UNIVERSITÀ DEGLI STUDI DI MODENA E REGGIO EMILIA

Dottorato di ricerca in Ingegneria dei materiali

(Scuola di Dottorato in Modellistica, Simulazione Computazionale e Caratterizzazione Multiscala per le Scienze dei Materiali e della Vita)

XXVI Ciclo

Design, development and testing of solar reflective ceramic based building materials

Candidato: Dr. Chiara FERRARI

Tutor: Prof. Cristina SILIGARDI

Co-Tutor: Dott Alberto MUSCIO

Direttore della Scuola di dottorato: Prof. Ledi MENABUE

Al nonno Egidio
spero tu possa essere fiero
del mio tentativo di ripercorrere i tuoi passi.

ABSTRACT

English abstract

Roofing solutions with high capacity to reflect incident solar radiation, the so-called cool roofs, can provide an effective answer to summer overheating of either individual buildings or whole urban areas. They, in fact are characterized by high infrared emissivity, which allows the roof to emit via thermal radiation, the maximum amount of radiation adsorbed, and high albedo properties reflecting the solar radiation incident on their surface. Nowadays, commercial cool roof products are mainly represented by organic membranes and coatings, but ceramic tiles can offer an interesting alternative or complement in view of their higher durability and low maintenance costs. A common cool surface is made by a very simple system where a substrate is coated with a two layer system: the basecoat is characterized by a strong Near infrared reflectivity and the transparent topcoat, with the eventual presence of pigments, which weakly absorb and, eventually, strongly backscatter Near Infra-Red radiations. This close resemblance to a common system tile-engobe-glaze, the high thermal emissivity of ceramic bodies, the interesting reflective properties of a white stoneware tile, which maintain high reflectance up to the whole NiR region investigated (700-2500 nm) and the good attitude of ceramics tile against weathering agents and ageing processes inspired the creation of a solar-reflective clay-based tile with the formulation of a solar reflective engobe and the formulation of new cool colored glazes. The first step was the formulation of a low cost engobe enhancing the solar reflectance of the ceramic substrate. This goal was carried out through the variation of the substrate, of the raw materials, of the thickness of the engobe and on the white or transparent glaze applied as a top coat on the substrate-engobe system. After this step a solar-reflective colored glaze was designed in order to evaluate how nonwhite surfaces affect the solar reflectance of the final product. In the glaze study both traditional stoneware tiles and clay roof tiles substrate were considered. Concerning clay roof tiles substrate three different glaze formulations, in which eight different pigment were embedded, were analyzed, while, concerning traditional stoneware tiles substrate

four different glazes formulations, in which eight different pigments were embedded, were studied. Another roofing product quite common as "Cool Roof" is represented by the asphalt shingle. In this case basalt or slate grit is applied on a bitumen layer in order to improve the aesthetical aspect of the final tile and preserve from ageing the bitumen base. Mineral grits are usually covered by a colored layer through a rotary kiln. The third part of this work is concerning the formulation of a new white ceramic glaze for basalt grit. Starting from a commercial formulation, implemented with a new pigment, two experimental plans were studied in order to analyze the influence of two pigments (TiO_2 and Talc), other raw materials and the firing temperature. For all the samples mineralogical and microstructural analysis were combined with solar reflectance (250-2500 nm) and thermal emissivity (4-40 μm) measurements in order to evaluate the behavior of the samples against solar radiations. Since a good cool roof product should keep its solar properties for at least three years, the fourth part of this work concerned the study of the influence of artificial and natural ageing on the solar reflectance performance of clay based roof tiles. Clay roof tiles samples, artificially and naturally aged, were then cleaned through wiping and rinsing in order to simulate the effect of wind and rain. The importance of creating solar-reflective ceramic-based surfaces and well understanding their behaviour after ageing processes is crucial in order to promote this new building product which, not only can mitigate the Urban Heat Island Effect, but can frame in a smart way in the national and European building policies.

Italian abstract

Coperture dotate di alta capacità di riflettere la radiazione solare, i "cool roof", possono rappresentare un'efficace risposta al sovra riscaldamento estivo sia di edifici singoli sia di aree urbane. Questi infatti sono caratterizzati da alta emissività nell'infrarosso che consente alla copertura di emettere come radiazione termica la massima quantità di radiazione assorbita, ed alti valori di albedo, ovvero capacità di riflettere la radiazione solare incidente.

La struttura tipica di un cool roof è un sistema dove il substrato è coperto da due strati: un base coat caratterizzato da alta riflettanza nel vicino Infrarosso (NiR) e un top coat trasparente, con eventuale presenza di pigmenti, che assorbe debolmente ed, eventualmente, riflette la radiazione NiR.

Questa somiglianza con un sistema piastrella-ingobbio-smalto, l'elevata emissività termica dei corpi ceramici e le interessanti proprietà di riflettanza di una piastrella a base bianca che mantiene alti valori in tutto il NiR investigato (0.7-2.5 μm) e la buona risposta dei ceramici contro l'invecchiamento e gli agenti atmosferici, ha ispirato la creazione di una piastrella ad alta riflettanza solare con un ingobbio alto riflettente e nuovi smalti cool colors.

Questo lavoro si articola in tre parti riguardanti differenti aspetti della ricerca cool roof: lo sviluppo di ceramici tradizionali e tegole smaltate, lo sviluppo di smalti ceramici per tegole canadesi e lo studio delle loro proprietà dopo l' invecchiamento.

La prima parte riguarda la formulazione di un ingobbio che migliori la riflettanza del substrato ceramico. Questo obiettivo è stato ottenuto studiando le variabili colore del supporto, tipo di materie prime, spessore dell'ingobbio e tipologia di smalto (bianco, trasparente e matt) applicato come top coat sul sistema ingobbio-substrato

Successivamente, per valutare come le superfici colorate influenzano la riflettanza finale del prodotto, uno smalto colorato ad alta riflettanza è stato preparato utilizzando fritte con finitura differente e diversi pigmenti. Come substrati sono state usate sia piastrelle in grés bianco sia tegole.

Le Tegole Canadesi sono un altro prodotto da copertura costituito da graniglia di basalti o ardesia applicata su uno strato bituminoso per migliorarne l'aspetto estetico del prodotto finale

e preservarlo dall'ageing. La graniglia minerale è solitamente coperta da uno strato colorato applicato in forno rotativo.

La seconda parte del lavoro riguarda la formulazione di uno smalto ceramico bianco per graniglia basaltica a partire da una formulazione commerciale, implementata con un nuovo pigmento. Due piani sperimentali DoE sono stati formulati per analizzare l'influenza dei due pigmenti (Talco e TiO2), altre materie prime e temperatura di cottura.

Un buon prodotto cool roof deve mantenere le proprietà solari per diversi anni quindi l'ultima parte di questo lavoro riguarda lo studio di invecchiamento naturale e artificiale sulla riflettanza di tegole e coppi. I campioni, invecchiati naturalmente e artificialmente, sono stati puliti simulando l'effetto del vento e della pioggia.

Di tutti i campioni le analisi mineralogiche e microstrutturali sono state integrate con misure di riflettanza solare (0.3-2.5 μm) ed emissività termica (4-40 μm) per valutare il comportamento dei campioni alla radiazione solare.

L'importanza della creazione di prodotti ceramici ad alta riflettanza e la corretta comprensione del loro comportamento dopo l'invecchiamento è cruciale per promuovere questi nuovo prodotti per edilizia che, non solo possono mitigare l'effetto isola di calore urbano, ma possono essere inserite in modo innovativo nel quadro normativo edilizio nazionale ed europeo

TABLE OF CONTENTS

LIST OF TABLES

LIST OF FIGURES

CHAPTER 1
INTRODUCTION

Research topic

Cool roof are one of the most successful mitigation strategies for the reduction of the Urban Heat Island effect. Since cool roof market is actually dominated by organic based products such as paint and membranes, in this work, new clay based building products are designed, created and then characterized in order to introduce these new solutions as effective strategies to improve indoor thermal comfort and building energy efficiency.

Motivations

Nowadays comfort, especially thermal comfort, is one of the main requirement for a building. It can be achieved through thermal insulation in summer and reduction of the solar gain through transparent and opaque element in summer. In particular, solar gain through opaque elements is one of the main causes of the Urban Heat Island effect (Fig.1.1). This phenomenon consists in the increasing of the environmental temperature of urban area generally up to 3 °C if compared with surrounding rural areas.

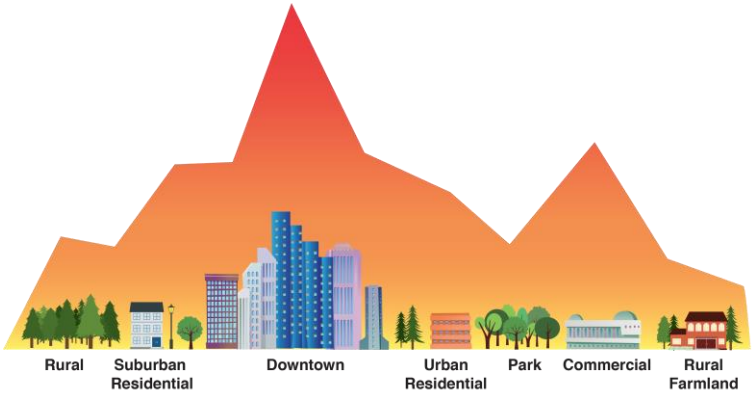

Figure 1.1 – Urban heat island effect

Residential areas energy demand is more than 30% of the total amount of energy required, and the demand for electricity increase every year (Swan et al, 2009). In particular the increasing cooling demands for both residential and commercial buildings and the increase in thermal comfort requirements highlighted the need of mitigation solution in a sustainable way (IEA, 2012)

One of the better strategies to reduce cooling demand is the optimization of roofs use, since roofs covering represents 20-25% of the whole area of four American Cities (Akbari and Rose, 2008). The same proportion can be referred to Italian and in general European cities. This high percentage of potentially unused surface is an interesting alternative for the application of technique aimed to reduce the Urban Heat Island Effect such as cool roofs and green roofs. Because of the current building policies cool roofs are preferable to green roofs because of their lower impact on the city skyline. A uniform skyline that must match also with several historical buildings, is in fact required by the majority of cities in Italy and in Europe.

Nowadays four different cool roofs generation were produced: the first cool roof generation, as reported by Santamouris (2012) was represented by naturally high solar reflective materials. Their reflective capacity, however, rarely were higher than 75% (Doulos et al, 2004, Bretz & Akbari, 1997) The second cool roof generation evolved thanks to the experimentally developed coverings with high performance in reflecting solar radiation, reaching better results with $\rho sol < 0.85$ (Synnefa et al, 2008; Kilikitsa et al, 2012). The third generation of cool roof tried to develope high performing reflective coatings characterized by high infrared reflectance, thus optimizing the cool roof effect with respect to the conventional ones of the same color (Levinson et al, 2005a, Levinson et al, 2005b)

A new cool roof generation, finally, is focused on innovative materials such as nanobased thermochromic paints or phase change materials (Ma et al, 2001, Karlessi et al, 2011)

The Italian tradition on ceramic based building materials put our attention on the creation of new solar reflective material ceramic based trying to conciliate these new technologies with the traditions of our manufacture.

Purpose of the work

In line with the background delineated above, the purpose of this work is the creation of new solar reflective building materials solutions for both cool pavement and cool roof solutions. Three different building products were taken into account: starting from a traditional system "ceramic support-engobe-glaze" a new ceramic tile was designed where a solar reflective engobe was protected with different glazes both white, in order to guarantee the higher reflectance possible for the system, and colored glaze. Since both pavement and roofing solution can be implemented in order to improve their solar reflectance, a solar reflective glaze for traditional clay roof tiles was designed. Another building product can be implemented through the application of a ceramic glaze in order to improve its solar reflectance: a new ceramic based glaze for asphalt shingles was designed, starting form an industrial formulation, in order to improve the solar performance but, at the same time, reduce the cost of the final product.

Finally, this work tries to approach the ageing problem. Considering the long exposure to weathering agents and pollution which both can reduce the solar reflectance of building materials, an ageing study was carried out on different samples. Possible differences between natural and artificial ageing were analyzed and an attempt was made to understand how different solar-reflective clay-based building products react not only to ageing and pollutants exposure but also to natural cleaning steps such as wind and rain.

Outline of the work

In this work four section can be identified.

Chapter 1, 2 and 3 try to frame Urban Heat Island Effect and, among its possible mitigation strategies, cool roof and cool colors development. A special attention is given to the development of inorganic based solar reflective building materials and as can be seen, although several studies concerning the use of cement both as cool roof and as cool pavements, ceramic based building products such as ceramic tiles and clay roof tiles are still not well studied. Moreover the actual state of the art concerning ageing studies is approached with attention not only to natural ageing procedures but also to artificial ageing protocols.

In this whole first section, both Cool Roof Rating Council and the European Cool Roof Council were taken as a reference. Chapter 3 is focused on the most used building materials for cool roof applications with particular attention for ceramic glazed tiles, clay roof tiles and asphalt shingles, the three building materials studied in this work. Since Solar Reflectance measure was widely used in this study, Chapter 4 present a special regard to this technique explaining the principles behind this measure, the facilities used in order to perform these characterization and the reason behind the choice of the irradiance spectrum used in this work.

Chapter 5 and 6 deals with the formulation, the preparation and the following characterizations of the building materials. In particular, Chapter 5 shows the production of solar reflective traditional ceramic tiles and clay roof tiles. Concerning the engobe formulation, the influence of raw materials, thickness and ceramic support was analyzed. In a second time the best engobe produced in this first section was covered with different glazes characterized by different frits and pigments. Since clay roof tiles are usually not engobed, different glazed, designed on purpose to fit clay roof tiles firing, were designed. The same pigments used for ceramic tiles were embedded into the formulations. In both sections attempts were made to correlate the measured Solar Properties with the microstructure and the mineralogy nature of the different surfaces.
In Chapter 6 a non-traditional ceramic products was studied. Asphalt shingles represents one of the most used cool roof product: a bitumen layer covered with mineral grits which is usually in order to reduce summer overheating and improve the skyline match of the product. Since traditional paints need to be refurbished after few year of exposure, it has been replaced with ceramic glaze applied on the mineral grit through a rotary kiln. The starting formulation was an industrial recipe, which was modified, through a mixture design approach, in order to evaluate the influence of the pigments, the liquid phase and the firing temperature.

Chapter 7 deals with ageing study. Two different approaches were adopted: the first part of the study compares natural and artificial ageing applied on monochromatic cool colored tiles. Natural exposure took place in Arizona, according to what prescribed by CRRC-1 Standard Test Method. Accelerated ageing protocols, which allow to condensate 3 years ageing in 3 days of lab activities, simulated both Arizona condition and an average soiling condition of Arizona, Ohio and Florida which are the three locations chosen by CRRC in order to have a comprehensive idea of US soiling conditions and was carried out in LBNL heat island group laboratories.

Finally chapter 8 summarizes the major findings of this work with the addition of some perspectives that should be developed in the next years in order to keep cool roof research updated in Italy.

Chapter references

Akbari H., Rose L.S. (2008) Urban surfaces and heat island mitigation potentials, Journal of Human–Environment System, 11(2) 85-101.

Bretz, S., and Akbari, H. (1997). Long-term performance of high-albedo roof coatings. *Energy & Buildings*, 25, 159-167.

Doulos L, Santamouris M., Livada I. (2004) Passive Cooling of outdoor urban spaces: the role of materials, Solar Energy, 77(2) 231-249.

IEA International Energy Agency: Report for the Clean Energy Ministerial: Transforming global markets for clean energy products. Technical report, 2010,

Karlessi T., Santamouris M., Synnefa A., Assimakopoulos D., Didaskalopoulos P., Apostolakis K. (2011) Development and testing of PCM doped cool colored coatings to mitigate urban heat island and cool buildings, Building and Environment, 46(3) 570–576.

Kolokotsa D., Maravelaki-Kalaitzaki P., Papantoniou S., Vangeloglou E., Saliari M., Karlessi T., Santamouris M. (2012) Development and analysis of mineral based coatings for buildings and urban structures, Solar Energy, 86(5) 1648-1659

Levinson R., Berdahl P., Akbari H. (2005a) Solar spectral optical properties of pigments— Part I: model for deriving scattering and absorption coefficients from transmittance and reflectance measurements, Solar Energy Materials and Solar Cells, 89(4) 319–349.

Levinson R., Berdahl P., Akbari H.(2005b) Solar spectral optical properties of pigments— Part II: survey of common colorants, Solar Energy Materials and Solar Cells, 89(4) 351–389.

Ma Y., Zhu B., Wu K.(2001) Preparation and solar reflectance spectra of chameleontype building coatings, Solar Energy, 70, 417-422.

Santamouris M., Cooling the cities – A review of reflective and green roof mitigation technologies to fight heat island and improve comfort in urban environments, Solar Energy, Available online 30 July 2012, ISSN 0038-092X.

Synnefa A., Santamouris M, Livada., I.(2006) A study of the thermal performance of reflective coatings for the urban environment, Solar Energy, 80(8), 968-981.

Swan L. G., Ugursal V. I. (2009) Modeling of end-use energy consumption in the residential sector: A review of modeling techniques, Renewable and Sustainable Energy Reviews, 13(8), 1819-1835.

CHAPTER 2
COOL ROOF: MITIGATION STRATEGIES FOR URBAN HEAT ISLAND

Urban Heat Island

First described by Luke Howard in the 1810s, (Luke Howard, 1820) the Urban heat island effect occurs when temperatures of urban areas are significantly warmer than temperatures of outlying rural areas causing, in addition to an increase in energy consumption and in pollutants and greenhouse gases emission, a decrease in comfort and human health and a reduction of water quality (EPA, 2008).

More closely Urban Heat Island effect can be distinguished in atmospheric and surface urban heat island effect. Atmospheric Urban Heat Island take into account the difference of air temperature between warmer air in urban areas and cooler air in surrounding rural areas. This effect is pronounced after sunset due to the slow release of energy from urban areas, while is quite weak throughout the day. The time distribution of this heating peak is strictly related to the properties of building materials used on both urban and rural surfaces, to the season and to the weather conditions. Atmospheric Urban Heat Island can be split into two different models: if the layer below and above the tops of the trees and roofs are compared, the model is called Canopy layer Urban Heat Island. The range of the lower region is extended up to ~1.5 Km from the surface, meaning starting from the treetop and rooftop level reaching the level where any influence of the urban landscape does not occurs, originate the boundary layer urban heat island (Oke, T.R., 1982).

Surface Urban Heat Island is characterized by more significant spatial and temporal variation. This model is observed both during night and day, and presents its peaks during day and summer. (Oke, T.R., 1982, 1987, 1997, Voogt J.A. et al, 2003, Roth M., et al 1989) and present a higher intensity if compared with Atmospheric heat island.(Oke T.R, 1997) This is highlighted by Voogt (2000) in Fig. 2.1 where the intensity of Canopy Layer Urban Heat Island (CLUHI), represented with continuous line, and Surface Urban Heat Island (SUHI), represented by dashed line, are compared. During daytime SUHI is more intense than

CLUHI, which present really slight temperature variations, while during nighttime both of UHI presents higher variations and almost the same trend.

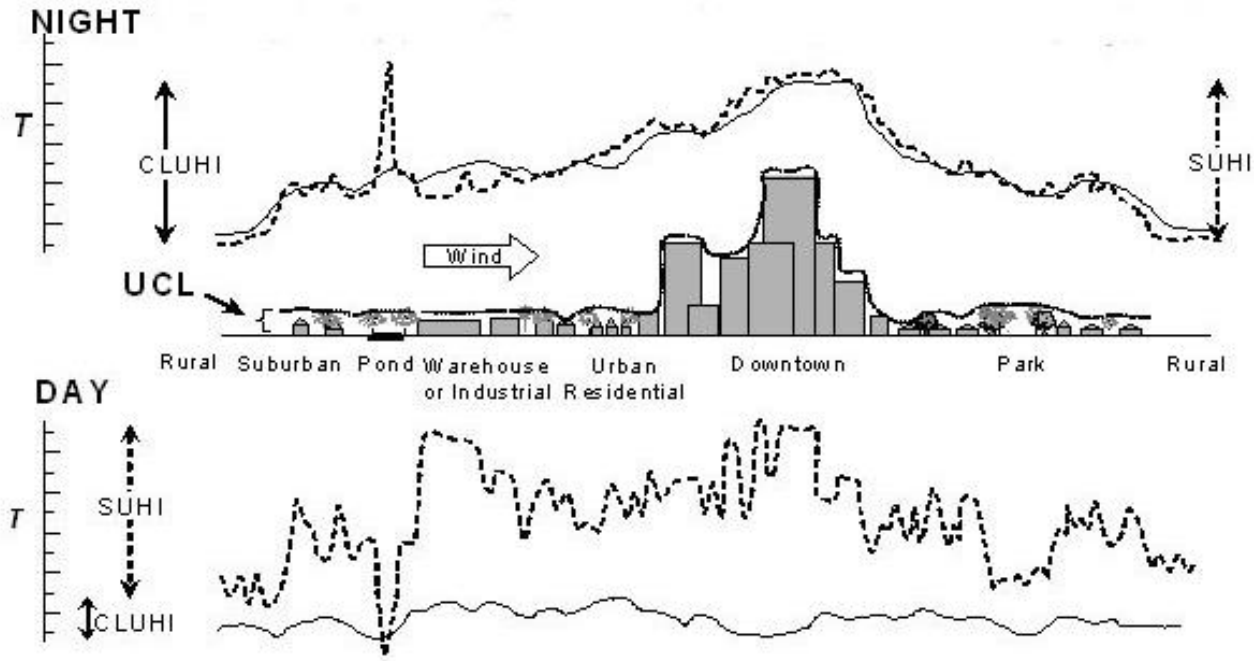

Figure 2.1 – Cross section of air temperature (dashed line) measured within the urban canopy layer (UCL) and surface temperature (continuous line) under optimum heat island conditions (calm and clear) during nighttime (top) and daytime (bottom) (Voogt, 2003)

More generally speaking Urban Heat Island effect is most intense with clear sky and no wind conditions because solar radiation is blocked by cloud cover with a reduction of daytime warming in the cities.

In order to mitigate Urban Heat Island effect is essential to know how this phenomenon is formed. In addition to the weather influence which can emphasize UHI, the release of anthropogenic heat, and the geographic location, the surface properties of the building and in general urban materials has an important influence on UHI formation, in fact all materials are characterized by solar radiation absorption properties which keep surfaces warmer than those of rural areas (Christen and Vogt, 2004). Moreover the lack of cool sink trees and vegetation in general contribute to the reduction of natural cooling effect given by tree shade and evapotranspiration. Among UHI causes also heat emission can contribute to the air warmth, which can also be enhanced by the distribution and the building shape, which can obstruct air circulation in urban canyons and increase the storage of solar radiation by the city structure (Sailor et al, 2002, Oke et al., 1991).

Mitigation Strategies

Several technological measures were developed in order to counterbalance the impact of heat island (Rosenfeld et al., 1995, Akbari et al., 2001, Adnot et al., 2007, Gaitaini et al., 2007, Kuttler, 2011). They tried to increase thermal losses and decrease the gains in order to balance the thermal budget. Three strategies were applied: the expansion of green spaces in cities, the use of natural heat sinks in order to dissipate the excess heat and the increasing of albedo in urban environment (Julia et al, 2009, Mihalakakou et al., 1994, Akbari et al, 2005) The United states Environmental Protection Agency suggest, as mitigation techniques the application of green roofs, the increase of vegetation and trees areas and solar reflective roofs and pavements. (Santamouris, 2012)

The increase of trees and vegetation areas is an effective and simple way for the reduction of UHI through evapotranspiration and shade with a reduction of 11-25 °C compared with unshaded areas (Akbari et al. 1997) while evapotranspiration can further help the peak summer temperature by 1-5 °C (Huang et al. 1990, Kurn et al). In practice, the use of trees and vegetation implies several benefits including the improvement of quality of life, the reduction of pavement maintenance, the improved air quality, reduction of greenhouses gases emission, the reduction of energy demand for air conditioning and the better stormwater management. (EPA, 2008 http://www.epa.gov/heatislands/mitigation/trees.htm)

The implementation of green roof, vegetative layer grown on rooftop, shades and removes heat from the hair thanks to evapotranspiration. They can be installed on both industrial facilities and private residence (http://www.greenroofs.com/projects/plist.php). In this case benefits are quite similar to benefits related to the increase of trees and vegetation areas. Even though the first solution is easily applicable in both Italian and European context, the use of green roof is still not so diffuse.

Since roofs, which represent a very high fraction of the exposed urban area, reached 20-25% for less or more dense cities (Akbari & Rose, 2008) this huge surface provide and excellent space to apply mitigation techniques. Beside green roof, the use of solar reflective roofs, which increase the albedo of the surface, is suggested.

Cool roof and cool pavements

The first step that has to be taken into account for cool roof comprehension is the analysis of the solar radiation reaching the earth. At the top of the atmosphere, solar radiation can be approximated to that of a

black body with T= 5800 K then, crossing the layer of atmosphere is filtrated and the spectrum is modified following the angle that the sun forms with the zenith (air mass) (Fig. 2.2a) and the portion of light taken into account (direct, diffuse and reflected) (Fig. 2.2b)

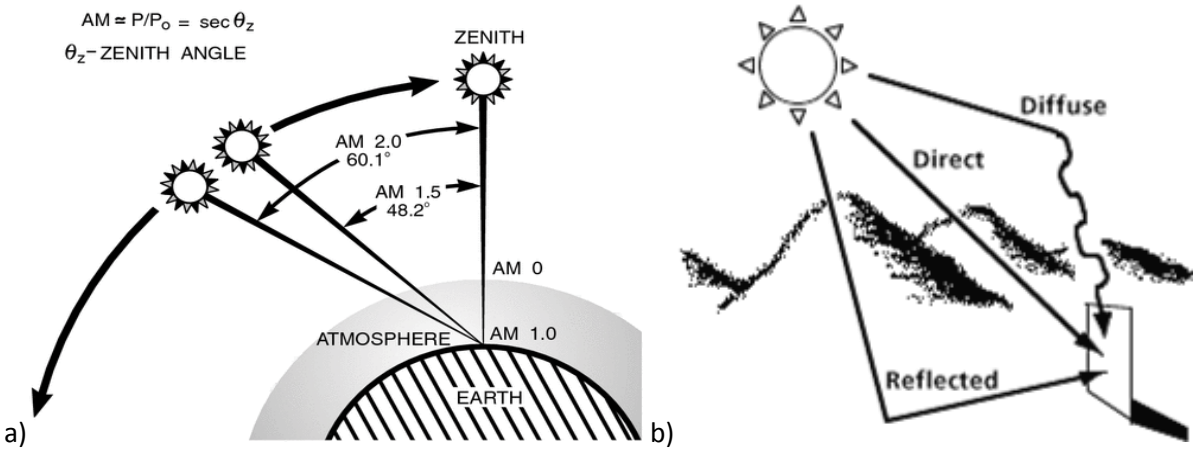

Figure 2.2 – Air mass definition according to the angle that the sun forms with zenith (a) and different portion of light reaching a surface (b)

The interaction between these two factors motivated the identification of various irradiance spectra i.e. spectral distribution curves, which correlate the solar radiation reaching the earth with the wavelength of these radiations. (Fig. 2.3) As it is evident in Fig 2.3 all the spectra considered cover both UV, visible and NiR fraction.

The UV fraction is the smallest while the visible and the NiR are the two dominant ones. Quantifying the two fractions, the percentage of NiR radiation is higher than the percentage registered for the Visible fractions. This allow us to consider that, in order to mitigate Urban heat island a surface should reflect as much radiation as it is possible mostly in the Visible and NiR range, as it can be read in table 2.1.

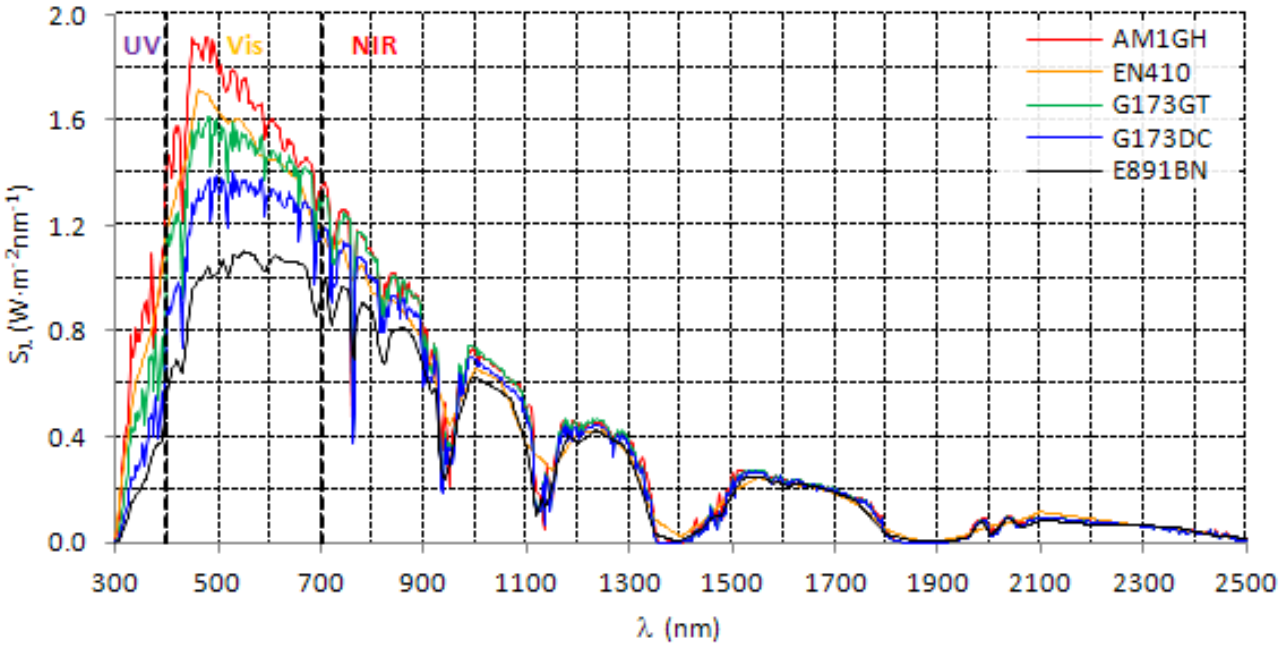

Figure 2.3 – Standard solar irradiance spectra (Ferrari, 2013)

Table 2.1 – Fraction of radiation reaching the earth according to different irradiance spectra (Ferrari et al 2013)

Initialism	***Description***	***UV/Vis/NIR (%)***	***Source***
AM1GH	*Clear sky AM1 global horizontal irradiance*	*6.5/45.0/48.5*	*NREL SMARTS 2.9.5*
EN410	*Clear sky AM1 global horizontal irradiance*	*6.2/44.3/49.5*	*EN 410:2011*
G173GT	*Clear sky AM1.5 global irradiance on a south facing surface tilted 37°*	*4.5/43.5/52.0*	*ASTM G173-03*
G173DC	*Clear sky AM1.5 direct irradiance on a surface normal tracking the sun*	*3.3/42.2/54.5*	*ASTM G173-03*
E891BN	*Hazy sky AM1.5 beam-normal irradiance*	*2.8/39.2/58.0*	*ASTM E981-87 (1992)*

Cool roofs refer to surfaces with high solar reflectance or albedo and high thermal emittance. (fig. 2.4)

Solar reflectance can be identified as the amount of solar radiation reflected by a surface in a range from 250 up to 2500 nm. Usually this parameter evaluates how well a material reflects energy at each solar energy wavelength, then the weighted average of these values, according to the irradiance spectrum considered, is calculated. Solar reflectance usually range from 0, for a totally absorbing material, to 1 for a total reflective material.

In order to evaluate a surface's contribution to urban heat island, solar reflectance should be integrated with thermal emissivity which express the ratio of the thermal radiation emitted from a surface and the

maximum theoretical emission at the same temperature. Its value ranges between 0 and 1 and the properties is measured in the range between 4000 and 40000nm. When a surface with high emittance is exposed to sunlight will reach thermal equilibrium at lower temperature since it gives off its heat more readily.

Another parameter can be used in cool roof evaluation: Solar reflectance index summarize, according to this equation $SRI = \frac{T_{black} - T_{surface}}{T_{black} - T_{white}} \times 100$ where T stands for steady state temperature. SRI ranges between 0 (as hot as a black surface) and 100 (as cold as a white surface).

Considering the importance of a correct measurement protocols, for each properties, standard were published by ASTM(Tab. 2.2)

Table 2.2 – Test methods (EPA, 2008)

Property	Test method	Equipment required	Test location
Solar reflectance	ASTM E 903 – Standard Test Method for Solar absorbance reflectance and transmittance of materials using integrating sphere	Integrating sphere spectrophotometer	Laboratory
Solar reflectance	ASTM C 1549 – Standard Test Method for determination of solar reflectance near ambient temperature using a portable solar reflectometer	Portable solar reflectometer	Laboratory or field
Solar reflectance	ASTM E 1918 – Standard Test Method for measuring solar reflectance of horizontal and low sloped surfaces in the field	Pyranometer	Field
Solar reflectance	CRRC Test Method #1 (for variegated roof products) used in conjunction with ASTM C1549	Portable solar reflectometer	Laboratory or field
Thermal emittance	ASTM E 408-71 – Standard Test Method for Total normal emittance of surfaces using inspection-meter techniques	Reflectometer or emissometer	Laboratory
Thermal emittance	ASTM C 1371 - Standard Test Method for determination of emittance of materials near room temperature using portable emissometer	Emissometer	Field
SRI	ASTM E 1980 – Standard practice for calculating solar reflectance index of horizontal and low sloped opaque surfaces	None (calculation)	-

Solar reflective surfaces, both cool roof and cool pavements, in order to keep cold the surface are characterized both by high solar reflectance and high thermal emissivity. In figure 2.4 how a cool roof, and in general a cool or solar reflective surface works, is easily explained through a comparison between a black , a metal and a white roof.

The black roof, due to its surface, is characterized by high thermal emissivity and low solar reflectance and can reach 180 °F (82 °C), a metal roof is characterized by high solar reflectance and low thermal emissivity and can reach 160 °F (71 °C).

Under solar exposure, both of them present a tangible increasing of temperature, while a white roof, which is characterized by the lowest temperature increase, is characterized by both very high solar reflectance and high thermal emissivity and can reach 120 °F (49 °C).

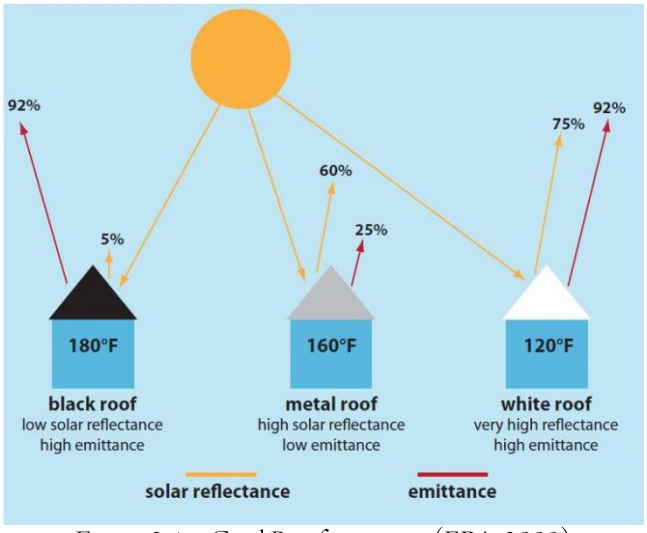

Figure 2.4 – Cool Roof structure (EPA, 2008)

Different kind of material can be adapted and used in order to create solar reflective surfaces.

Concerning the installation of cool pavements not only commonly employed clear resin binders, cementitious and elastomeric coatings, light colored aggregates and cements can be used, but also permeable pavements such as porous asphalt cement, pervious Portland cement concrete and reinforced grass pavement can be used with an added value since they also provide storm water management (Cool roof Toolkit).

Concerning the cool roof market an important distinction should be made since roofing products vary widely if they are designed for low sloped or steep sloped roof.

Low sloped roofs are flat roofs with a really low slope just to provide water drainage. The most suitable solutions for low-sloped roofs are single ply membranes, liquid applied coatings, built up roof, modified bitumen shingles and metal roofs. Steep sloped roofs present higher pitch as it can be observed in the majority of residential building. Since steep sloped roofs are more visible to the street, a special attention should be given to the aesthetical aspect of these products which can be made not just by Clay and Concrete tiles, like south Europe building tradition, but also from metal roof, wood shanks, asphalt shingles and liquid applied coatings like paint applied on the roof tiles.

In particular concerning steep sloped roof, as said above, the appearance acquire an increasing role since the most reflective cool roofs are generally white. In order to allow the use of building materials with lower visual impact, cool color were implemented: they are characterized by high infrared reflectance optimizing the cool roof effect with respect to the conventional ones of the same color as it can be seen in fig. 2.5

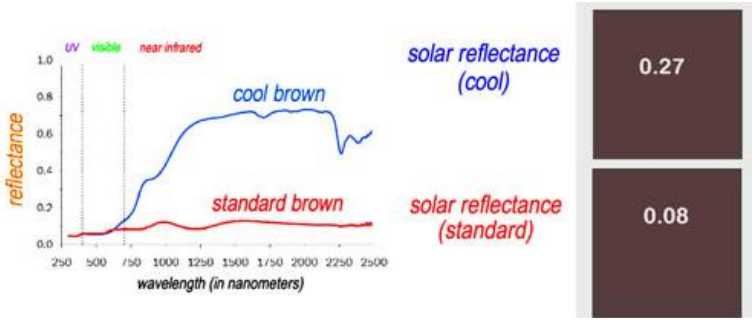

Figure 2.5 – Spectral differences between cool colors and standard colors (courtesy of BASF coatings, Source: http://eetd.lbl.gov/newsletter/nl19/)

Both cool pavements and cool roofs present a significant amount of benefits that, once balanced with costs and weakness allow us to state that this solution can represent an effective mitigation strategy for Urban Heat Island that should be widely used, even in Italy.

Since the installation of roofs, in a building, is a relevant cost, before the installation of a solar reflective surface a lifecycle analysis and a quick review of benefits, costs and penalties should be approached.

In order to analyze the lifecycle of cool roof, four aspects must be taken into account: Upfront and Ongoing costs and expenses and non-financial benefits.

For an easier comprehension Upfront and Ongoing cost will be considered as unique aspect as well as Upfront and Ongoing Savings.

Among Upfront and Ongoing costs, materials and labors should be considered as well as disposal and replacement if a traditional roof will be replaced by a cool roof. In any case maintenance cost should be taken into account. This aspect varies a lot considering different roofing coverage and considering different roof durability.

Considering Savings several aspects are quite relevant: first of all energy savings which are the main benefit of cool roof, rebates and incentives for people installing cool roof are usually offered both for new roofs and for the replacement of a traditional roof in the US. It is important to remember how cool roofs can extend roof lifetime, moreover this feature can be enhanced by a correct maintenance protocol. Another important saving skill of cool surfaces is the reduction of power plant emissions, both for houses and for cars in case of cool pavements Finally, considering cool pavements, additional savings is represented by the water management, in particular storm water.

The last aspect which is considered are the non-financial benefits such as indoor comfort and improvement in life quality starting from the reduction of air pollution and cooling of ambient temperatures. Both cool surfaces, moreover, slow the climate change reducing surface temperature and heat flow into the atmosphere counteracting warming because of greenhouse gases.

Another aspect that has to be considered in order to have a comprehensive idea of cool roof technology are the penalties related to solar reflective surfaces.

Despite the benefits of cool surfaces are observed in almost every part of the world, their effectiveness varies, not only depending on local factors, the climate, but also the type of building, the topography and the weather in the region. In particular cool roofs and cool pavements are strongly recommended in tropical zones characterized by long warm seasons. In temperate areas, where hot seasons are shorter, benefits of cool roofs are evident even when evaluating only net energy cost saving despite of winter heating penalty. Since cool roof presents, as a strength point, the ability to lessen cooling demands of a building, the risk to increase heating requirements is reasonable. Despite all, considering both the cooling savings and the net savings reported in Fig. 2.6, almost in every case winter heating penalties are less than cooling energy savings (Cool Roof Toolkit)

In the US cool surfaces are more widely used than in Europe and, in order to organize and rate cool roof products and stimulate their installation several agency were organized . These agencies can be grouped in four different families:

Among roof rating programs the Cool Roof Rating Council (CRRC) is the most important organization, founded in 1998, which keep a neutral rating program for measuring and reporting radiating properties of solar reflective surfaces without stating minimum requirements for a surface to be "cool". Through CRRC-1 Program Manual all measuring system required are shown in order to allow accredited independent testing laboratory to measure radiative properties of both unexposed and aged roofing products. CRRC stated which are the locations where the exposure of samples for natural ageing protocols has to take place and how this process should be carried on.

Complimentary to the CRRC, Environmental Protection Agency's Energy Star Program set minimum requirements for both low slope and steep slope roofs and for both unweathered and weathered surfaces.

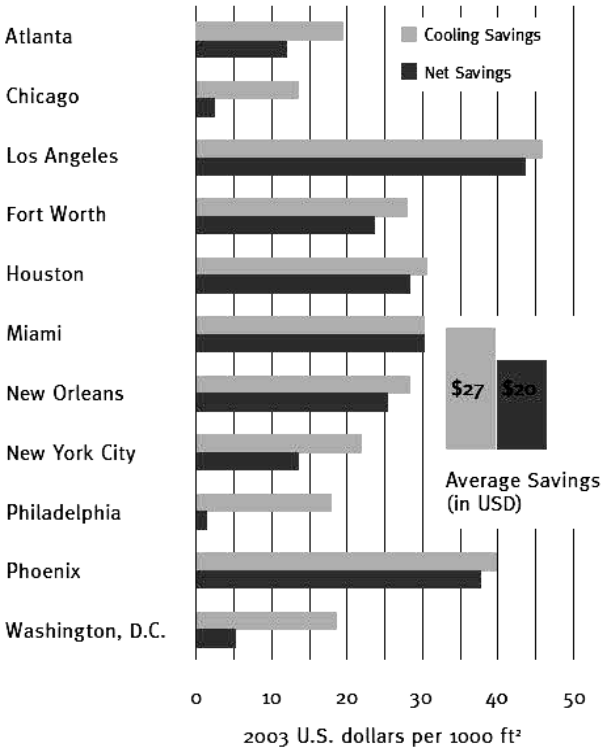

Figure 2.6 – Annual net energy cost savings in various U.S. Cities from widespread use of cool roofing. Source: Adapted from Dallas Urban Heat Island, Houston Advanced Research Center, 2009. sciencedirect.com/science/article/pii/S0360544298001054, Cool Roof Toolkit.

The second category is represented by energy codes, not mandatory document until a jurisdiction adopts these documents as part of regulation or law. Among energy codes the most widely used are ASHRAE standards.

In addition to energy codes, US state and city can adopt their own codes such as California's title 24 which establish requirements for solar reflective roofs both in new constructions or major re-roofing project.

The last category Is represented by green building programs, growing both in the US and in Europe. The two most known programs are the Green Globes program which is an online questionnaire-based program which give points for different aspects of the building and is comparing each category with EPA's target finder. The second, and well-known also in Europe, program is the Leader in Energy and Environmental Desing (LEED) program, a voluntary certification program for sustainable buildings which references CRRC and Energy Star as source of rated products.. For each of these two programs solar reflective roofs or pavements help to increase the point related to energy efficiency aspects.

In Europe, ten years later than in the US, the European Cool Roof Council (EU-CRC) was found in order to provide the same function of the American one. Eu-CRC started from the Cool Roof Project, co-financed by the European Union in the framework of the Intelligent Energy Europe Programme. In june 20013 an European Project financed by the Programme MED started. The project MaIn, Matériaux Intellingents, led by Dr. Alberto Muscio working at UniMoRe EELab (Energy Efficiency Laboratory) is aimed at dissemination of smart materials such as cool roofs and cool pavements by intervening in any chain cycle for their usage.

Ageing issues

Among the building materials suitable for cool surfaces applications, the durability, once applied vary deeply as suggested by tab2.3 and 2.4. In order to find a good compromise between durability and solar properties CRRC requires both unexposed and aged solar reflectance and thermal emittance values. In order to standardize sample exposure, three different locations in the US were chosen to obtain a comprehensive idea of what ageing in the US is. Samples are exposed for three years in test farms located in Arizona, representative for a dry hot climate, Florida, for a hot and humid climate and Ohio, for a cold temperate climate.

Since building materials are deeply subjected to atmospheric factors and ageing, therefore not only good aesthetical and surface properties but also mechanical ones are required. The combination of the features of ceramic products, their shock resistance properties, and the design of a coating characterized by excellent solar reflective behavior make roof tiles an ideal product to be applied on modern buildings. Cool

roof tiles have the potentials of saving energy, limiting summer overheating, and mitigating the urban heat island effect (Konopacki et al 1997; Akbari, 2005; Levinson & Akbari, 2010).

Table 2.3 – Durability of common cool pavement materials

Common cool pavement	**Pavement surface life (years)**
Clear resin binder	20
Coatings	1 – 5
Light-colored aggregates	2 – 5
Light-colored cement	40
Ceramic tiles	50+
Porous cement, concrete and reinforced grass pavement	Varies
Portland porous concrete	40

Table 2.4 – Durability of common cool roof materials

Common cool roofs	**Slope**	**Roof surface life (years)**
Asphalt shingle	Steep slope	15-30
Built-up roof	Low slope	10-30
Clay tile	Steep slope	50+
Concrete tile	Steep slope	30-50+
Liquid applied coating	Both slope	5-20
Metal roof	Both slope	20-50+
Modified bitumen	Low slope	10-30
Single ply membrane	Low slope	10-20
Wood shake	Steep slope	15-30

Studies about ageing processes affecting roofing materials were carried out in the last 15 years. In particular Bretz et al (1997) demonstrated that the decrease in solar reflectance due to ageing of solar reflective coatings is not a significant barrier to the use of these materials for the improvement of energy efficiency in buildings. The study was carried out in collaboration with three different suppliers, analyzing three different coatings made by a white polymer coating with an acrylic base, a white acrylic-based coating and a white cementitious coating applied on horizontal and low sloped (<25%) roofs. Albedo values were measured in the warmest hours of the day, in clear days using a pyranometer, and reflectance measurements were carried out with a double beam spectrophotometer with 150 mm integrating sphere according to ASTM

Standard Test Method E903-96 (ASTM, 1996). The main finding of that paper was the change in albedo depends mainly on the coating, the surface texture, the slope of the roof, and the nearby sources of dirt and debris, quantifying the albedo reduction in 0.15 during the first year and much more gradual decline after the first year of ageing. Bretz et al. assume also that the albedo can be restored from 90 to 100% of the estimated original value just washing the surfaces.

Levinson et al (2005) studied the effect of cleaning processes on the reflectance and, in general, on solar heat gains of light colored roofing membranes. In that study white or light grey PVC membrane samples taken from roofs across the United States were analyzed. On the sample's surface black carbon and inorganic carbon was found. These contaminants reduce the solar reflectance of the membranes. To analyze the influence of several cleaning processes on the solar reflectance values, the sample surfaces were firstly wiped to simulate wind action, then rinsed to simulate rain action, and as a third step the surfaces were washed simulating a homemade cleaning process using a phosphate-free dishwashing detergent. As a final step all the surfaces were treated with a mixture of sodium hypochlorite and sodium hydroxide to simulate professional cleaning processes. After rinsing and washing processes almost all the dirt deposited on the surface was removed except for thin layers of organic carbon and some isolated dark spots of biomass. Bleaching processes cleared these last two contaminants recovering the loss of solar reflectance.

The same cleaning processes were used by Akbari et al. (2005) studying unweathered and weathered single ply roofing membranes collected from various sites across the US and Canada. In that study, 16 samples were analyzed at LBNL, following all the cleaning processes concerning the weathered samples surface treatment, and 25 samples were studied at National Research Council of Canada, applying just wiping processes on the samples surface. All cleaning processes were effective with recovery of almost 90% of their unweathered reflectivity. In some cases, an anti-algae product was required to restore the reflectivity level.

Among several studies concerning solar properties of building materials, Berdahl et al (2012) highlighted how solar reflectance changes during sample exposure to weathering agents. Asphalt shingles with granules coated by inorganic metal oxide pigment were studies. The very stable nature of the coatings helps to keep the properties of the granules constant on time, but initial solar reflectance values changed due to the loss of processing oils which coat the granules. These oils are particularly sensible to UV induced Photo Oxidation, which produces dark hydrophilic substances that are removed by rain or dew. Both hot dry and hot humid climates were considered in this study. In hot dry climates the changes in solar reflectance are mainly related to the annual cycle of accumulation of atmospheric particles and their removal by wind and

rain; in hot humid climate, instead, algae grow easily on granule surfaces, creating coatings which reduce reflectance by as much as 0.06 after 3 years. In this case, anti-algae additive addition to the asphalt shingles is suggested. If algae growth is absent, solar reflectance does not change deeply in the first year (0.02 or less).

Considering the importance of the atmospheric particles deposited on the roof tiles, Cheng et al (2012) studied the nature of dust deposited during natural ageing processes. According to that study, the knowledge taken from Bretz et al (1997) concerning the black and organic carbon deposited by ageing and weathering processes on the roofing material was integrated with the definition of two different kind of atmospheric particles belonging to rural and urban/industrial sites. Moreover, Cheng et al performed elemental analysis on atmospheric particle and they highlighted that Iron is the most abundant contaminant, and Iron, Chromium and Carbon are the major contributors to the change of solar reflectance on soiled samples (after about 4 years exposure)

Accelerate ageing experiments (Sleiman, 2010 and Sleiman 2014) have been formulated to simulate the natural weathering conditions. On the sample surface a suspension of water and soiling agents is sprayed from a nozzle. Artificial soiling mixture is made by sooty particles, salty particles and organic particulate matters trying to reproduce, in the most repeatable way possible, particles that can be found in the atmosphere. After the deposition of a known amount of soiling mixture, the samples will be dried under a heating lamp. The soiling mixture recipe is aimed at reproducing in a quite standard way a natural one, but it must be integrated with insoluble dust surrogate to optimize the wet and dry deposition and create a mixture that can be industrially adoptable. This mixture should be flexible and tunable to better represent different climate zones across the globe.

The first studies on solar reflective materials using tiles as substrate were made by Synnefa et al (2006, 2007) using concrete tiles as support for cool colored coatings, while the importance of clay roof tiles as a possible solutions for cool roof surfaces was highlighted by different previous studies.

Noelia et al (2014) made a classification of building materials used in urban envelopes and, considering tiles with different composition, finishing and color, they highlighted that, if comparing clay and cement tiles with the same finishing and color, the tiles made by clay presents a better behavior.

The same comparison was made with two different finishing and different colors: natural/enameled and matte/aged were compared as well as terracotta, grey and black colors. The first finishing style (natural/enameled) presented better solar properties as well as terracotta color. A study made by Ferrari et

al (2013) regards the design of a low cost solar reflective coating for porcelain stoneware tiles analyzing different pigments and different raw materials influence.

Another study made by Pisello et al (2013) concerns the development of coatings for traditional roof tiles for application in historical building in particular thanks also to the low embodied energy, the great ability to regulate indoor humidity, reduced toxicity and relatively low price if compared with other roofing products.

Clay roof tiles were also studied by Levinson et al (2007) where, testing pitched NiR reflective concrete or clay tile roofs a reduction of tile temperature, building heat gain and cooling power demand were achieved. Moreover the importance of this study carried out on cool colors instead of white cool roof is related to the need to apply cool roof technology on historical building which represents the majority of the buildings in Italy and in general in Europe in order to preserve the architectural heritage of these areas.

The development of cool tiles, more specifically of selective pigments with traditional colors, raises strong interest also in completely different geographical areas such as India and China, see among the others the work by George et al. (2011) and by Zhao et al (2013).

Chapter references

Adnot, J., Alvarez, S., Klitsikas, N., Lopes, C., Orphelin, M., Sànchez, F., Santamouris, M., (2007) Cooling the Cities- Rafraıˆchir les villes, Energy Efficient Cooling Systems & Techniques for Urban Building. Ecole des Mines, Paris.

Akbari, H., Pomerantz, M., Taha, H., (2001) Cool surfaces and shade trees to reduce energy use and improve air quality in urban areas. Solar Energy 70 (3), 295–310

Akbari, H., Berhe, A., Levinson, R., Graveline, S., Foley, K., Delgado, A.H., and Paroli, R.M. (2005). Aging and weathering of cool roofing membranes. Proceedings of the First International Conference on Passive and Low Energy Cooling for the Built Environment, May 17, 2005, Athens, Greece, Also published as Lawrence Berkeley National Laboratory Report LBNL-58055, Berkeley, CA.

Akbari, H., KurnD., et al. (1997). Peak power and cooling energy savings of shade trees. Energy and Buildings 25, 139–148.

Akbari H., Rose L.S. (2008) Urban surfaces and heat island mitigation potentials, Journal of Human–Environment System, 11(2) 85-101.

ASTM (1996). ASTM E 903-96 – Standard test method for solar absorptance, reflectance, and transmittance of materials using integrating spheres. Standard of the American Society for Testing and Materials.

Bretz, S., and Akbari, H. (1997). Long-term performance of high-albedo roof coatings. Energy & Buildings, 25, 159-167.

Berdahl, P., Akbari, H., Levinson, R., Jacobs, J., Klink, F., and Everman, R. (2012). Three-year weathering tests on asphalt shingles: Solar reflectance. Solar Energy Materials and Solar Cells, 99, 277-281.

Cheng, M.D., Miller, W., New, J., and Berdahl, P. (2012). Understanding the long-term effects of environmental exposure on roof reflectance in California. Construction and Building Materials 26, 516–526 (2012) Doi: 10.1016/j.conbuildmat.2011.06.052

Christen, A. and Vogt, R. (2004), Energy and radiation balance of a central European city. Int. J. Climatol., 24: 1395–1421.

EEDT newsletter: http://eetd.lbl.gov/newsletter/nl19/

Environmental Protection Agency.EPA, (2008) Reducing Urban Heat Islands: Compendium of Strategies: Basic and Cool Pavements Compendium

Ferrari C., Libbra A., Muscio A., Siligardi C., (2013), Influence of the irradiance spectrum on solar reflectance measurements, Advances in Building Energy Research 7(2), 244-253

Gaitani, N., Michalakakou, G., Santamouris, M., (2007) On the use of bioclimatic architecture principles in order to improve thermal comfort conditions in outdoor spaces. Building and Environment 42 (1), 317– 324.

George, G., Vishnu, V.S., Reddy, M.L.P. (2011). The synthesis, characterization and optical properties of silicon and praseodymium doped Y6MoO12 compounds: Environmentally benign inorganic pigments with high NIR reflectance. Dyes and Pigments, 88(1), 109-115.

Green Roofs: http://www.greenroofs.com/projects/plist.php

Huang, J., H. Akbari, and H. Taha. (1990). The Wind-Shielding and Shading Effects of Trees on Residential Heating and Cooling Requirements. ASHRAE Winter Meeting, American Society of Heating, Refrigerating and Air-Conditioning Engineers. Atlanta, Georgia.

Julia, E., Santamouris, M., Dimoudi, A., (2009) Monitoring the effect of urban green areas on the heat island in Athens. Environmental Monitoring and Assessment 156 (1–4), 275–292.

Konopacki, S.J., Akbari H., Pomerantz M., Gabersek, S., and Gartland, L.M. (1997). Cooling Energy Savings Potential of Light-Colored Roofs for Residential and Commercial Buildings in 11 US Metropolitan Areas. Lawrence Berkeley National Laboratory Report LBNL-39433, Berkeley, CA.

Kurn, D., S. Bretz, B. Huang, and H. Akbari. (1994). The Potential for Reducing Urban Air Temperatures and Energy Consumption through Vegetative Cooling (PDF) (31 pp, 1.76MB). ACEEE Summer Study on Energy Efficiency in Buildings, American Council for an Energy Efficient Economy. Pacific Grove, California.

Kuttler, W., 2011. Climate change in urban areas – Part 2, measures.

Kuttler Environmental Sciences Europe, 21–23.Levinson, R., Berdahl, P., Berhe, A., and Akbari, H. (2005). Effects of soiling and cleaning on the reflectance and solar heat gain of a light-colored roofing membrane. Atmospheric Environment, 39, 7807-7824. Also published as Lawrence Berkeley National Laboratory Report LBNL-57555, Berkeley, CA.

Levinson R., Akbari H., Reilly J.C. (2007). Cooler tile-roofed buildings with near-infrared-reflective non-white coatings, Building and Environment, 42 (7) 2591-2605, DOI:10.1016/j.buildenv.2006.06.005.

Levinson, R., and Akbari, H. (2010). Potential benefits of cool roofs on commercial buildings: conserving energy, saving money, and reducing emission of greenhouse gases and air pollutants. Energy Efficiency, 3(1), 53-109.

Liu, K. and B. Baskaran. (2003). Thermal Performance of Green Roofs Through Field Evaluation (PDF) (11 pp, 401K) National Research Council of Canada. Report No. NRCC-46412. http://archive.nrc-cnrc.gc.ca/obj/irc/doc/pubs/nrcc46412/nrcc46412.pdf

Luke Howard, 1818-20) The climate of London, deduced from Meteorological observations, made at different places in the neighbourhood of the metropolis, 2 vol., London,

Mihalakakou, G., Santamouris, M., Asimakopoulos, D., (1994) On the use of ground for heat dissipation. Journal of Energy 19 (1), 17–25.

Oke, T.R., Johnson, D.G., Steyn, D.G., Watson, I.D., (1991) Simulation of surface urban heat island under 'ideal' conditions at night – Part 2: diagnosis and causation. Boundary-Layer Meteorology 56, 339–358.

Oke, T.R. (1982). The Energetic Basis of the Urban Heat Island. Quarterly Journal of the Royal Meteorological Society. 108, 1-24.

Oke, T.R. (1997). Urban Climates and Global Environmental Change. In: Thompson, R.D. and A. Perry (eds.) Applied Climatology: Principles & Practices. New York, NY: Rout ledge. pp. 273-287.

Oke. T.R. (1987). Boundary Layer Climates. New York, Routledge.

Pisello, A.L., Cotana, F., Nicolini, A., Brinchi, L. (2013). Development of Clay Tile Coatings for Steep-Sloped Cool Roofs. Energies 6, 3637-3653

Rosenfeld A. H., Akbari H., Bretz S., Fishman B.L., Kurn D.M., Sailor D., Taha H. (1995) Mitigation of urban heat island: materials, utility programs, updates, Energy and Buildings, 22, 255-265.

Roth, M., T. R. Oke, and W. J. Emery. (1989). Satellite-derived Urban Heat Islands from Three Coastal Cities and the Utilization of Such Data in Urban Climatology. Int. J. Remote Sensing. 10, 1699-1720

Sailor D. J., Fan H., (2002) Modeling the diurnal variability of effective albedo for cities, Atmospheric Environment 36(4), 713-725

Santamouris, M. (2012). Cooling the cities – A review of reflective and green roof mitigation technologies to fight heat island and improve comfort in urban environments. Solar Energy, In press (2012).doi:10.1016/j.solener.2012.07.003.

Sleiman, M., Kirchstetter, T., Berdahl, P., Gilbert, H., Francois, D., Spears, M., Levinson, R., Destaillats, H., and Akbari, H.(2010).Development of an accelerated soiling method that mimics natural exposure of roofing materials.Proceedings of the 3rd International Passive and Low Energy Cooling for the Built Environment (Palenc 2010), September 29 to October 1, 2010, Rhodes, Greece, pp. 19-21.

Synnefa A., Santamouris M., Apostolakis K.,(2007) On the development, optical properties and thermal performance of cool colored coatings for the urban environment, Solar Energy, 81(4), 488-497, 10.1016/j.solener.2006.08.005.

Synnefa A., Santamouris M., Livada I., (2006) A study of the thermal performance of reflective coatings for the urban environment, Solar Energy, 80(8), 968-981, 10.1016/j.solener.2005.08.005.

Voogt, J.A. and T.R. Oke. (2003). Thermal Remote Sensing of Urban Areas. Remote Sensing of Environment. 86. (Special issue on Urban Areas): 370-384.

Pisello, A.L., Cotana, F., Nicolini, A., Brinchi, L. (2013). Development of Clay Tile Coatings for Steep-Sloped Cool Roofs. Energies 6, 3637-3653

Zhao, M., Han, A., Ye, M., Wu, T. (2013). Preparation and characterization of Fe3+ doped Y2Ce2O7 pigments with high near-infrared reflectance. Solar Energy, 97, 350-35

CHAPTER 3
BUILDING MATERIALS FOR COOL ROOF APPLICATIONS

In chapter 2, building materials suitable for cool roofing are exposed. Among all these materials it was evident how inorganic based ones were characterized by interesting durability properties. In this work our attention was focused, in particular, on clay based materials with a special regard to ceramic tiles and clay roof tiles. Another building product, even if not properly ceramic based, was considered, since mineral grit, on asphalt shingle, is usually covered with a ceramic glaze applied through a rotary kiln. In this chapter the three building product studied will be briefly illustrated in order to provide an easy comprehension of the different experimental step.

Ceramic tiles

The cool roof market is nowadays dominated by organic membranes and coatings, which can reach very high values of solar reflectance (ρ_{sol}=0.80÷0.90 for white products). The solar reflectivity spectrum of organic coatings, however, often shows a sharp decrease as one moves from the visible range in the near infrared (NIR). On the other hand, white ceramic tiles are generally characterized by slightly lower solar reflectance values (ρ_{sol}=0.60÷0.80) (Ferrari et al, 2013), but their reflectivity spectrum, in contrast to organic materials and coatings, can show a high and nearly flat trend in the NIR (Libbra et al, 2011a; Libbra et al, 2011b). When a given reflectivity spectrum in the visible range is required to obtain a certain non-white color, a true cool color product can be achieved by maximizing the reflectivity in the NIR and, in this context, ceramic tiles can provide an interesting alternative or complement to organic materials and coatings.

A traditional porcelain stoneware tile is made by at least three different layers: a ceramic support, a thin engobe application and one or more glaze applications. This is the same structure of advanced cool color products (Levinson et al, 2007), consisting of a support material, a high reflectance basecoat deposited onto the support surface, and an IR-transparent topcoat placed onto the basecoat. Solar radiation is allowed to pass through the topcoat, so that infrared radiation is reflected from the basecoat, crosses again the topcoat and eventually leaves the material, whereas the optical color is obtained by the visible reflection/absorption spectrum of selective pigments embedded in the topcoat (Levinson et al, 2005; Thongkanluang et al, 2011).

In this work we focused on a completely new product, and not just a cool coating, in which we considered as support the traditional ceramic body, the basecoat is represented by the engobe and the NIR-transparent topcoat is the glaze, and all components are managed in the framework of a conventional production process of the ceramic industry.

The engobe is a very important step in the tile production process because this thin layer between the ceramic support and the glaze prevents reactions between chromophore impurities, ensures a good opacity and a high whiteness degree, improves the dilatometric match between the support and the glaze. It also improves impermeability and, consequently, it prevents staining due to colored solutions that may come in contact with the fired tiles. It is made by several raw materials such as ball-clay, which provides plasticity, various frits (30-40%) helping the glassy phase formation and, sometimes, feldspar and quartz, which allow control of mixture melting point and thermal expansion coefficient. In order to improve the engobe whiteness, other raw materials can be added.

Glazes are vitreous coatings applied onto the exposed tile surface in order to make it waterproof, tougher and more resistant to dirt, as well as to improve its aesthetic aspect. Glaze composition is extremely variable and complex, consisting mainly of frits and other additional components in variable percentages such as kaolin, ball-clay, bentonite, opacifiers, pigments, or additives to control the glaze rheology during application (Applied Ceramic Technology).

Clay Roof Tiles

Among ceramic products, clay roof tiles were previously studied (Kültür et al, 2012; Libbra et al, 2011, Libbra et al, 2012) concerning both natural ageing and organic coatings formulation, and one of the main faced issues was related to the relatively unnatural aspect given by the deposition of paints on roof tiles, if compared with the natural terracotta aspect of these covering materials.

Clay roof tiles is one of the most durable roofing product. They are made by clay minerals (38-50%), quartz-feldspatic inert (36-50%) and carbonates (around 8-18%). Due to the low cost of the final product, the raw materials used in order to produce it has to be as more economic as the can. Usually economic raw materials are characterized by the presence of oxides which affect the color of the final manufact (iron oxides let the tile become reddish) and may create sulphates, in particular if considerably high percentages of carbonates are involved (sulphates and sulphides). It is important to observe how quartz feldspatic raw material, in this case, acts like inert while in ceramic tiles acts like fondent. This can be explained observing the firing temperature of clay roof tiles. Usually clay roof tiles are, in fact, fired with heating treatment reaching maximum of 950 °C while ceramic tiles reach temperatures up to 1200 °C. In order to modify the surface color. can be added, once the mixture was pressed into molds, and before firing process, engobes, glazes or cromophore element soluble salts.

In this case the engobe is made by a thin layer of partially dried clay which could present a lower amount of undesired minerals. The glaze, as well as glaze for ceramics, is a vitreous layer, which should reduce the water absorbance of the tile increasing also the resistance to weathering agents and mechanical properties.

The presence of soluble salts made by cromophore elements is used as finishing process before the firing cycle in order to improve the aesthetical aspect of the final product.

Recently, in particular in Mediterranean area and in Italy, roof tile industry developed a trend concerning the decoration of clay roof tiles surface. Most of the roofs in the Mediterranean area are characterized by the presence of moss and lichens because of their porosity where moss seeds can be blown by wind or carried by birds, and, moreover, due to their high durability, most

of the roofs in Mediterranean are tiled on ancient building. In order to decrease the impact of new roof in a city skyline made of "aged" roofs, and to improve the integration of new clay roof tiles as replacement of broken ones, a new product simulating with inorganic engobes and glazes the surface of aged tiles, is designed.

Asphalt Shingles

Among the studied materials, asphalt shingles are the most recent, since their use started at the beginning of 1900s. They are characterized by formerly living or inert matrix embedded into a bitumen/asphalt layer to improve their impermeability (figure 3.1). In order to protect the bitumen layer from the solar radiation, avoiding the reaction with UV radiation, which causes bitumen deterioration, asphalt shingles are covered by mineral or ceramic grit (Table 3.1).

Finally the backside of each shingle is covered by sand, talc or mica in order to avoid the adhesion of the piled tiles during storage operations. (EPA, 2010)

Table 3.1 – Asphalt shingle composition (CIWBM, 2007)

Component	Organic shingles (wt %)	Fiberglass shingles (wt %)
Asphalt cement	30-36	19-22
Felt	2-15	2-15
Mineral granules/aggregate	20-38	20-30
Mineral filler/stabilizer	8-40	8-40

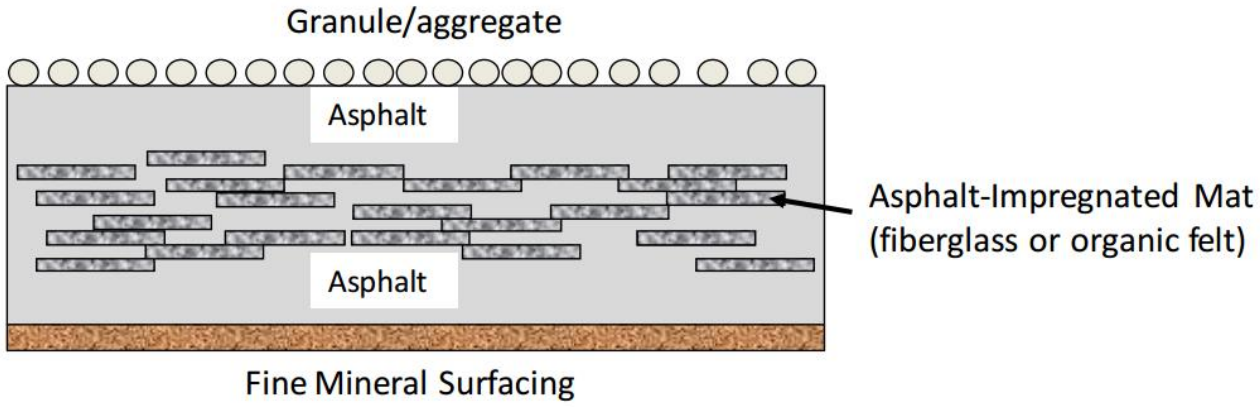

Figure 3.1 – Asphalt shingle composition (Kingcounty)

Considering the wide application of asphalt shingles not only in the US but also in the northern part of Europe, the production of this building product is related to some specifications developed by American Society of Testing Materials. In particular the production of asphalt shingles made with an organic felt based mat surfaced with mineral granules is regulated by ASTM D 225-07 (ASTM, 2007) while asphalt shingles made by a fiberglass felt mat and surfaced with mineral granules is regulated by ASTM D3462 (ASTM, 2010)

In order to improve the final aspect of the asphalt shingle mineral grit is often painted with field-applied coatings or glazed with ceramic glazes applied through a rotary kiln. These operations, besides the enhancement of aesthetical properties, can improve also other features such as the resistance to moss and algae through the application of Copper or Silver or the improvement of the solar reflectance of the substrate (basalts presents ρ_{sol}= 0.18) reaching interesting values for cool roofing application.

Chapter references

ASTM Standard D225, 2007, " Standard Specification for Asphalt Shingles (Organic Felt) Surfaced With Mineral Granules (Withdrawn 2012)" ASTM International, West Conshohocken, PA, 2003, DOI: 10.1520/D0225-07, www.astm.org.

ASTM Standard D3462 / D3462M - 10a, 2010, " Standard Specification for Asphalt Shingles Made from Glass Felt and Surfaced with Mineral Granules" ASTM International, West Conshohocken, PA, 2003, DOI: 10.1520/D3462_D3462M-10A, www.astm.org

Applied Ceramic Technology (2nd edition), vol. 1La Mandragola, Bologna, Italy (2005), pp. 139–174

CIWMB (2007). "Asphalt Roofing Shingles Recycling: Introduction." <http://www.ciwmb.ca.gov/ConDemo/Shingles/> (Accessed 20th January 2014).
G.P. Emiliani, F. Corbara, Tecnologia ceramic: le tipologie, Gruppo editorial Faenza Editrice, 2000, ISBN: 8881380439

EPA, 2010, http://www.epa.gov/climatechange/wycd/waste/downloads/asphalt-shingles10-28-10.pdf (Accessed 20th January 2014).

Ferrari C., Libbra A., Muscio A., Siligardi C.,(2013) Design of ceramic tiles with high solar reflectance through the development of a functional engobe, Ceramics International, 39(8) 9583-9590

S. Kültür, N. Türkeri, (2012) Assessment of long term solar reflectance performance of roof coverings measured in laboratory and in field, Building and Environment, 48, 164-172

Levinson R., Berdahl P., Akbari H., Miller W., Joedicke I., Reilly J., Suzuki Y., Vondran M. (2007) Methods of Creating Solar-Reflective Nonwhite Surfaces and their Application to Residential Roofing Materials, Solar Energy Materials & Solar Cells, 91(4), 304-314.

Levinson R., Berdahl P., Akbari H.(2005) Solar Spectral Optical Properties of Pigments – Part II: Survey of Common Colorants, Solar Energy Materials & Solar Cells, 89(4) 351-389.

Libbra A., Muscio A., Siligardi C., Tartarini P. (2011) Assessment and Improvement of the Performance of Anti solar Surfaces and Coatings, Progress in Organic Coatings, 72(1-2), 73-80.

Libbra A., Tarozzi L., Muscio A., Corticelli M.A. (2011) Spectral Response Data for Development of Cool Coloured Tile Coverings, Optics and Laser Technology, 43(2), 394-400.

Thongkanluang T., Limsuwan P., Rakkwamsuk P. (2011) Preparation and Application of High Near-Infrared Reflective Green Pigment for Ceramic Tile Roofs, Int. J. Applied Ceramic Technology, 8(6), 1451-1458.

Kingcounty - http://your.kingcounty.gov/solidwaste/linkup/documents/shingles-CMRA-environmental-issues.pdf (Accessed 20th January 2014).

CHAPTER 4
CHARACTERIZATION TECHNIQUES

Structural characterization

In order to characterize not only the structure but also the thermo-physical properties of the samples involved in this study, different experimental techniques have been employed.

Mineralogical analysis were performed through a X-ray diffractometer X'pert PRO (PANalytical, Almelo, The Netherlands) employing a Cu-Kαradiation. Data were collected in the 2θ range of 5°-80° with a step of 0.017° and a time interval of 19.68 s (X'Celerator detector). For the X-ray diffraction analysis both Bracket and MPSS setup were adopted. The powders analyzed were crushed in a mortar to a fine powder while the massive glazed samples (except for ageing study) were blown with canned compressed air.

Microstructural analysis have been carried out with scanning electron microscope, SEM (SEM XL-30 and ESEM Quanta 200, FEI Co., Eindhoven, The Netherland). Moreover, a local semi-quantitative chemical analysis was performed by X-ray energy dispersion spectroscopy, EDS (Inca, Oxford Instruments, UK). The ESEM was operated in high vacuum mode. Cross section samples were cut using a diamond cutter and then ground by SiC abrasive paper, followed by polishing with diamond paste (3 and 1 μm) and lapping oil.

In addition to these characterizations, in chapter 5 roughness analysis were approached through a roughness tester (Diavite DH-5 V1.50) equipped with a tracer (Diavite 5478). Moreover Hunter's parameters L*a*b*, an objective and numeric way to identify colors, were measured with a X-Rite colorimeter SP-60.

Solar reflectance characterization

In order to investigate Solar Reflectance of the samples two different strategies were adopted (Levinson et al, 2010 a, 2010 b) which accomplish to ASTM E903 and ASTM C1549. Both techniques are based on the comparison of the samples properties with a completely absorbing standard (black body) and a completely reflective sample (usually a Spectralon sample is used). Calibration procedure is required before each test session.

ASTM E903 measurement are performed with two Uv-Vis-NiR Spectrophotometer: V-670 (Jasco, Easton, Maryland) and Lambda 1050 (Perkin Elmer, Massachussets), while ASTM C1549 measurement are carried out with a Solar Spectrum Reflectometer (Devices and Services, Dallas, Texas).

Both of these techniques are nondestructive on the samples but, as the ASTM C1549 do not have any extension limitation for the surface to be analyze (CRRC-1 Test Method), samples should be cut (6x6 cm) in order to be placed into the measurement chamber of the spectrophotometer.

Solar Spectrum Reflectometer

SSR assumes that the diffuse directional spectral reflectance of a surface is equal to its directional-hemispherical spectral reflectance using a diffuse light to illuminate a surface and then measuring the amount of light reflected at near-normal incidence. The diffuse light source is represented by a chamber painted with BaSO4, a white high reflective paint where a tungsten lamp is placed in, protected by a baffle.

There are four physical detector (iR, Red, Blu, UV @ ~ 3125 K) and two virtual detector (iR and red @ ~ 2300 K), made by silicon or lead sulfide covered with spectrally selective light filters, which receive the amount of light which is reflected by the surface through a collimating tube which is angled 20° from the surface's normal.

The sample is placed facing on a 2.5 cm diameter aperture and the instrument registers the reflectance after the selection of the irradiance spectrum. In SSR v.6.0 11 irradiance spectra

are available and, in addition, the amount of light reflected reached by each physical and virtual detector can be obtained. (Levinson et al. 2010, b)

Sample preparation

The sample surface should be plain and smooth in order to accomplish to the principle illustrated above. No particular treatments of the surface are required in order to carry out the analysis. If the sample presents a slight curvature or a rough surface a ring-shaped white foam sheet thin layer can be added to the aperture.

UV-Vis-NiR Spectrophotometer

To perform this measurement method, a flat surface, not larger than 6x6 cm, is illuminated by a monochromatic light at near normal incidence ($\theta \approx 8°$), the reflected light is collected through a 150 mm integrating sphere and measured. In order to cover the whole range of wavelength reaching the earth (300-2500 nm) the measurements were carried out with variable step size. A step size of 5nm is sufficient in order to capture spectral details of most surfaces. As the output for SSR measurements is directly the solar reflectance of the sample analyzed, the output obtained by the Spectrophotometer analysis is the spectral reflectivity of the sample. Solar reflectance can be obtained through the mean of spectral reflectivity weighted by solar spectral irradiance.

Sample preparation

Usually samples can be put in the measurement chamber without any preparation, but since our samples present not a regular shape, a white foam sheet thin layer frame should be attached with adhesive tape to the measurement aperture. If the sample is bigger than the measurement aperture the analysis should be carried out in a dark room and the spectrophotometer should be covered with a thick black tissue panel in order to avoid any interference between the room and the spectrophotometer.

Irradiance spectrum

The solar reflectance value ρsol was determined through the integration over the range from 300 to 2500 nm the measured spectral reflectivity ρλ (ratio of reflected part and total amount of incident radiation at the considered wavelength λ), weighted by the standard spectral irradiance of the sun at the earth surface, Isol,λ [Wm−2 nm−1]

$$\rho_{sol} = \frac{\int_{300}^{2500} \rho_{\lambda} I_{sol,\lambda} d\lambda}{\int_{300}^{2500} I_{sol,\lambda} d\lambda}$$

Actually, the most widely used irradiance spectrum in solar reflectance measurements is represented by E891BN (ASTM E891). This spectrum refers to Hazy Sky, Air Mass 1.5 Beam Normal conditions, but two irradiance spectra suits in a better way the peak solar heat gain for low-sloped or horizontal surfaces typical of mainland USA or Southern Europe. These two spectra are AM1GH (Clear Sky, Air Mass 1, Global Horizontal) (Levinson, 2010a) and the spectrum proposed by EN410 (EN410:2011) (Clear Sky, Air Mass 1, Global Horizontal). Average conditions can be modeled by the irradiance spectra proposed by G173DC and G173GT (ASTM G173). (Ferrari et al, 2013).

In this study, for both methodologies, AM1GH was selected as the irradiance spectrum to calculate Solar Reflectance.

Chapter references

ASTM C1549. (2009). ASTM C1549-09 – standard test method for determination of solar reflectance near ambient temperature using a portable solar reflectometer. West Conshohocken, PA: ASTM International.

ASTM E891. (1992). ASTM E891-87(1992) – tables for terrestrial direct normal solar spectral irradiance for air mass 1.5. West Conshohocken, PA: ASTM International.

ASTM (1996). ASTM E 903-96 – Standard test method for solar absorptance, reflectance, and transmittance of materials using integrating spheres. Standard of the American Society for Testing and Materials.

ASTM G173. (2003). ASTM G173-03 – standard tables for reference solar spectral irradiances: Direct normal and hemispherical on 37° tilted surface. West Conshohocken, PA: ASTM International.

Cool roof Rating Council. (2013) Product rating program manual (CRRC-1). Retrieved from www.coolroofs.org/ documents/CRRC-1-2012_Standard.pdf

Devices & Services Co. TN 09-1 Solar Spectrum Reflectometer Version 6.0

EN 410. (2011). EN 410:2011 – glass in building – determination of luminous and solar characteristics of glazing. Brussels: European Committee for Standardization.

Ferrari C.,. Libbra A., Muscio A., Siligardi C., (2013) Influence of the irradiance spectrum on solar reflectance measurements, Advances in Building Energy Research 7(2), 244-253

Levinson R., Akbari H., Berdahl P. (2010a), Measuring solar reflectance—Part I: Defining a metric that accurately predicts solar heat gain, Solar Energy, 84(9), 1717-1744

Levinson R., Akbari H., Berdahl P. (2010b), Measuring solar reflectance—Part II: Review of practical methods, Solar Energy, 84(9), 1745-1759,

CHAPTER 5
FORMULATION OF A NEW COOL COLORED TILE

Brief introduction

Limiting summer overheating of buildings and mitigating the urban heat island effect are the principles behind cool roofs (Akbbari et al, 2012, Santamouris, 2012), roofing solutions with high capacity to reflect incident solar radiation. Among direct benefits of lower building overheating there are lower costs for air conditioning and greater comfort inside buildings, as well as lower structural stress, chemical or physical material degradation and roof maintenance cost. Among indirect benefits, coming from mitigation of the urban heat island effect, there are smog reduction, public health and also energy benefits such as peak energy saving and grid stability (Akbari et al, 2012, Santamouris, 2012, Taha et al, 1998, Akbari et al 2001, Shi et al, 2011, De Brito Filho et al, 2011, Synnefa et al, 2012).

Roofing solutions with high capacity to reflect incident solar radiation, the so-called cool roofs, can provide an effective answer to summer overheating of either individual buildings or whole urban areas. Nowadays, organic membranes and coatings mainly represent commercial cool roof products, but ceramic tiles can offer an interesting alternative or complement in view of their high durability. This chapter presents the procedure through which a traditional white engobe and a glazed tile with high solar reflectance are developed by the introduction of suitable raw materials and pigments, in the perspective of production by commonly used industrial processes. The solar performances was checked for both light and dark supports and for different engobe thicknesses up to 250 μm; the estimated solar reflectance values were correlated with surface properties such as (microstructure, mineralogical composition, and roughness). The best performing engobe, applied as a 200 μm layer, improved solar reflectance of the sample up to 0.90. Three different glazes without pigments were then applied on engobed samples and were found to slightly affect the reflectance and improve the resistance to mechanical stress or

weathering. A white gloss glaze was found to be the best performing one in terms of solar reflectance. The cool roof concept has also evolved into cool colors (Synnefa te al, 2012, Synnefa et al., 2007), coating solutions which combine aesthetic requirements with material functionality.

Aim of the project

The main aim of this work is to design an inorganic engobe with high solar reflectance, as well as to investigate the glaze influence on the reflectance.

A white cool roof material can be obtained in case of white engobe and non-pigmented glaze, whereas cool color ceramic coatings can be derived by adding proper pigments with selective absorption in the visible-NIR spectrum to the glaze. With regard to the industrial process, the study is carried out using the same production methods and the same average composition of traditional porcelain stoneware tiles, products of Italian manufacture worldwide appreciated for their special features, first of all for resistance to sun, rain and frost. At this first stage of the work, the attention is focused only on white pigments, in order to obtain the highest reflectivity throughout the solar spectrum. Among the different white pigments currently in use in the ceramic industry, two ones have been selected, alternative but very different from each other, to be included in the formulation of an engobe with high and flat reflectivity spectrum. Thereafter, three different types of glaze were applied onto a tile support coated with the best performing engobe, in order to check how the glaze itself affects solar reflectance. The three glazes are characterized by three different finishing: transparent, white matt and white gloss. The second stage of this work started from the substrate-engobe system, which was completed with a colored glaze. In this part, starting from the most performing engobe obtained in the first stage, four different glazes were formulated and each one was added with eight different pigments in order to study the solar reflectance response to the colored surface. Since cool surfaces are mainly applied as roofing system, therefore, the third stage analyze three different glazes were formulated on purpose for clay roof tiles, were added with the pigments used in the second stage. These glazes were finally applied on a red substrate simulating clay roof tiles in order to obtain a new cool colored glazed clay roof tile.

Experimental approach: engobe

The engobes were prepared according to formulations detailed in Tab. 5.1. Two sets of formulations were considered, the first set made of samples characterized by the presence of $ZrSiO_4$ (64.00% $ZrSiO_4$+HfO_2, 35.2% SiO_2, 0.40% Al_2O_3, 0.25% TiO_2, 0.15% Fe_2O_3) while TiO_2 (92.7% TiO_2, 0.73% SiO_2, 0.40% Al_2O_3, 0.98% Fe_2O_3, 5.19% others) is the pigment introduced into the second set of samples. In the second set, $ZrSiO_4$ is replaced by the same number of moles of TiO_2. The two selected pigments, $ZrSiO_4$ and TiO_2, are commercial and relatively cheap products widely used in traditional ceramic formulations. The main difference between them is that both ones are characterized by high refraction index n, but the n value of $ZrSiO_4$ is around 1.94 while the n value of TiO_2 is around 2.52 (I.Cer.S., 2003).

To ensure that the grain size distribution of the two pigments is the same and it does not affect the optical properties of the raw material, a laser grain size analysis was performed on both raw materials using a particle size analyzer (Tab. 5.2).

Table 5.1 – Engobes composition (wt%).

	Set 1					Set 2			
Sample	A2	B2	C2	D2	N2	A3	B2	C3	D3
Na feldspar	45	30			30	45	32		
Recycled Glass			30	45				30	43
Nepheline Syenite					15				
Alumina	10	25	25	10	10	9	25	23	10
Quartz	10	15	15	10	10	11.5	16	14	10
Kaolin	10	10	10	10	10	10	10	10	10
$ZrSiO_4$	10	10	10	10	10				
TiO_2						4.4	4.8	4.3	4.1
White clay	15	10	10	15	15	15	15	10	15
Sodium Tripolyphosphate	0.2	0.2	0.2	0.2	0.2	0.2	0.2	0.2	0.2
Carboxymethyl cellulose	0.2	0.2	0.2	0.2	0.2	0.2	0.2	0.2	0.2

Table 5.2 – Pigments granulometric distribution

	D_{10}	D_{50}	D_{90}
$ZrSiO_4$	0.44 μm	1.70 μm	4.76 μm
TiO_2	0.47 μm	2.23 μm	4.49 μm

Sample with label N2 is characterized by the presence of Nepheline Syenite (60.14% SiO_2, 23.5% Al_2O_3, 9.3% Fe_2O_3, 7.06% others) as partial replacement of Na Feldspar (68.9% SiO_2, 19.30% Al_2O_3, 0.02% Fe_2O_3, 0.02% TiO_2, 11.40% others). In both formulation sets, samples with label starting with C or D are characterized by a high amount of recycled glass. Entering in detail, a recycled boric glass made of (in wt%) 73.70% SiO_2, 6.30% Al_2O_3, 0.87% K_2O, 6.62% Na_2O, 1.10% CaO, 10.40% B_2O_3, and 1.01% BaO was used . The granulometric distribution analysis of the glass powder returned an average diameter of 87 μm at D_{90}.

The above described raw materials, selected among the most widely used in the Italian ceramic district according to their optical properties, were mixed with Kaolin (44.10% SiO_2, 31.35% Al_2O_3, 0.12% Fe_2O_3, 0.05% TiO_2, 12.50% others), White clay (52.50% SiO_2, 31.70%

Al_2O_3, 1.00% Fe_2O_3, 1.05% TiO_2, 13.75% others), Alumina (0.01% SiO_2, 99.4% Al_2O_3, 0.01% Fe_2O_3, 0.01% TiO_2, 0.57% others) and Quartz (96.20% SiO_2, 2.40% Al_2O_3, 0.12% Fe_2O_3, 0.05% TiO_2, 1.23% others).

Raw materials were poured in an alumina jar with the addition of 40 wt% of water with respect the studied mix and alumina milling balls having different diameters. After the milling process, the engobes presented a density of 1.53 g/ml. They were subsequently dried and wet sieved using the fraction passing though a 100 μm mesh sieve as a common practice, and then applied in two layers onto the ceramic support by means of an airbrush.

Two different types of tile were used as the ceramic support, shaped 30cm x 30cm, one white ($\square_{sol}$=0.48) and the other one red ($\square_{sol}$=0.37) in order to analyze the effect of the support color. Moreover, two, three and four layers of engobe were applied by an airbrush onto different red tiles, in order to verify the engobe opacity in the diverse conditions. Since the airbrush application is deeply influenced by the manual skill of the operator, the engobe thickness was measured in cross section by means of a SEM and it was quantified in about 200 μm for two airbrush applications (after SEM observation, fig. 5.5), while it increases to about 250 μm with three applications and to about 30 μm with four applications. The sample weight was also checked after every engobe application to verify the amount of engobe applied onto the tiles.

All the samples were fired in an industrial roller kiln at the maximum temperature of 1195°C for 6 min, in a cold to cold cycle which totally lasts 47 min.

The solar properties of all the engobed samples were eventually measured and three different commercial glazes, a transparent one, a commercial white gloss glaze and a commercial white matt glaze, were applied on the two best performing formulations, using either white or red ceramic supports. The investigation was aimed at analyzing the interaction of the glaze with the engobe and at understanding the behavior of the 'cool' engobe-glaze system. The glazes were obtained from different frits to promote the particular features of each glaze, with the addition of kaolin and other raw material to improve rheological behavior.The glazed samples were also fired at the same conditions of unglazed engobed tiles.

Method

X-ray Diffraction (XRD) analysis was conducted using Cu Kα radiation limited to 40 kV and 40 mA and a X'Celerator counter (X'pert PRO, Panalytical) in order to determine the mineralogical phases present in both the glaze or the engobe. XRD spectra were collected on the sample surface with a scanning rate of 0.1°/min for 2θ from 10° to 70°

A SEM analysis was performed by means of a scanning electron microscope (FEI XL-30), in order to investigate the surface of unglazed and glazed samples and study the engobe thickness influence on solar properties. In the thickness investigation, the analyzed samples were cut using a diamond cutter and then ground by SiC abrasive paper, followed by polishing with diamond paste (3 and 1 μm) and lapping oil. The samples were coated with a 10 nm thick gold layer using the sputtering technique.

A UV-Vis-NIR spectrometer (Jasco V-670) with a 150 mm integrating sphere was used to measure the spectral reflectance of each sample, following the ASTM E903 Standard Test Method. More specifically, the solar reflectance value ρ_{sol} of every analyzed surface was calculated by integrating over the range from 300 to 2500 nm the measured spectral reflectivity ρ_λ (defined as the ratio of reflected part and total amount of incident radiation at the considered wavelength λ), weighted by the standard spectral irradiance of the sun at the earth surface, $I_{sol,\lambda}$ [W/(m²×nm)]:

$$\rho_{sol} = \frac{\int_{300}^{2500} \rho_\lambda I_{sol,\lambda} d\lambda}{\int_{300}^{2500} I_{sol,\lambda} d\lambda} \quad (5.1)$$

Surface roughness allows understanding the level of soil resistance of a sample. A rougher surface usually retains more easily the dirt that is deposited on it. This causes a deterioration of optical properties. The surface profile was analyzed with a roughness tester (Diavite DH-5 V1.50 with a DIAVITE 5478 tracer) that records the roughness along a length L (4.8mm), thus providing a profile from which the synthetic parameters that characterize the roughness itself are extracted. The three measured parameters are R_z, R_{max} and R_a. R_z is the distance between two straight lines parallel to the middle line drawn at distances equal to the average of the five highest peaks and the average of the five lowest valleys in the range of the length L. R_{max} is the distance between two lines parallel to the middle line, the first tangential to

the highest peak and the second tangential to the lower valley. R_{max} is therefore the maximum of the profile irregularities. The roughness R_a is a mean roughness value that, however, does not reveal the type of irregularity.

$$R_a = \frac{1}{L}\int_0^L |y| dx \qquad (5.2)$$

Results and discussion

An XRD analysis was performed in order to more accurately classify, in qualitative terms, the mineralogical phases present in the engobes (Table 5.3). The diffraction analysis was performed on the engobed surface of the samples.

Table 5.3 – XRD semi-quantitative analysis of unglazed samples.

	Corundum	Quartz	Albite	Mullite	Cristobalite	Zircon	Rutile	Anatase	Anorthite
B2	**	****	**	**		***			
C2	**	***				***			
D2	*	***				***			
N2	*	****	***	*		***			
B3	**	****	**	*			*		
C3	**	***					*	*	
D3	*	**			*		*	*	

Abundance: ****: dominant (50-100%), ***: abundant (20-50%), **: common (5-20%) , *: present (0-5%)

Among samples in Set 1, crystal structures of sample B2 are formed directly from the raw materials used in the engobe after heat treatment. As it can be seen on the table, during the firing process two new phases, Mullite and α-Cristobalite, formed as a consequence of the heat treatment. The crystalline phases in the sample result from the crystallization of the high percentage of frits introduced in the formulation and the heat treatment of raw materials. Sample C2 is also characterized by the presence of an amount of vitreous phase, given mainly by the 30%wt of frits used into the formulation. An even stronger presence of vitreous phase occurs in sample D2 because of the high percentage of recycled glass employed into the formulation as

replacement of Na Feldspar. Sample N2, instead, is characterized by a degree of crystallinity higher than C2 and D2 highlighted by the well-defined peaks shape. This behavior is comparable to that of sample B2; and is caused by the mineralogical composition of sample N2: the percentage of recycled glass, which was introduced in C2 and D2, is replaced by nepheline syenite and Na-feldspar.

The behavior of samples in Set 2 (i.e. formulations B3, C3, or D3) can generally be assimilated to that of samples in Set 1. The main difference regards the presence of the crystalline phases formed from TiO2 (Anatase and Rutile) in place of that formed from ZrSiO4 (Zircon) in Set 1 samples. More specifically, the XRD analysis shows that the phase forming ZrSiO4 is inert to heat treatment, while TiO2 seems to be more reactive as two distinct crystalline phases are formed in samples C3 and D3 as a result of heat treatment of the engobe. The presence of cristobalite, in the sample D3, let us know that the duration of the firing cycle was not sufficient to conclude the crystallization of quartz considering that the rate of transition from quartz to Cristobalite exceeds the rate of quartz dissolution. (Carty et al, 1998, SIligardi et al, 2014)

Engobed unglazed samples

The morphological study is based on examination of the surface of the samples by SEM. Sample B2 (Fig. 5.1) presents a surface where raw materials seem almost incoherent. It appears that the high refractoriness of the formulation prevents cohesion of powders. Instead, sample C2 presents a surface significantly different. The presence of frit allows the formation of glassy phase binding the crystalline phases and contributing to a more effective consolidation. Sample D2, containing recycled glass as a replacement of Na Feldspar, is characterized by the presence of a glassy phase and presents a smooth surface, in which porosity is absent. In all SEM images of Set 1 samples, one can easily recognize the crystalline phase from $ZrSiO_4$ crystals completely surrounded by glass. Sample N2 presents a surface more similar to that of sample C2 due to the similar amount of the vitreous phase, that, in this case, is formed also thanks to thermal transformation of nepheline. With regard to samples in Set 2, a good overlap with the microstructure of corresponding samples in Set 1 can be observed, in perfect analogy with what occurs in the XRD analysis, and SEM images are therefore omitted.

Glazed samples

Figure 5.2 shows how the surface of sample B2 looks like with the three different glazes (Clockwise: White gloss glaze, transparent glaze, white matt glaze). A very interesting microstructure can also be observed on the surface of sample "B2+white gloss glaze" applied, as $ZrSiO_4$ originates a crystallization with internal acicular (*i.e.* slender needle-like) crystals. As one can see, in "B2+transparent glaze" micrograph, the surface area is flat and smooth, thus allowing a shiny surface. To achieve this effect it is necessary that, at the formation temperature of the coating, the crystalline phases formed during the heating phase melt completely and subsequently do not crystallize during the cooling process.

The last SEM image shows the surface of sample "B2+white matt glaze", where the presence of some crystals can again be observed. The matt effect on the surface depends on the type and quality of crystals in the coating, and the glaze component that originates such structures is nepheline. Generally speaking, a strong difference can be observed in SEM images between the three glaze types.

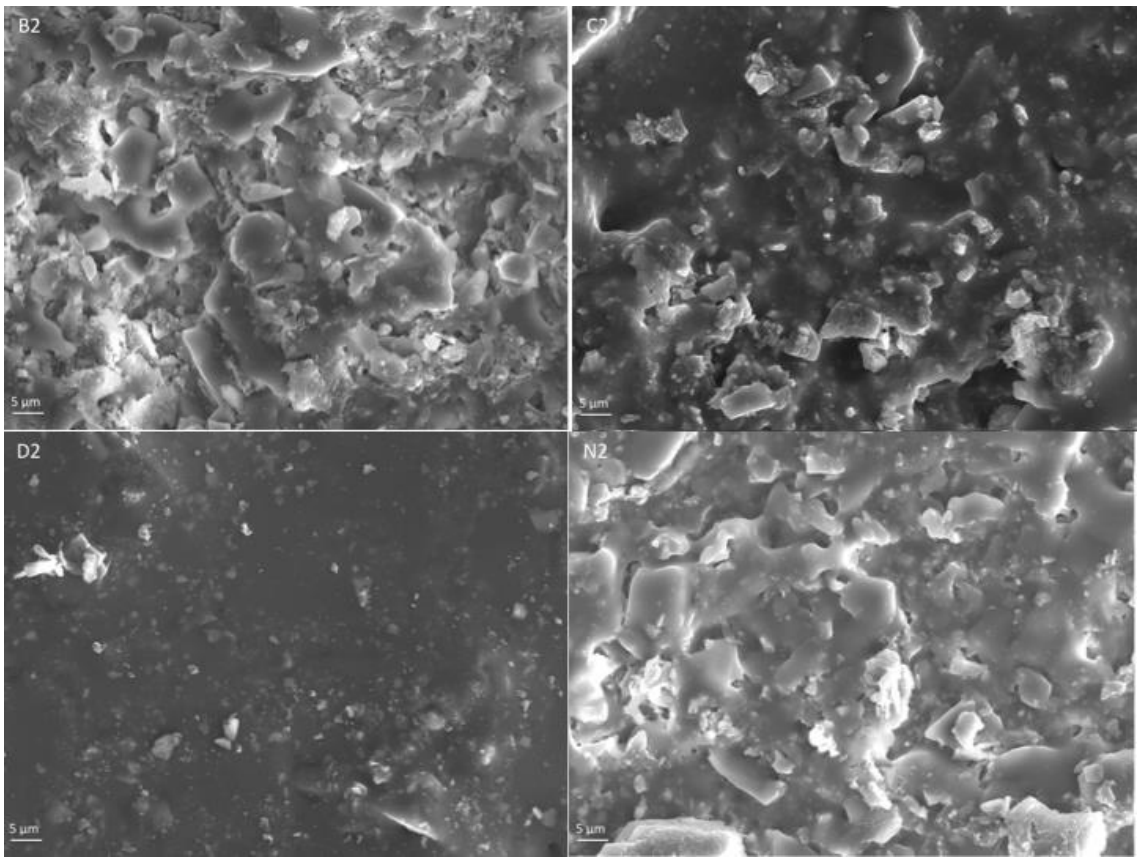

Figure 5.1 – Set 1 unglazed samples surface micrographs SED image 1000x.

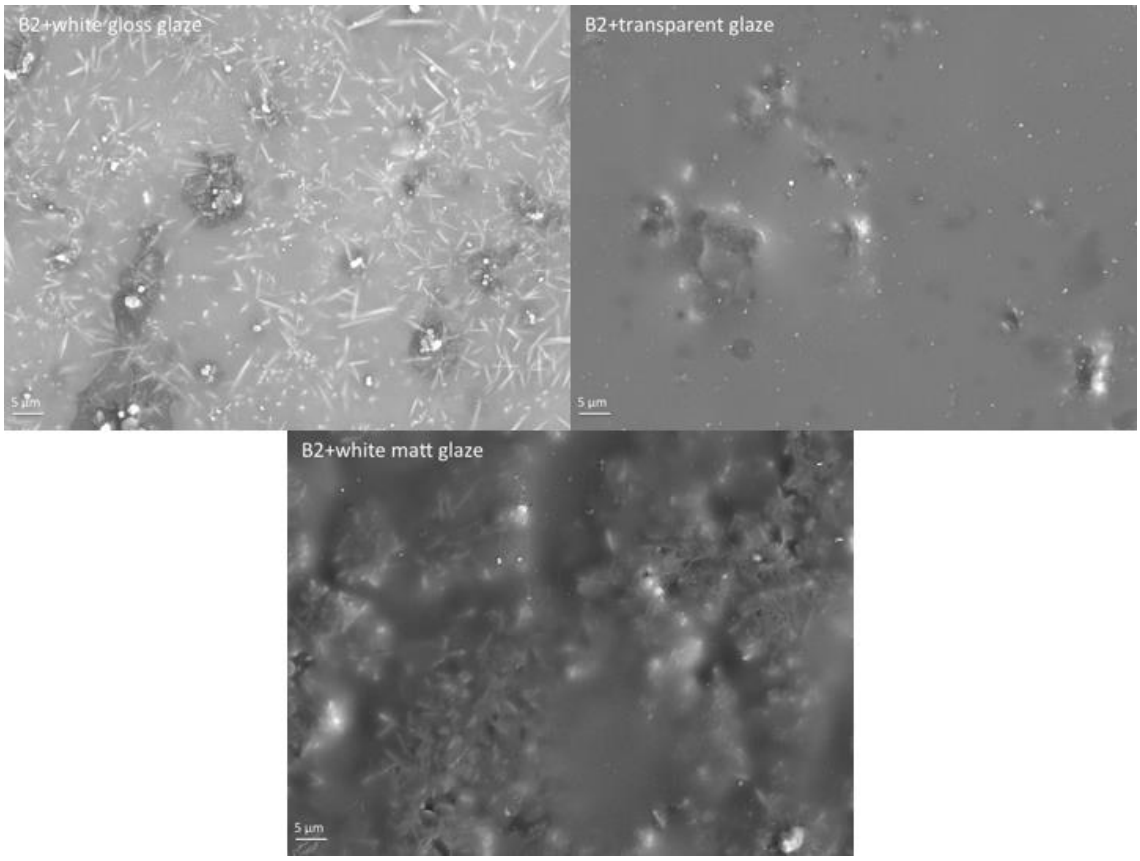

Figure 5.2 – B2 glazed samples surface micrographs SED image 1000x.

Solar reflectance values, measured for both sets of engobed unglazed samples are shown in Tab. 5.4, where one data column is related to red ceramic support and the other one is related to white support. All the samples presents interesting values ranging from 0.63 to 0.90 for the sample on the red support and from 0.66 up to 0.90 for the engobes applied on the white support. Engobes sprayed onto the white support are always better performing than those sprayed onto the red support.

Table 5.4 – Solar reflectance of unglazed and glazed samples in Set 1 and Set 2.

ρ_{sol}	Red support	White support
A2	0.80	0.82
B2	0.90	0.90
C2	0.81	0.82
D2	0.65	0.70
N2	0.79	0.81
A3	0.70	0.72
B3	0.81	0.81
C3	0.73	0.74
D3	0.63	0.66
B2 (transparent)	0.84	0.86
B2 (glossy white)	0.85	0.86
B2 (matt white)	0.84	0.86
C2(transparent)	0.78	0.81
C2 (glossy white)	0.82	0.83
C2 (matt white)	0.80	0.80

In the first sample set (Set 1), samples with engobe composition B2, on both red and white supports, and samples with engobe composition C2, on white support, are the best performing ones, with solar reflectance as high as 0.90 and 0.82, respectively (see Tab. 5.4 and Fig. 5.3).

Samples with engobe formulation A2, on both red and white support, achieve good reflectance values as well, but the formulation was not considered for more investigation as it is vey similar to B2.

Samples with engobe formulation N2 also show good reflectance values, but the added raw material is relatively expensive and, therefore, they have been dropped in favor of cheaper engobes with similar or superior performance. It is interesting to highlight how these spectra does not decrease in Spectral Reflectivity with the increasing of wavelength, if compared with polymeric coatings.

The small variation on each spectrum in the 1900-2500 nm λ is not oustsanding, especially if we consider the small amount of solar spectral irradiance in that range

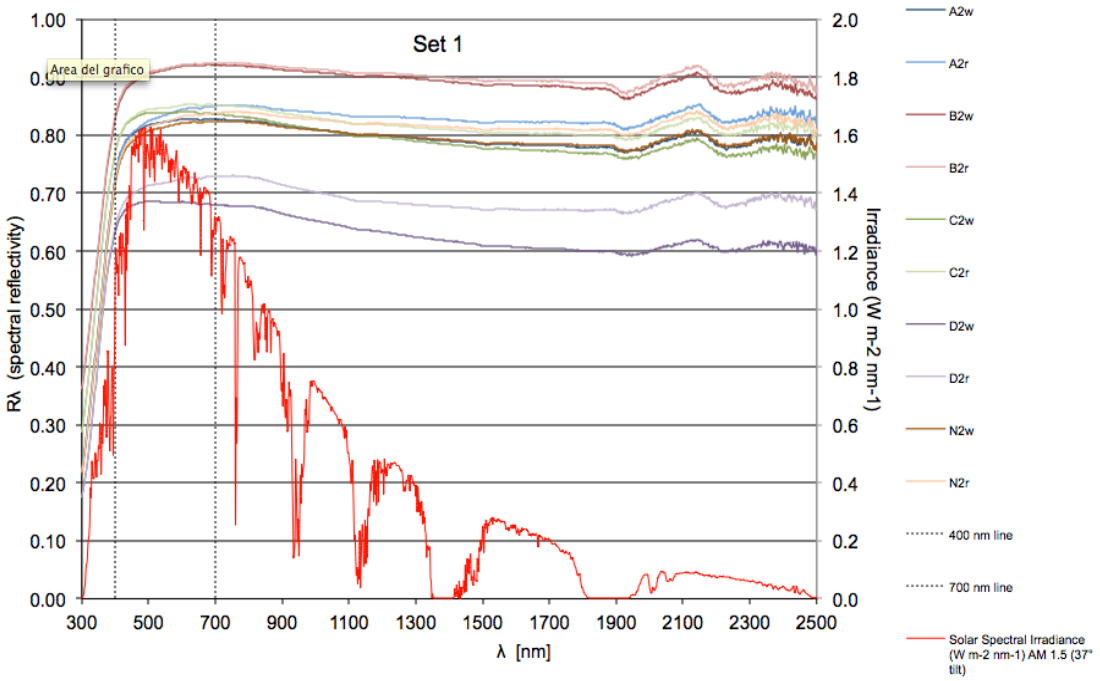

Figure 5.3 – Set 1 UV-Vis-NiR spectra.

In the second sample set (Set 2), a reduction of the solar reflectance values is generally observed between samples with similar compositions (see Tab. 5.4 and Fig. 5.4). The reason is the replacement of $ZrSiO_4$ by TiO_2 and, consequently, of the mineralogical phases added to the formulation. Samples with engobe composition D2 and D3 present the lowest reflectance values, probably because the high glass percentage in the formulation (45%wt) makes the engobes more vitreous.

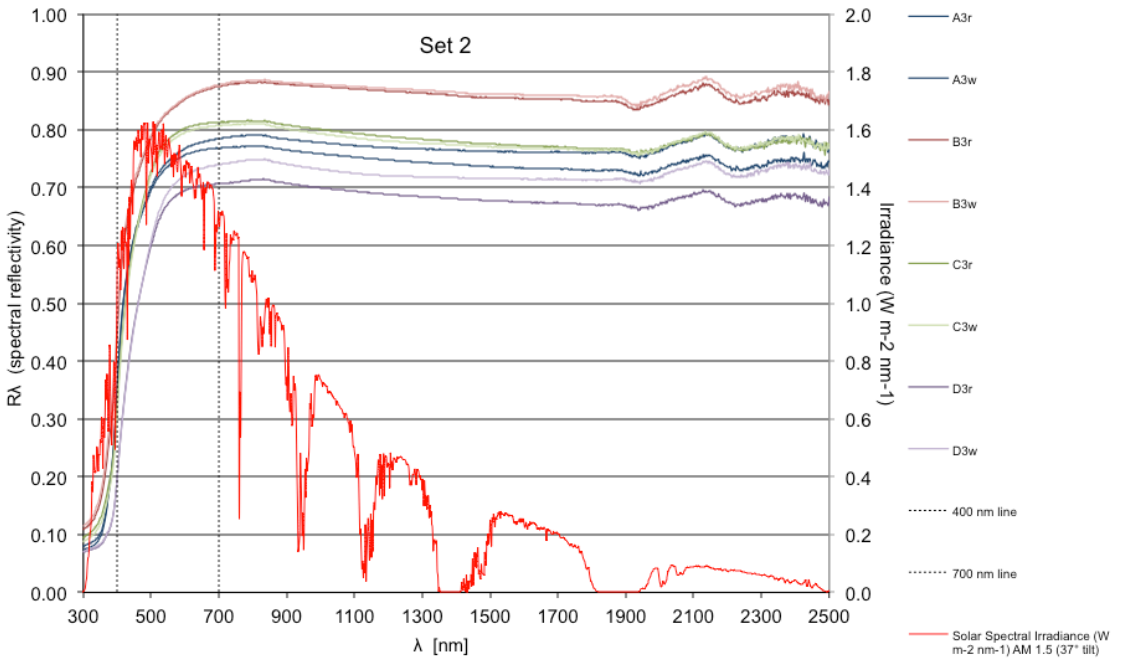

Figure 5.4 – Set 2 UV-Vis-NiR spectra.

In an industrial context it is important to apply an engobe with thickness providing an adequate effect but, at the same time, to achieve a good compromise on the amount of employed material. Therefore, different numbers of layers have been applied onto the same support to investigate the effect of the engobe thickness. Entering in detail, two, three and four layers of engobe were applied onto the red support. The selected formulation was that of sample B2, which reaches the best performance in terms of solar reflectance. The results, summarized in Tab. 5.5, show that just 0.01 increase of solar reflectance is obtained passing from one to two engobe layers, and that the same solar reflectance is practically obtained increasing the number of layers from two to three or four. Generally speaking, the thickness analysis shows that excellent levels of coverage can be reached, and just two engobe layers are enough to mask also a relatively dark (red) support and ensure the best performance.

The application of a vitreous glaze does not allow the samples to obtain the same performance of unglazed coupons, although they can reach very good values of solar reflectance (Tab. 5.3).

Table 5.5 – Solar reflectance of unglazed samples with different engobe thickness.

B2 (Unglazed), Support: layer number	Red ρ_{sol}
1	0.90
2	0.91
3	0.91
4	0.91

In this work, three glaze types where tested: transparent, glossy white, and matt white. Samples with transparent glaze are characterized by a smooth glossy and transparent surface, through which the color of the engobe below can be clearly seen. Samples with glossy white glaze have a smooth surface as well, but the glaze is opaque white and not transparent. Samples with matt white glaze, instead, show a smooth but matt surface, and it is impossible to see the engobe color because of the glaze.

Glazed samples with engobe composition C2, which is characterized by the presence of recycled glass in replacement of Na-feldspar, show solar reflectance values always lower than those for glazed samples with composition B2. For both compositions, a non-negligible drop of solar reflectance is observed with respect to the unglazed samples, showing that the glaze affects performance. Samples with engobe composition B2 and white gloss glaze seems to provide the highest reflectance values, as high as 0.85 on red support and 0.86 on white support. Transparent and white matt glazes, however, yields approximately the same results. As a comparison, white-colored clay or concrete tiles generally provide reflectance values between 0.60 and 0.75 (Sacmi, 2005). Despite the decrease of ρ_{sol}=0.04 glazed samples are characterized by excellent solar performances and moreover enhanced mechanical properties.

The roughness test was carried out on both sample B2 (Fig. 3) and sample C2 (Fig. 4). The extracted profiles are very similar; therefore one can assume that the microscopic surface defects evidenced by SEM analysis do not influence the results. Samples coated with transparent glaze and white gloss glaze have very similar profiles, as seen on the SEM cross section in Fig. 5.

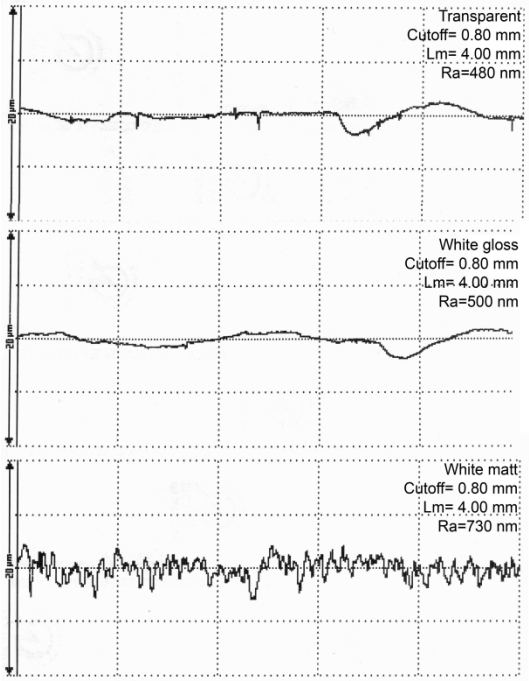

Figure 5.3 - roughness profile of B2 glazed samples.

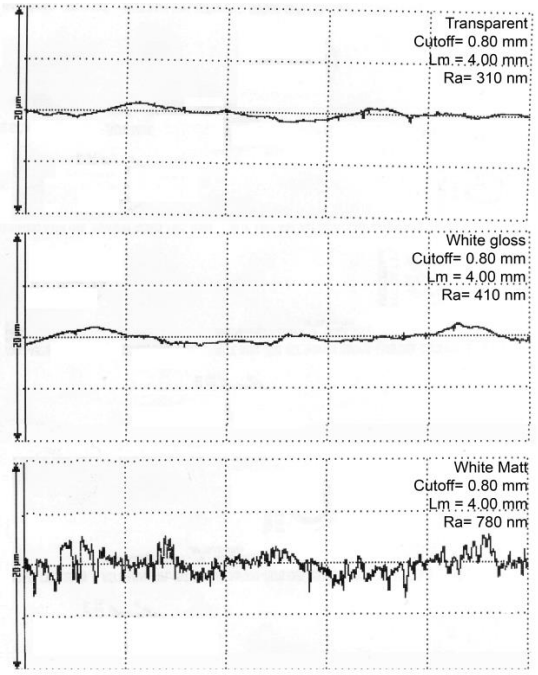

Figure 5.4 - roughness profile of C2 glazed samples.

The values of R_a recorded for those samples are about 0.40 μm and 0.42 μm, respectively, while the roughness of the matt glaze is approximately doubled, with R_a equal to 80 μm. A functional consideration can lead to the conclusion that the surfaces with less dirtying problems are the gloss ones as the pronounced roughness of the matt glaze gives a higher chance of dirt to lock into the surface asperities and reduce solar reflectance. Moreover, the white matt glaze has a

lower soil resistance, and potentially higher maintenance cost. A correlation between surface roughness and solar properties seems also to exist because the white matt glaze has lower reflectivity in comparison with the white gloss glaze or the transparent glaze (Tab. 5.3). It should be noted, however, that samples with similar roughness like those with transparent glaze and glossy white glaze have different reflectance values, therefore it is not possible to directly correlate the roughness to the optical properties without taking into account the mineralogy of engobe and glaze.

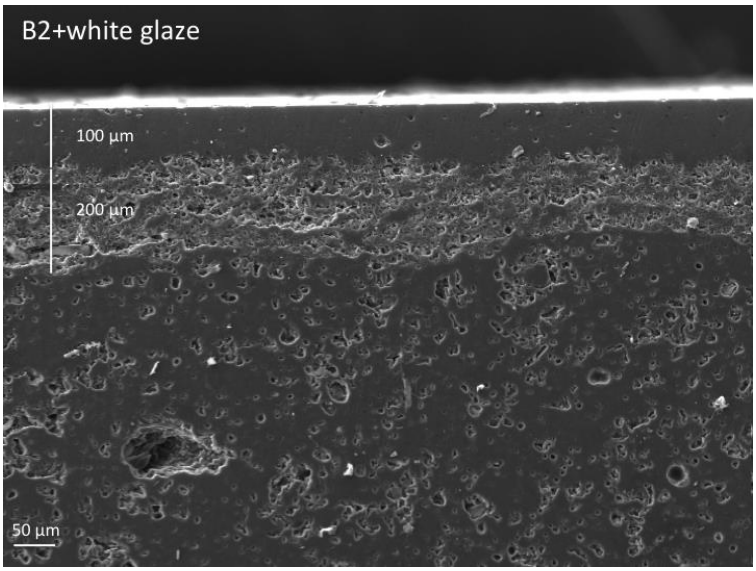

Figure 5.5 - Sample B2 and white gloss glaze cross section SED image 1000x

Experimental approach: ceramic glazes

The second part of this study is focused on the formulation of glazes suitable for tiles and for roof tiles. Four different formulations were prepared for the ceramic substrate each formulation is characterized by the presence of different frits, which develop different surface finishing. In particular transparent (Tab 5.6), matt (Tab 5.7), white gloss (Tab 5.6) and a recycled glass (Tab 5.6) glaze were produced.

Table 5.6 – Formulations of Transparent glaze and recycled glass based glaze

Wt (%)	Transparent Glaze (T)	Recycled glass based glaze (R)
Frit	95.0	23
Kaolin	5.0	17.2
Calcite		15.2
Quartz		9.5
Dolomite		9.0
Ball Clay		11.0
ZnO		1.5
Alumina		4.6
Feldspar		9.0
Carboxymethyl cellulose	0.2	0.2
Sodium Tripolyphosphate	0.3	0.3
Water	45.0	45.0

Table 5.7 – Formulation of White gloss and White matt glaze

Wt (%)	White Matt (M)	White glaze (Wbis)
Frit	47.5	55.0
Kaolin	5.0	12.5
Nepheline Syenite	47.5	11.5
Quartz		16
Ball clay		3
$ZrSiO_4$		2
Carboxymethyl cellulose	0.2	0.2
Sodium Tripolyphosphate	0.3	0.3

The frit in the T glaze is made by 68% SiO_2, 13% CaO, 4.7% Al_2O_3, 1.7% MgO, 2.9% Alkali, 9.7% others, the frits in R glaze are made by 56.8% SiO_2, 7.6% Na_2O, 5.3% B_2O_3, 5.2%

BaO, 4.2% K_2O, 4.1% Al_2O_3, 3.9% SrO and 12.9% others. The frit used in M glaze is made by 48.0% SiO_2, 22.0% CaO, 18.0% Al_2O_3, 9.0% MgO and 3.0% Other, while the frit in the white glaze is composed by 62.8 % SiO_2, 7.9% CaO, 6.8 % ZnO, 6.1 % Al_2O_3, 4.8 ZrO_2, 4.3 %B_2O_3 and 7.3 others.

Raw materials were poured in an alumina jar with 45 wt% of water and alumina grinding balls with different diameters. All the glazes were milled for 30 minutes. Eight different pigments (Tab 5.8) were then embedded at 0.3 wt% into liquid glazes and then 32 pigmented glazes and 4 colorless glazes were applied on porcelain stoneware tiles. Before glaze application on the white support was applied the most performant engobe obtained in the previous part of the study. The glazes applied onto engobed tiles are characterized by 200 μm and 400 μm thickness. The glazed tiles were fired in an industrial roller kiln at the maximum temperature of 1200 °C for 6 min in a cold-to-cold cycle, which totally lasts 40 min.

Solar reflectance of the fired samples was measured and, similarly to what performed into the previous part of the study, a correlation between solar reflectance and surface properties were checked, in addition, were analyzed possible correlations between solar reflectance, the four glazes and the pigments presence.

Table 5.8 – Pigments chemical composition

	Beige	Brown	Brick	Grey	Black 1	Black 2	Green 1	Green 2
ZrO_2	39.5							
Pr_6O_{11}	4.0							
Fe_2O_3	4.0	16.5	30.5	13.5	25.0	31.5		
SiO_2	52.5			67.0				18.0
ZnO		50.2	24.5					
Al_2O_3		22.0	13.5					12.0
Cr_2O_3		11.0	31.5	12.5	25.0	31.5	70.5	70.0
CoO				4.0	25.0	24.0	29.5	
Ni				3.0	25.0			
MnO_2						13.0		

Method

Similarly to what performed in the first stage first of all Solar reflectance measurements were performed in accomplishment to ASTM E903 with a UV-Vis-Nir Spectrophotometer (Jasco V-670) equipped with a 150 nm integrating sphere. The solar reflectance was calculated by integrating over the range from 250 to 2500 nm with a step size of 5nm. On the samples presenting ρ_{NiR} higher than ρ_{Vis} L*a*b* measurements are carried out in order to check if correlations between Hunters parameters and reflectance are present.

Microstructural characterizations were performed by means of Environmental Scanning Electron Microscope (FEI Quanta-200). The surface of the samples was analyzed after being sputtered with a 10nm thick gold layer. Chemical analysis were carried out on the samples through X-EDS Oxford INCA-350

Then mineralogical analysis was conducted using a X'Pert Pro Panalytical diffractometer equipped with X'Celerator detector. CuKα radiation limited to 40kV and 40 mA was used. The spectra were collected with a scanning rate of 0.1 ° min-1 in a 2θ range from 10° up to 80°.

In order to compare the results with the previous obtained, moreover, the surface roughness was measured with a roughness tester (Diavite DH-5 V1.5 with a DIAVITE 5478 tracer). This instrument measured the roughness along a 0.8mm length providing two different parameters. Ra and Rz were calculated for each no pigmented sample, analyzing both the glaze thickness.

Results and discussion

Solar reflectance was measured for each glaze both with and without (TQ) pigments considering both the thickness (tab. 5.9). The values presents a wide range from 0.869 - 0.863 obtained by the white glazes for 200 and 400 μm to 0.161 – 0.137 reached for the Black 2 glazes for 200 and 400 μm.

Table 5.9 – Reflectance data of glazed samples according to ASTM E903 using AM1GH irradiance spectrum

	TQ	Beige	Brick	Black 1	Black2	Brown	Green1	Green 2	Grey
M02	0.853	0.726	0.479	0.208	0.155	0.421	0.381	0.411	0.577
R02	0.843	0.740	0.463	0.199	0.161	0.448	0.338	0.411	0.618
Tr02	0.840	0.753	0.517	0.164	0.197	0.441	0.328	0.444	0.593
W02bis	0.869	0.734	0.495	0.207	0.179	0.473	0.398	0.377	0.576
M04	0.845	0.694	0.437	0.160	0.142	0.380	0.315	0.394	0.531
R04	0.832	0.686	0.441	0.154	0.137	0.386	0.297	0.394	0.561
Tr04	0.840	0.709	0.474	0.142	0.149	0.398	0.301	0.430	0.536
W04bis	0.863	0.703	0.456	0.177	0.171	0.440	0.377	0.372	0.508

All the collected data are plotted into Fig. 5.6. The error bar, in this case, represent the 2σ to better approximate the standard deviation of the samples. In order to facilitate the graph comprehension, each line represent the color to which the data are referred to. Considering the labels of the samples, M stands for matt glaze, R for recycled glass based glaze, Tr for transparent glaze and Wbis for white glossy glaze. The two numbers refers to the thickness: 02 stands for 200 μm while 04 for 400 μm.

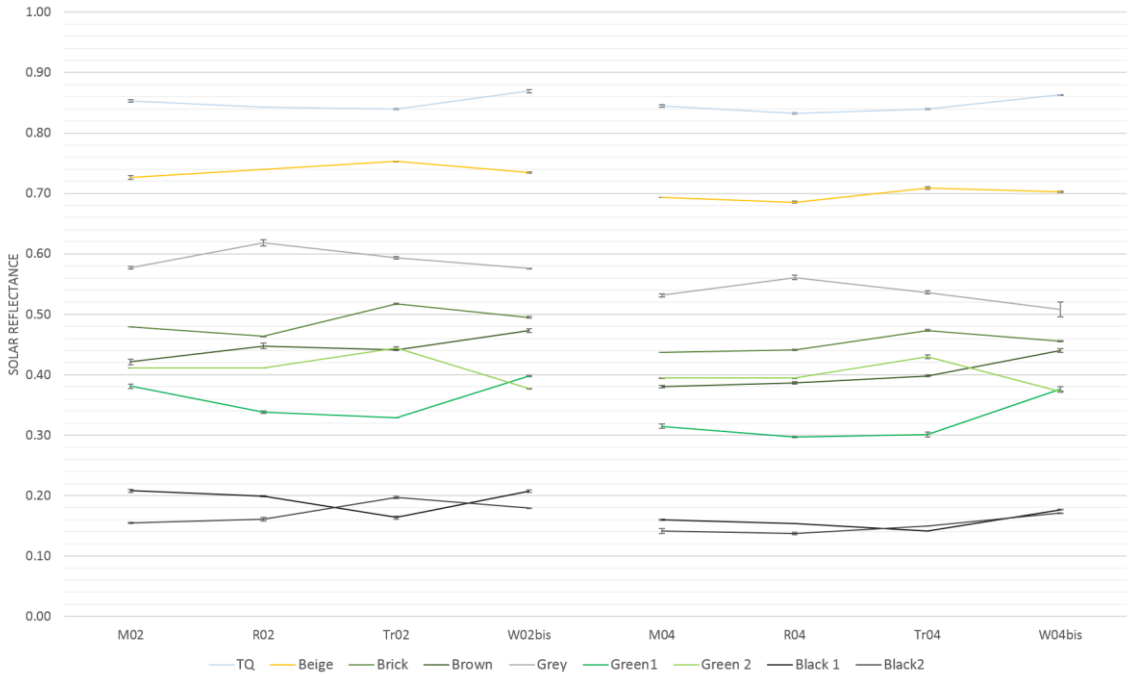

Fig. 5.6 – Summary of sola reflectance measured in accomplishment of ASTM E903 with irradiance spectrum AM1GH. (Left: 200 μm thick coatings; Right: 400 μm thick coatings)

From the chart several observations can be made. First of all, as expected, the most performing glaze is the one without pigments. Among pigmented samples, Beige is the most performing while the black ones are the less reflective glazes. Moreover, as it is shown by fig. 5.6 the surfaces characterized by a thinner layer of glaze reach higher values of solar reflectance if compared with the same glaze applied with 400 μm.

Considering the difference in the thickness, as expected, no pigmented glazes present the lower difference with the increasing of the thickness, in particular the sample with the transparent glaze does not change its reflectance, while, as the biggest difference, the sample with the recycled glass based glaze presents a difference in reflectance of 0.011. Among the cool colors "Green2" glazes are the ones with a lower difference between thin and thick coatings varying from 0.007 up to 0.017 while the "Grey" glazes present relevant variation ranging from 0.046 for the pigment embedded into the matt up to 0.068 for the pigment in white glaze.

Another data elaboration allows the creation of the plot in fig. 5.7 which analyze the influence of each glaze on each pigment. As it is reported by the image, TQ glaze is the one reporting the lower difference among all the glazes. Considering cool colored samples, then, the pigment most affected by the glaze presence is Green 1 where there is a difference of 0.100 from the lowest and the higher value while the pigment Black 2 is less affected by the presence of the

glaze with a difference between the minimum and the maximum values of 0.06. In both the glazes the higher value is referred to the pigment embedded into the White glaze with a thickness of 200 μm while the lowest value for the Green 1 sample is referred to the recycled glass based glaze with a thickness of 400 μm and for the Black 2 sample was measured in the matt glaze with a thickness of 400 μm.

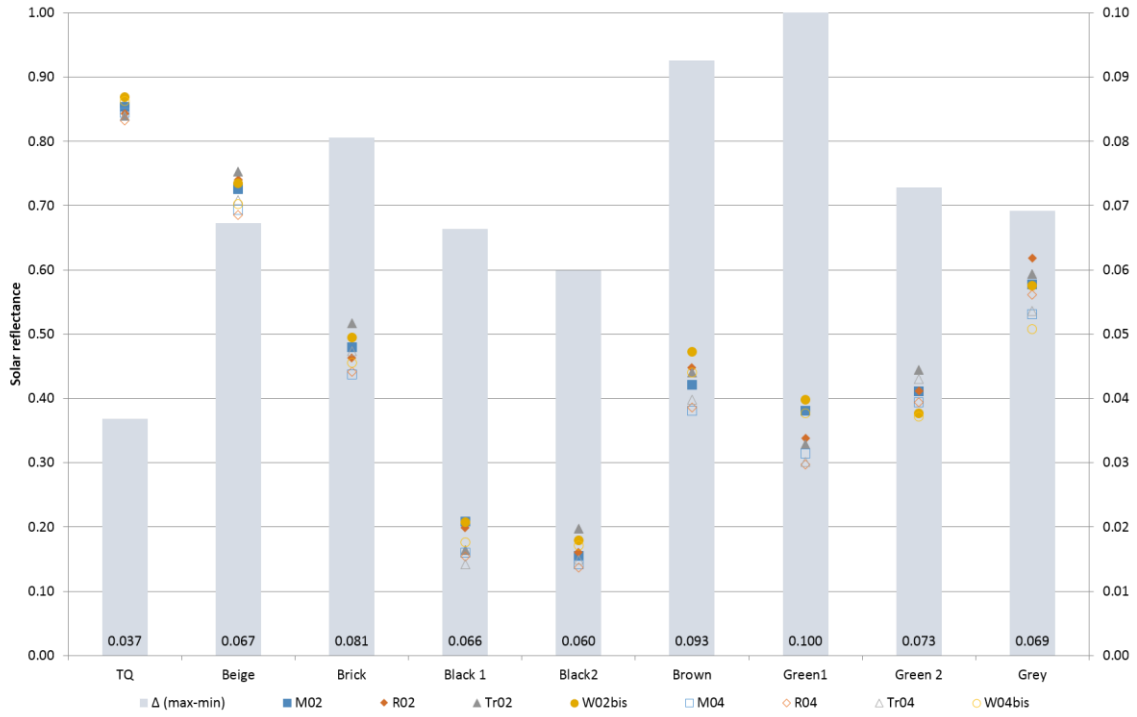

Figure 5.7 – Solar reflectance of each pigment considered the glaze differences and difference between max and min value of solar reflectance for each pigment

In order to evaluate the effect of the different wavelength ranges on the solar reflectance of each sample it is useful analyze solar reflectance is divided among Ultra Violet, Visible and Infra-Red. In figure 5.8 histogram representing the fraction of solar reflectance in each band of light. UV radiation is calculated between 250 and 400 nm, visible from 400 up to 700 and NiR from 700 up to 2500 nm. The blue band represents the UV reflectance, the Red band the Visible reflectance, which is responsible for the color of the samples perceived by the human eye and the Green band is referred to the NiR fraction, responsible for more than 50% of the total solar radiation.

It is possible to notice how the only three samples where solar reflectance in the infra red range higher than the values measured in the visible range are the TQ samples, the Beige and the Brick ones. Moreover it is interesting to notice how the Brick samples present ρ_{NiR} significantly

higher than the ρ_{vis} while White samples (TQ) present almost the same values for both ρ_{NiR} and ρ_{vis}.

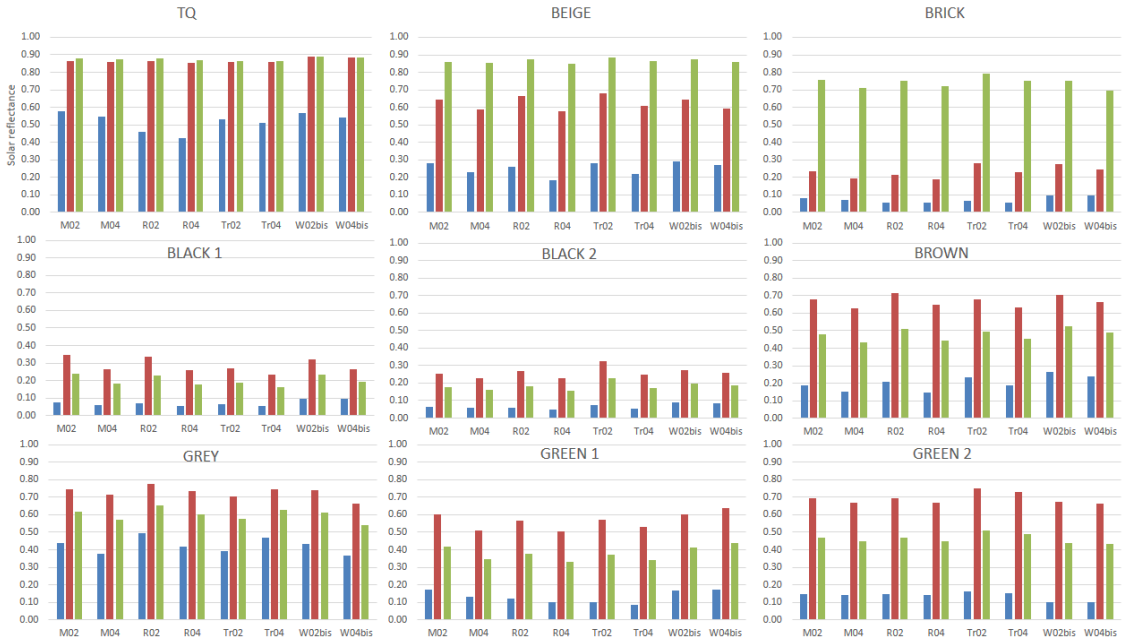

Figure 5.8 – Solar reflectance of the glazed samples calculated according to ASTM E903 with AM1GH irradiance spectrum divided for Uv-Vis-Nir wavelength range. The blue bar identify ρ_{UV}, red bar identify ρ_{Vis}, while green bar identify ρ_{NiR}

In addition to solar reflectance measurements, Hunter's parameters were measured for samples presenting ρ_{NiR} higher than ρ_{Vis}. The results were reported in Fig 5.9 and shows how L* is related to ρ_{Vis} since both of them maintain the same trend for each color. It is interesting to notice how as ρ_{Vis} decrease as the difference between L* and ρ_{Vis} decrease. Concerning solar reflective materials it is important to emphasize that L*, a* and b* do not have any direct relations with ρ_{sol} since Hunter's parameters are just related to the visible wavelength range which represent less than 50% of the total energy amount considered in solar reflectance measurements.

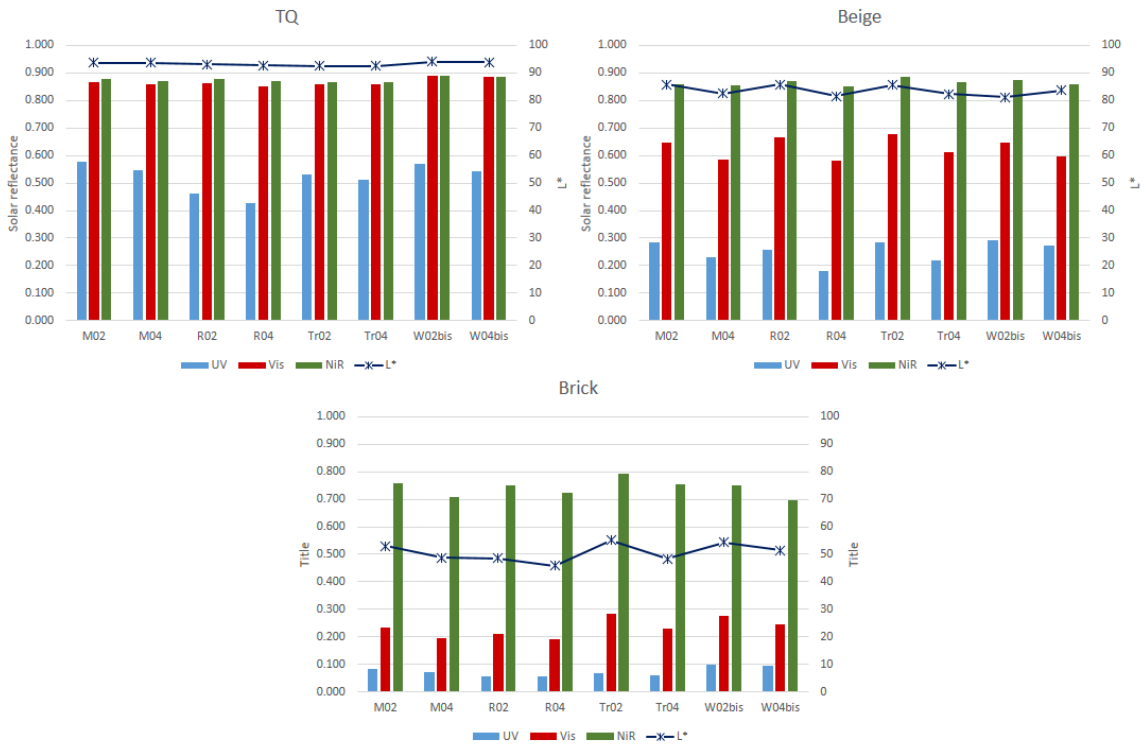

Figure 5.9 – Relations between solar reflectance and L*

In order to easily compare the samples created into this second stage and the ones created in the previous stage, among the images taken through ESEM analysis, 1000 x images, obtained through secondary electron detector are shown.

First of all, in Fig. 5.9 the comparison between the TQ samples with each glaze are shown. On the left of the picture the samples coated with 200 μm of glaze while on the right samples coated with 400 μm are reported. In this image t can be observed how there are no particular differences on the microstructure between the samples with different thickness. In fig 5.10 the samples with beige pigment embedded are shown. In this case all the micrographs are referred to the samples coated with 400 μm of glaze. Finally in Fig 5.11 the samples with all the eight pigments embedded into 400 μm thick transparent glazes are shown.

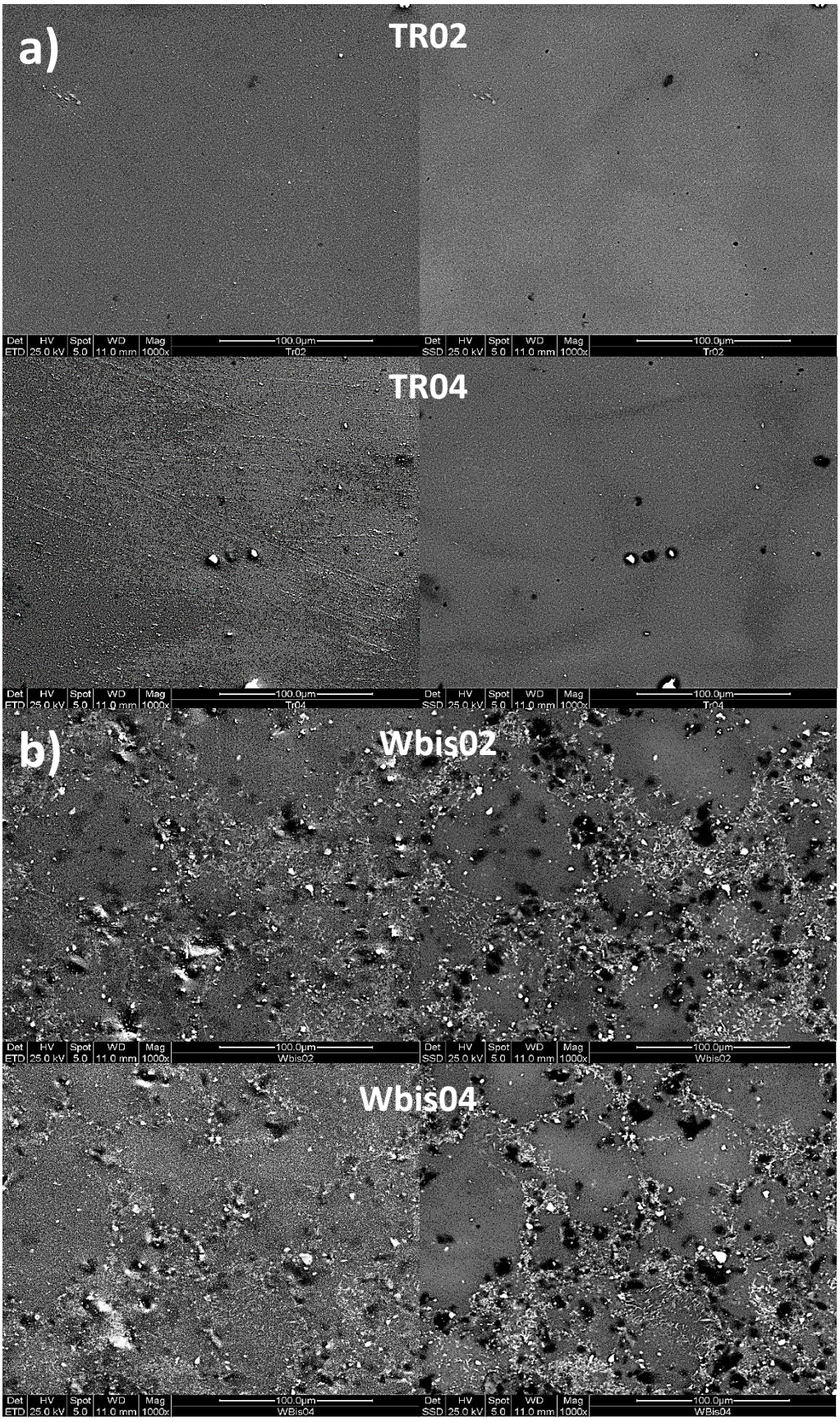
a)
TR02
Det HV Spot WD Mag
ETD 25.0 kV 5.0 11.0 mm 1000x
100.0µm
Tr02
Det HV Spot WD Mag
SSD 25.0 kV 5.0 11.0 mm 1000x
100.0µm
Tr02
TR04
Det HV Spot WD Mag
ETD 25.0 kV 5.0 11.0 mm 1000x
100.0µm
Tr04
Det HV Spot WD Mag
SSD 25.0 kV 5.0 11.0 mm 1000x
100.0µm
Tr04
b)
Wbis02
Det HV Spot WD Mag
ETD 25.0 kV 5.0 11.0 mm 1000x
100.0µm
Wbis02
Det HV Spot WD Mag
SSD 25.0 kV 5.0 11.0 mm 1000x
100.0µm
Wbis02
Wbis04
Det HV Spot WD Mag
ETD 25.0 kV 5.0 11.0 mm 1000x
100.0µm
WBis04
Det HV Spot WD Mag
SSD 25.0 kV 5.0 11.0 mm 1000x
100.0µm
WBis04

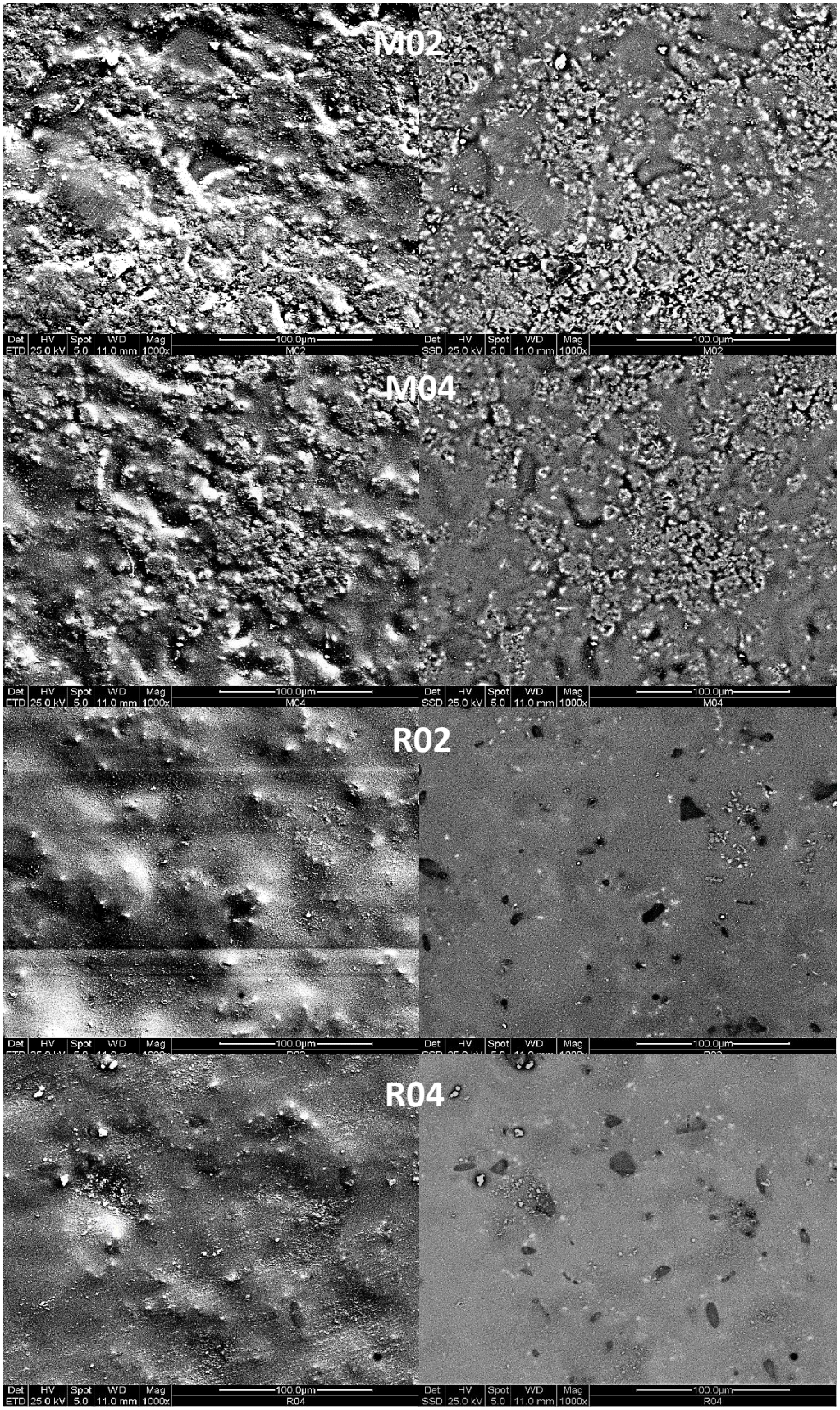

Figure 5.9 - TQ glazed both 200 μm and 400 μm samples surface micrographs both ETD and SSD image 1000x (5.9a Transparent glaze, 5.9b White glaze, 5.9c Matt glaze, 5.9d Recycled glass based glaze)

From the micrographs it is evident how TR samples presents an amorphous surface while White, M and W presents crystal formations. The nature of these crystals will be checked with mineralogical analysis of the fired surfaces. In order to provide a comprehensive image of the samples' surface, in the following figures will be reported micrographs collected with a mix detector combining both ETD (by secondary electrons detector) and SSD (by back scattered electrons detector).

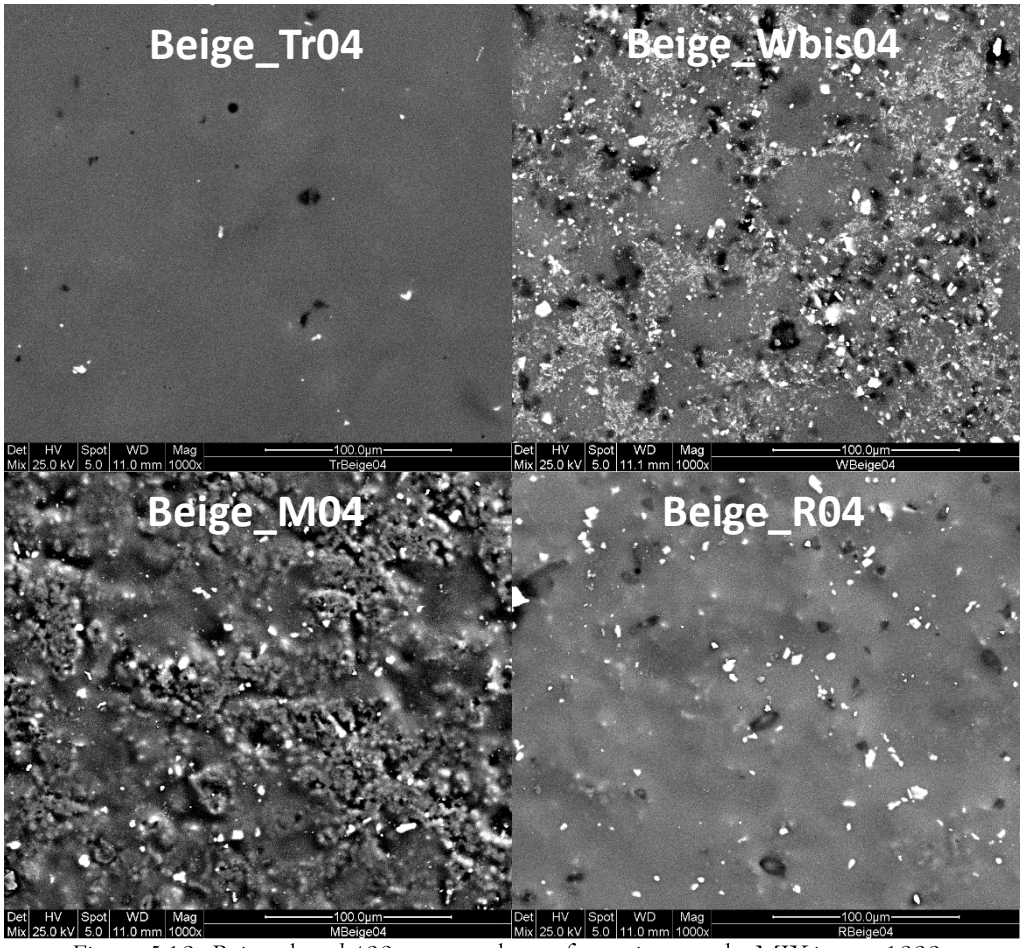

Figure 5.10 - Beige glazed 400 µm samples surface micrographs MIX image 1000x

From Fig. 5.10 it is evident how the presence of the pigments does not affect the microstructure of the samples except for the light spots if compared with the homologue samples in fig. 5.9.

In order to compare the microstructure of the colored samples, the simplest surface, the transparent one, was compared for each pigment used. Fig 5.11 reports the comparison among the different micrographs of the samples taken with both ETD and SSD detector in the same image.

This allows us to report in just one micrograph both the information gathered by the secondary electron detector and the backscattered electron detector.

The dark spot on the surfaces represents small pinhole on the sample's surface, while the light spot represents the pigment embedded into the glaze.

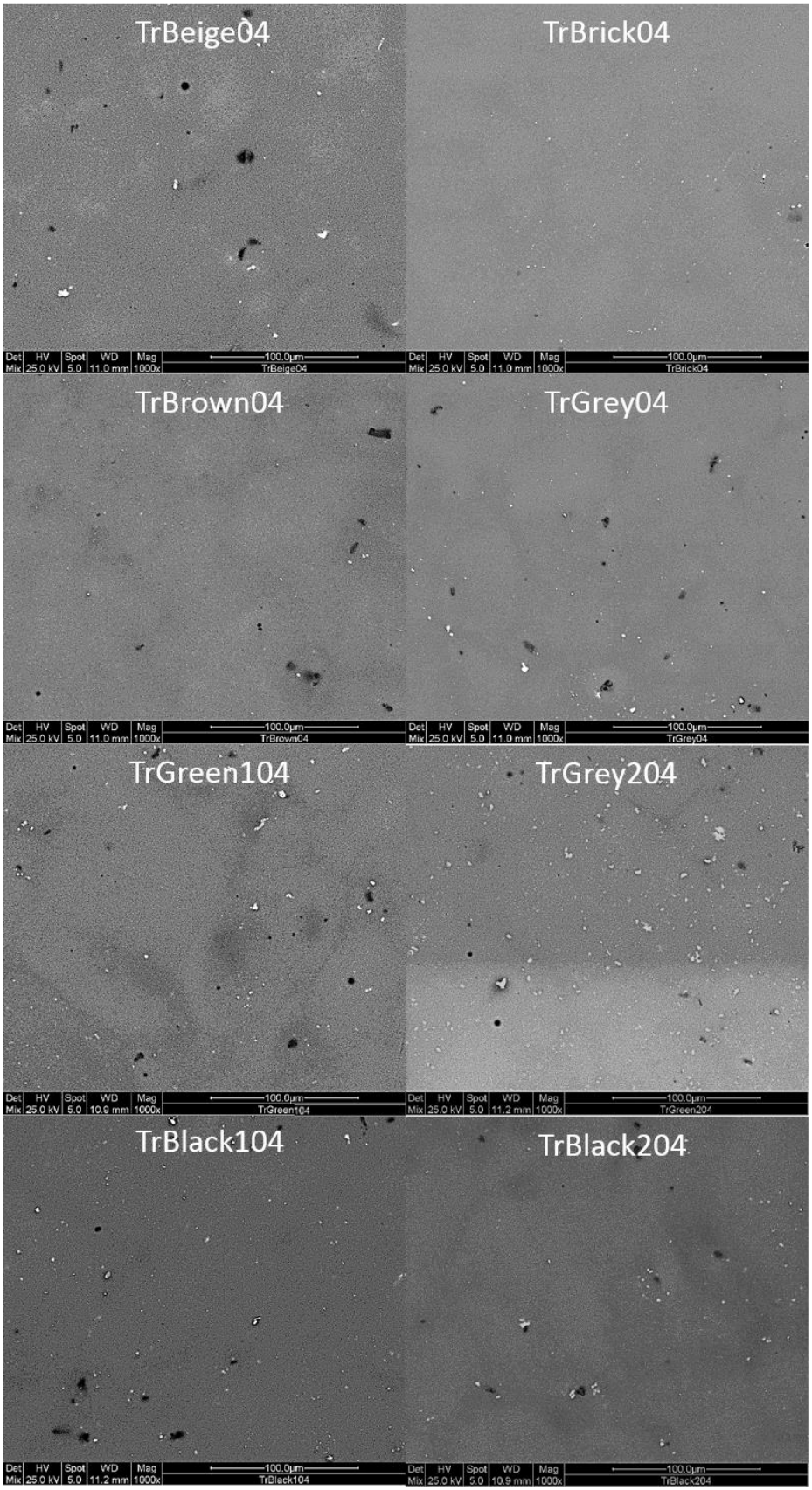

Figure 5.11 - Pigmented glazed 400 µm samples surface micrographs MIX image 1000x

The mineralogical analysis was first of all carried out on samples without pigments in order to establish which phases are formed during the heating treatment.

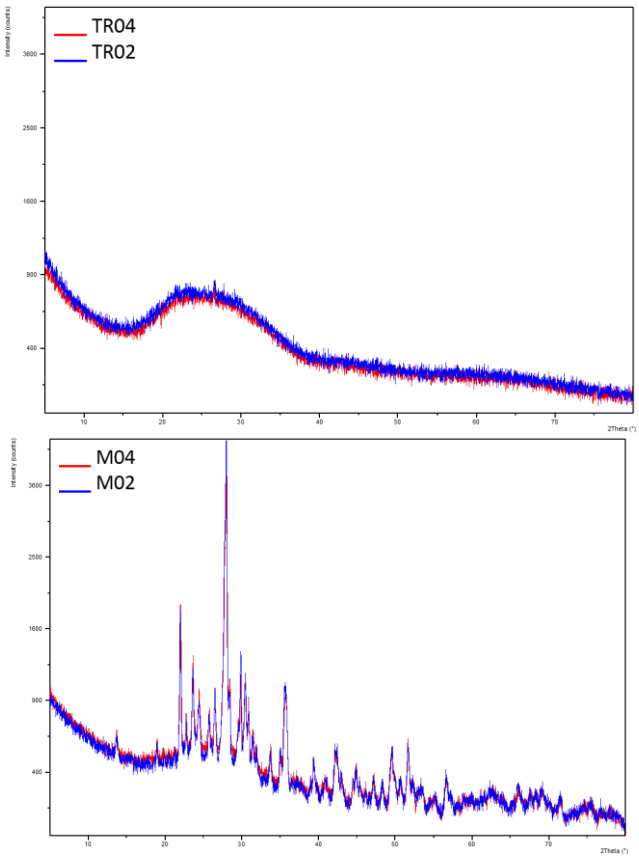

Figure 5.12 – Comparison between diffraction patterns of 200 μm and 400 μm Transparent and Matt Glazes

In Figure 5.12 a comparison between the two thickness applied on the glaze is shown. Both transparent and matt glaze are reported in order to show that there is no influence in phase formation with 200 and 400 μm.

According to what demonstrated in fig.5.12, the samples coated with 400 μm of glaze are discussed. In order to facilitate the interpretation of the data, the samples characterized by the transparent glaze with a 400 μm thickness will be discussed.

According to what presented by Fig. 5.9, concerning transparent glaze, as it is visible in fig. 5.12, no crystalline phases were formed during firing treatments while, both in recycled glass based glaze, white and matt glaze different phases were formed, in particular in the recycled glass based glaze was found presence of Quartz, anorthite ad alumina, into white glaze both Zirconium Silcate, as main constituent and Zirconium Oxide and Quartz as minor constituents were found. In the Matt glaze both albite and anorthite sodian were found.

Another important step is understand if there is any reaction between the glaze and the pigments during heating treatment. To better understand these interactions, in figure 5.13 the spectra of Green 1and Black 1 colored samples are overlapped to the TR04 sample and to the related powdered pigments diffraction patterns. As it is shown by the figure the peaks of the pigment are present also in the glazed sample meaning that there is no formation of new crystalline phases due to the interaction of the pigment and the glaze.

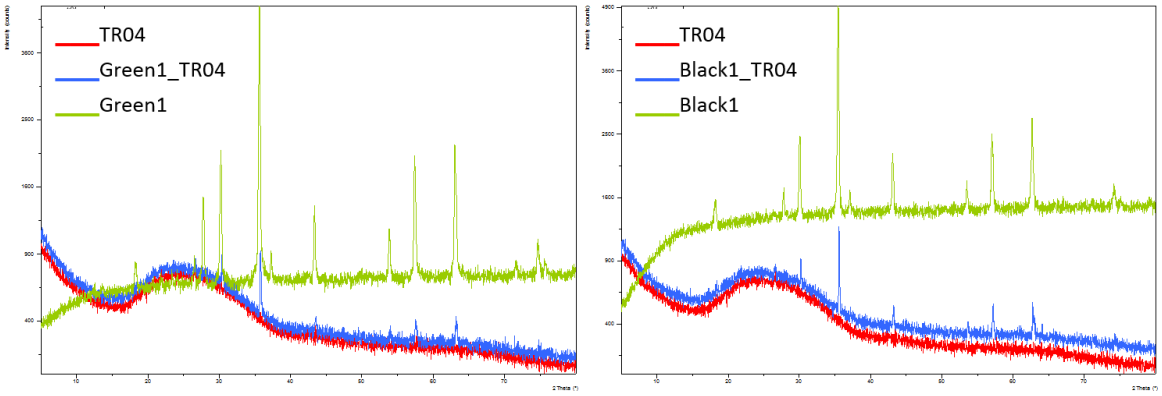

Figure 5.13 – Comparison between pigment powder, glazed unpigmented and glazed colored samples for both Green1 and Black 1 samples. Red pattern represent the unpigmented sample, blue pattern the colored one and the green pattern represent the powdered pigment.

Roughness measurements were performed on the no pigmented samples considering both the thickness. In this stage Ra were taken into account and the attempt was to find correlation between reflectance and roughness and eventually roughness and thickness.

Table 5.10 – Roughess (Ra) values for TQ samples and ratio between Ra for samples coated with the same glaze.

Sample	Ra (μm)	σ	Ra_{02}/Ra_{04}
Tr02	0.224	0.091	0.80
Tr04	0.280	0.107	
Wbis02	0.470	0.094	1.39
Wbis04	0.339	0.087	
R02	0.827	0.146	1.25
R04	0.661	0.121	
M02	3.321	0.694	1.98
M04	1.681	0.440	

From table 5.10 and fig. 5.14 it is evident how the roughness generally decrease with the increasing of the glaze thickness. Moreover the difference between 200 μm and 400 μm samples is higher with the increasing of the roughness.

Considering the interaction between the solar reflectance and the roughness it is important to observe that in this case there are no relations between Ra and solar reflectance (fig. 5.15) and no relations between the reflectance of the samples and their roughness. However the effect of the roughness on the surface of the sample will increase its influence if on the samples ageing studies. Since soiling particles and contaminants are deposited into the asperities, will be hardly to remove them from the surface of the samples if compared with ones deposited on smooth samples.

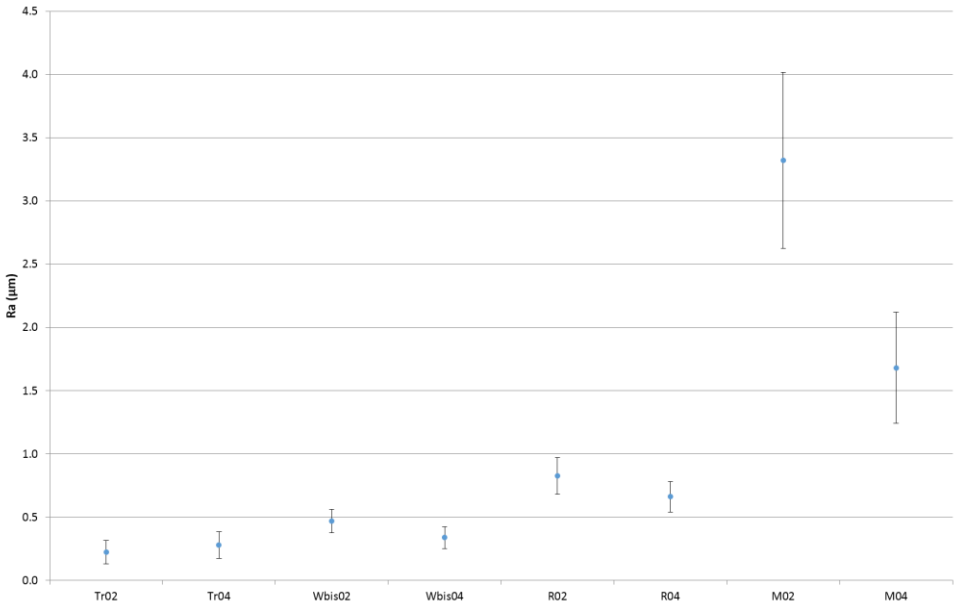

Figure 5.14 – Roughness of the no pigmented samples.

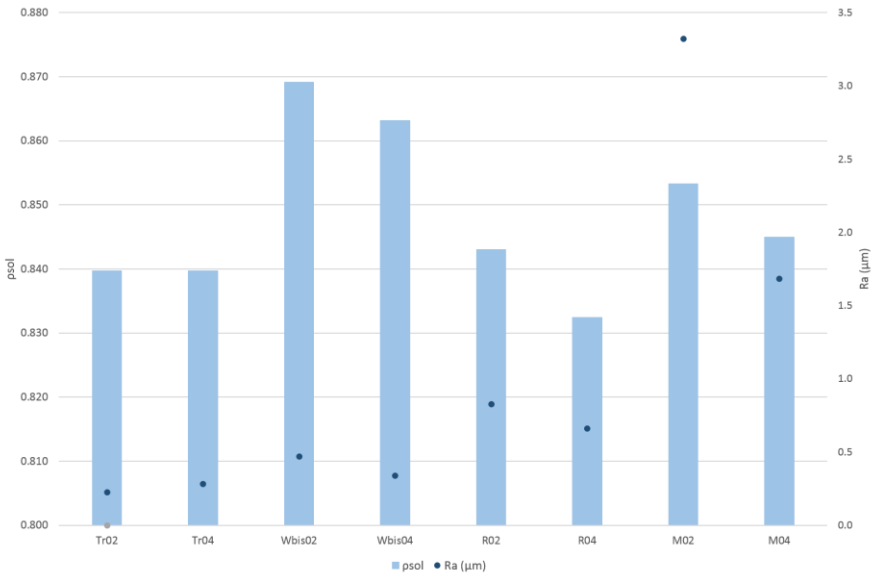

Figure 5.15 – Effect of roughness on solar reflectance

Experimental approach: glazes for clay roof tiles

Considering the interesting behavior of the glazes on traditional ceramics, and considered that solar reflective surfaces are commonly used as a roofing system, the same pigments embedded into glazes formulated in the previous part of the study, were used also into glazes designed on purpose for clay roof tiles. Considering the structure of a clay roof tile, on the substrate was applied just one layer made by a transparent glaze with the possible addition of pigments. In this case the engobe is not applied on the surface of the samples in order to better approximate the production process.

Three different glazes for clay roof tiles were designed using three different frits made by recycled glass (R), low thermal coefficient glass (T) and alkaline glass (A). In Table 5.11 the glaze formulation is presented. In each sample 0.3% of pigment was embedded.

Table 5.11 – Formulation of clay roof tile glazes

Wt (%)	Glaze formulation
Frit	95.0
Kaolin	5.0
Peptapon	0.3
Water	50.0

Peptapon is an industrial additive made by hydrocolloid preparation commonly used to improve glaze rheology.

The recycled glass based frit is composed by 10.5% B_2O_3, 5.7% Al_2O_3, 74.5% SiO_2, 1.0% K_2O, 6.1% Na_2O, 1.4% CaO, 0.8% Others, the Low thermal coefficient frit by 7.0% B_2O_3, 7.0% Al_2O_3, 58.0% SiO_2, 11.0% CaO, 11.0% ZnO, 6.0% Others, and the Alkaline frit is composed by 28.4% B_2O_3, 9.3% Al_2O_3, 56.7% SiO_2, 2.8% CaO, 2.5% Li_2O, 0.3% Others.

Likely to what performed in the second stage, all the raw materials except for the pigments, were poured in an alumina jar with 50 wt% of water and alumina grinding balls with different diameters. All the glazes were milled for 40 minutes. The same pigments used in the second stage (Tab 5.8) were then embedded at 0.3 wt% into the liquid glazes and both pigmented glazes and colorless glazes were applied on red ceramic substrates like clay roof tiles with a 200 μm thickness. All the glazed tiles were then fired in a muffle furnace for 3 hours at the maximum temperature of 950 °C.

Solar reflectance of the fired samples was measured and, once again, correlations between solar reflectance and surface properties were checked. Possible correlations between solar reflectance, the three glazes and the pigments were also analyzed.

Method

As well as what performed in the previous stages, first of all the solar reflectance of the samples was measured. The measurements, in accomplishment with ASTM E903, were performed through a Uv-Vis-Nir spectrophotometer (Jasco V-670). The solar reflectance was obtained integrating over the range from 250 nm up to 2500 nm with a step size of 5nm. The irradiance spectrum used do calculate solar reflectance was AM1GH.(Levinson et al, 2010). Hunter's parameters were measured for all the samples. In particular L* parameter was compared with ρvis.

Moreover microstructural characterizations were performed by means of ESEM (FEI Quanta-200) after sputtering the surface with 100nm of Gold. Mineralogical analysis was conducted through a X'Pert Pro Panalytical diffractometer equipped with X'Celerator detector. CuKα radiation, limited to 40kV and 40mA was used. All the spectra were collected with a scanning rate of 0.1 °min-1 in a 2θ range from 10° to 80°.

Results and discussion

Solar reflectance was measured for each glaze with and without pigments (Tab. 5.12). The solar reflectance of the unglazed surface is 0.445 and as it can be noticed from the table all the glazes reduce the solar reflectance value of the substrate. Fig. 5.16 plot how solar reflectance varies for each glaze according to each pigment. Likely to fig. 5.6, the error bar represents the 2σ to better approximate the standard deviation of the samples

Table 5.12 – Solar reflectance of glazed clay tiles according to ASTM E903 using AM1GH irradiance spectrum

	TQ	Beige	Brick	Black1	Black2	Brown	Green1	Green2	Gray
T	0.152	0.182	0.175	0.125	0.119	0.160	0.155	0.193	0.160
A	0.200	0.217	0.203	0.155	0.123	0.185	0.182	0.218	0.197
R	0.351	0.352	0.323	0.165	0.126	0.269	0.240	0.294	0.319

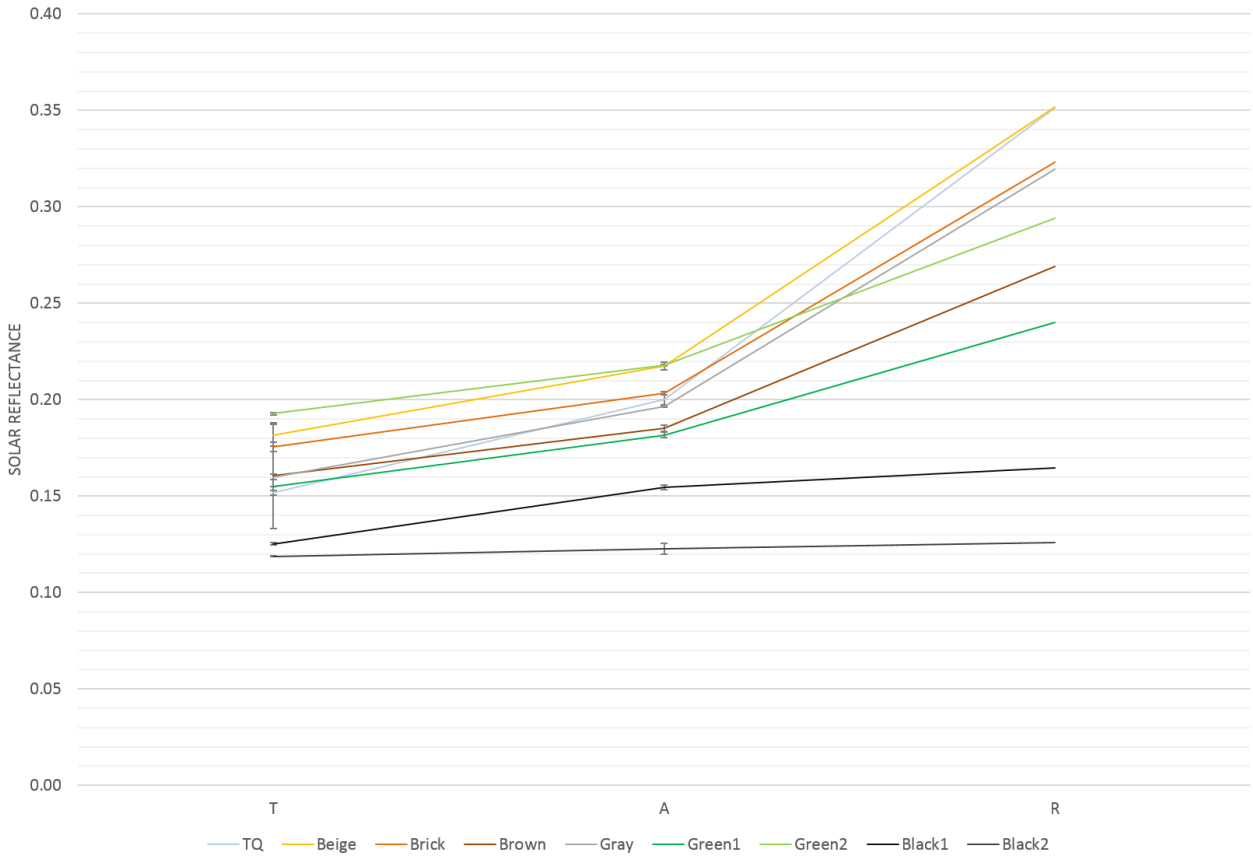

Fig. 5.16 – Summary of solar reflectance measured in accomplishment of ASTM E 903 with irradiance spectrum AM1GH.

Fig. 5.16 show an increasing in solar reflectance for the samples from the left to the right where pigments embedded in low thermal coefficient glaze present values lower than recycled glass based glaze. In particular for T and A samples the range of solar reflectance is approximately 10% while for R samples the variation of soar reflectance reaches around 25%.

In fig. 5.17 the influence of each pigment was approached. As much ρsol for R samples is higher, as much the difference between the higher value of solar reflectance and the lower one is more significant. In particular for beige sample the difference is 0.017 while for black2 sample is around 0.07.

Significant difference can be observed if solar reflectance of ceramic tiles and clay roof tiles are compared, first of all concerning clay roof tiles the different pigments present all the same trend with the glaze variations, while this does not occur on ceramic tiles. Moreover while solar reflectance of ceramic tiles with pigments is always lower than the solar reflectance of no pigmented tiles, concerning clay roof tiles different trends are presented by the data. Concerning T samples just Black1 and Black2 samples presents a reflectance lower than samples without

pigments, among A samples the number of samples which presents solar reflectance lower than the tile without pigments increases (Brown, Gray, Green1 and both Black1 and Black2) while, concerning R glazes, only Beige samples presents a solar reflectance higher than the sample without pigments.

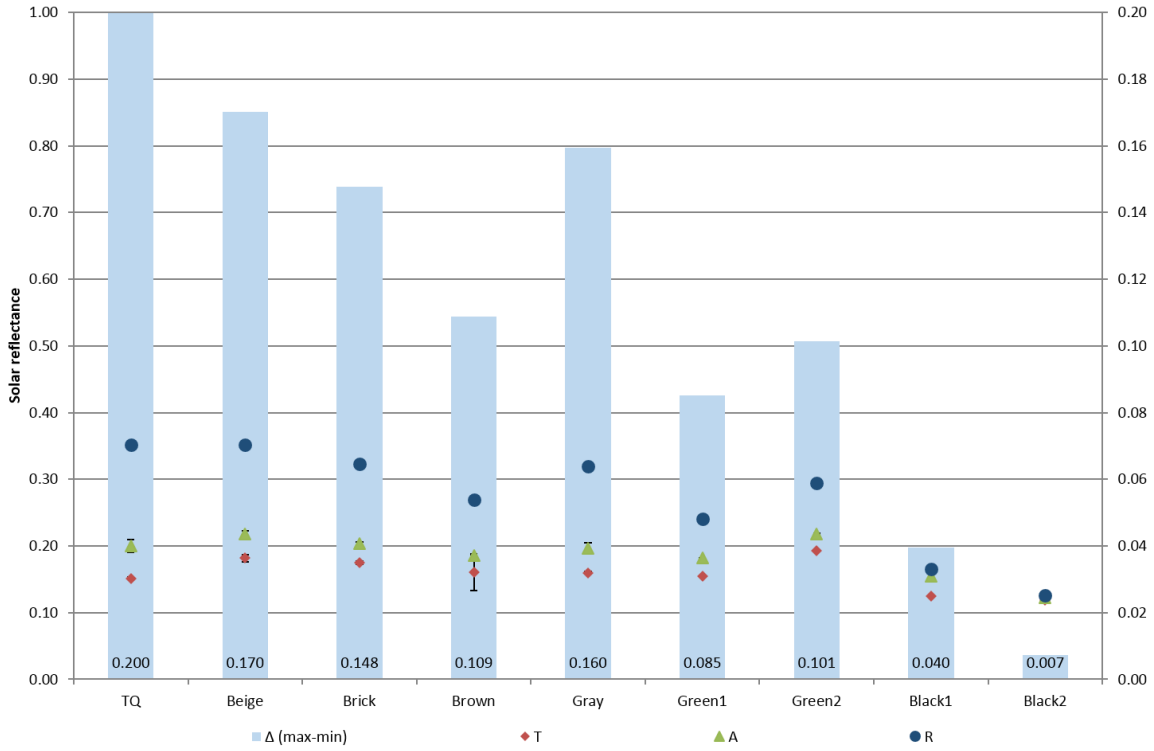

Figure 5.17 – Solar reflectance of each pigment considered the glaze differences and difference between higher and lower value of solar reflectance for each pigment.

Likely to second stage, the amount of solar reflectance for each wavelength range is reported in Fig. 5.18. In this stage the solar reflectance of the NiR fraction is significantly higher than the Vis fraction meaning that, according to the definition of cool color as a material where solar reflectance in NiR fraction is higher than solar reflectance in Visible wavelength range, all the samples can be considered as cool colors. According to the classification of cool colors as a building material characterized by a ρ_{sol}>0.50 no one of clay roof tiles produced can be classified like cool colors.

In Fig. 5.19 three representative glazes, TQ, beige and brick, each solar reflectance histogram was integrated with the L* parameter measured with a X'Rite colorimeter. The three glazes were selected in order to allow comparison between clay roof tiles (Fig. 5.19) and ceramic tiles (Fig. 5.9). Considering clay roof tiles samples, L* parameter follow the trend presented by

ρ_{vis} likely to what observed in Fig. 5.9. Despite the relation of L* and ρ_{vis} it is important to remember that since L* is related to the visible fraction and considered that this fraction is lower than 50% of the total energy amount, L* and solar reflectance are not necessarily linked to each other.

Figure 5.18 – Solar reflectance of glazed samples calculated according to ASTM E903 with AM1GH irradiance spectrum, divided for Uv-Vis-NiR wavelength range. The blue bar identify ρ_{Uv}, red bar identify ρ_{Vis}, while green bar identify ρ_{NiR}

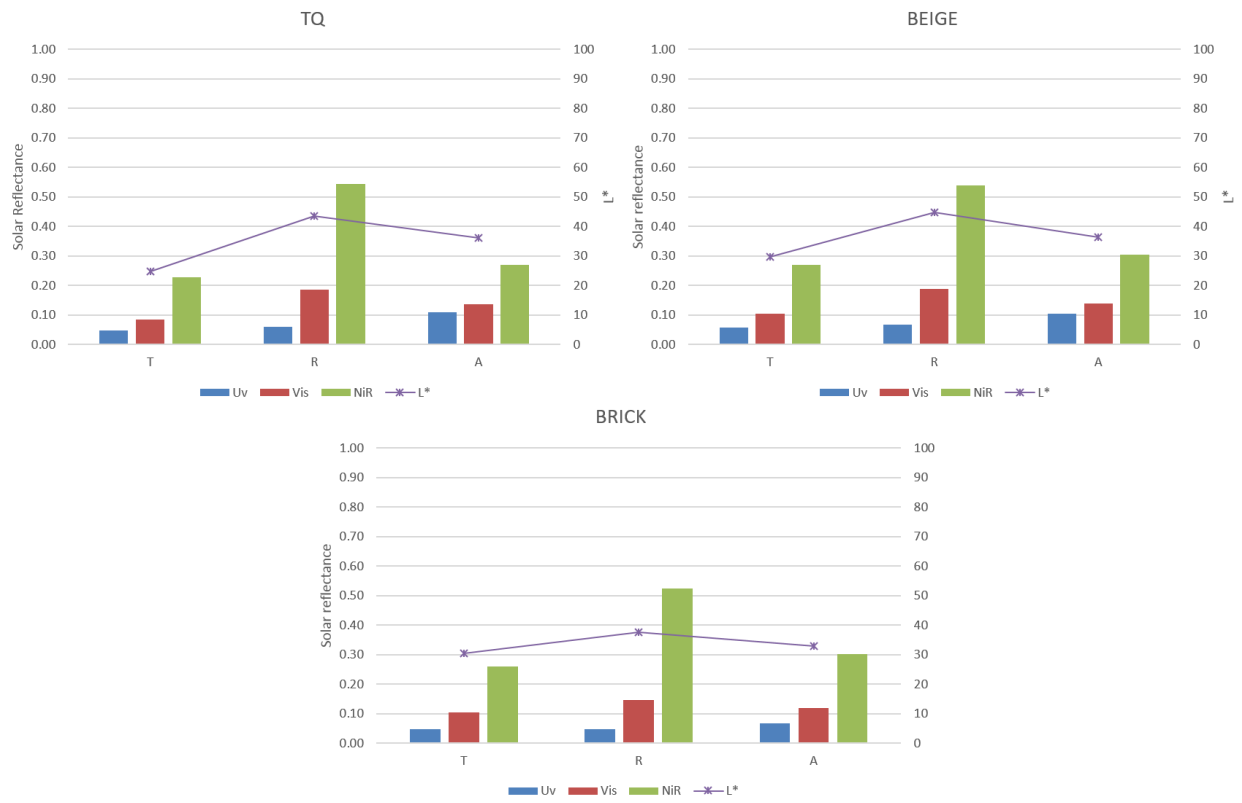

Figure 5.19 – Relation between solar reflectance and L*

First of all the microstructure of the samples without pigment was analyzed (Fig. 5.20). On the left micrographs obtained with ETD detector are reported while on the right micrographs obtained with SSD detector are shown. The three surfaces appear smooth and, in particular on R samples, small crystals appear on both ETD and SSD micrographs.

In figure 5.21 the microstructure of colored samples with higher solar reflectance is reported. All micrographs are collected using MIX detector which synthetize in one image information obtained both from ETD and SSD. The light spots on the images represent pigment powder embedded into the R glaze.

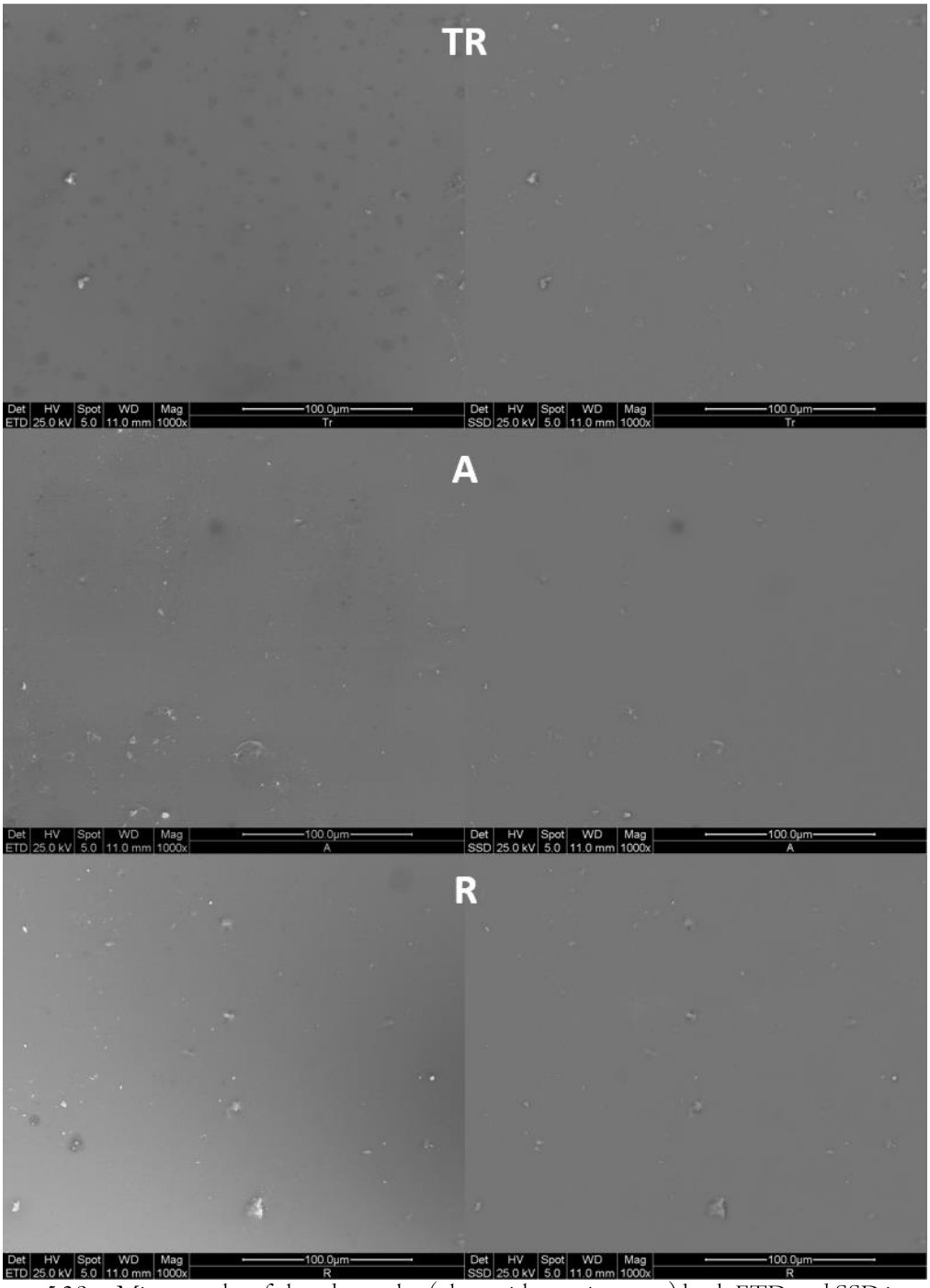

Figure 5.20 – Micrographs of glazed samples (glaze without pigments) both ETD and SSD images (1000x)

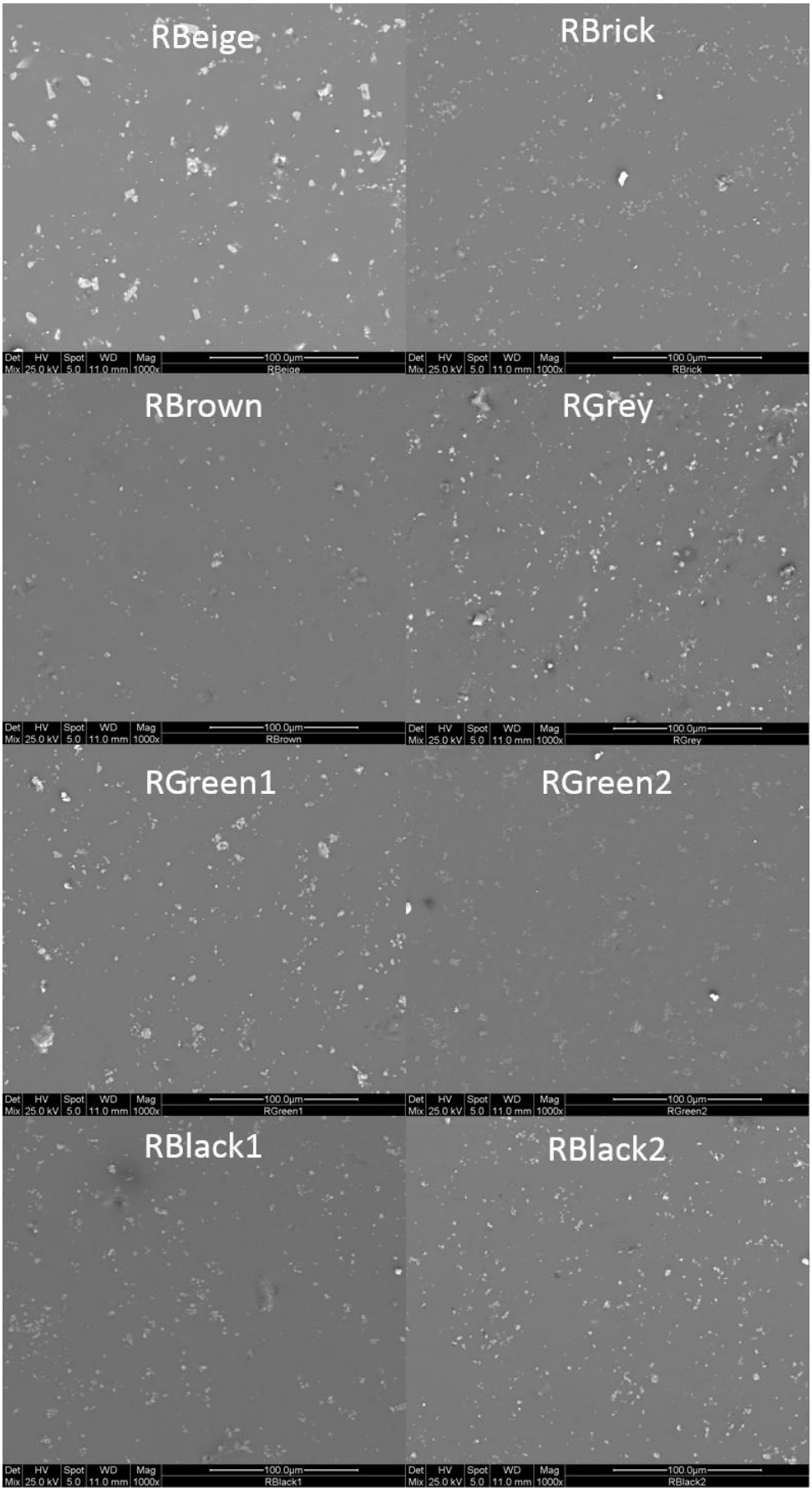

Figure 5.21 – Pigmented glazes surface micrographs MIX detector (1000x)

After the reflectance data results, both microstructural and mineralogical analysis were performed on the samples without pigments, in order to understand if the glazes themselves, during the firing temperature, form new crystalline phases. In particular, in this case, glaze with low thermal coefficient does not form any crystalline phase while small peaks appears on Alkaline glaze and recycled glass based glaze. The peaks detected at 26.67 °2θ, 26.67 °2θ and 36.59 °2θ can be related to the formation of quartz, while for recycled glass based glaze, the peak detected at 21.78 °2θ can be related to the presence of cristobalite. (Fig. 5.22)

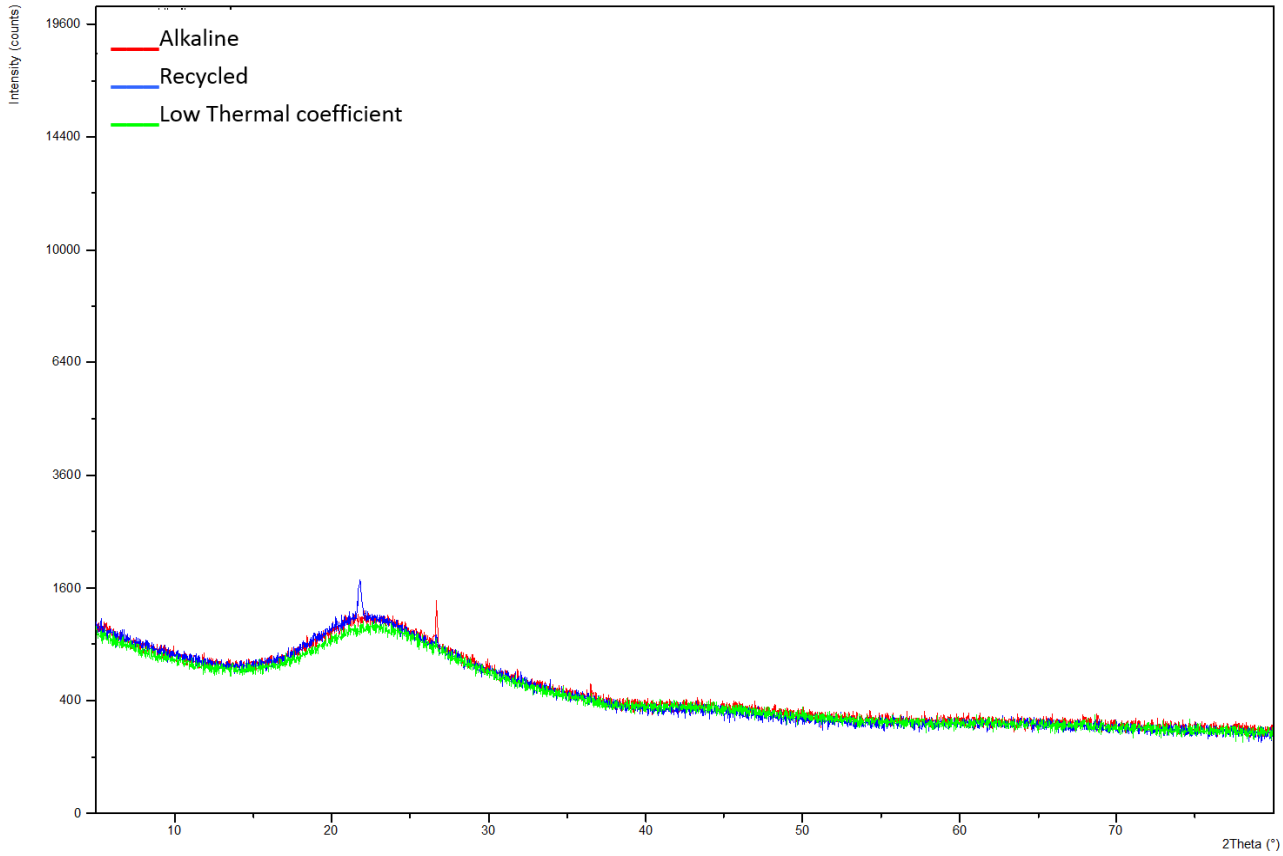

Figure 5.22 – Comparison between diffraction patterns of glazes without pigments

Considered the simple diffraction pattern of the glazed samples, likely to what is shown in Fig. 5.13, the comparison between powdered pigment, no colored glaze and colored glaze is reported in Fig. 5.23. It is evident how the peaks characteristic of the pigment appears, smoother, in the blue X-ray pattern, which shows the colored glazed sample. In this case the pigment does not react with the glaze with the formation of new phases.

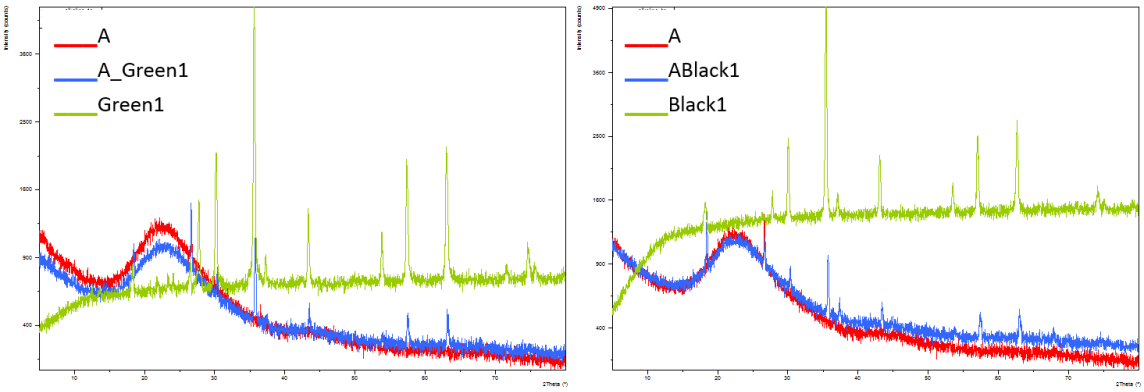

Figure 5.23 – Comparison between pigment powder, glazed samples without pigments and glazed colored samples for both Green1 and Black1 samples. Red pattern represents the glazed sample without pigments, blue pattern the glazed colored sample while green pattern represent the powdered pigment diffraction pattern

Conclusion

This work describes the procedure through which an engobe with high solar reflectance is obtained, using common production materials and processes of the ceramic tile industry. Two relatively inexpensive pigments were chosen to obtain a white engobe and one of them was selected after comparison of several formulations using both pigments. A solar reflectance of the engobe as high as 90% was obtained with either white or red ceramic support, with the chance to add one percent point by doubling the engobe thickness up to 200 μm.

In order to protect the engobe and improve its resistance to mechanical stress and weathering, the application of a glaze coating was subsequently investigated. Among the tested solutions, a white gloss glaze was found to give the best performance in terms of solar reflectance and functionality of the glazed tile, providing a white product with solar reflectance as high as 0.86 and the same predictable resistance to sun, rain and frost of ceramic tiles. On the other hand, a transparent gloss glaze was also produced with performance very close to that of the white gloss glaze. This can pave the way to the development of cool colored (*i.e.* non-white) tiles based on the same engobe and proper selective pigments added to the glaze.(Ferrari et al, 2013)

Concerning the formulation of cool colored ceramic tiles different glazed, transparent, white and colored, with different surface finishing are applied on the most performing engobe formulated in the first stage of the study. As expected, beige samples reach higher values of solar reflectance. Both beige and brick samples are characterized by a ρ_{nir} higher than ρ_{vis} . In order to create a surface that can be easily applied on European roofs a combination of beige, brick and brown should be formulated, even if the bright color of the glazes origin a surface, which hardly can be integrated into city skyline.

The formulation of cool colored clay roof tiles involves the application of just one layer of glaze on the substrate. In this case the samples coated with the recycled glass based glaze present the most promising values of solar reflectance even though the values remains quite low. The ρ_{nir} higher than ρ_{vis} represent a strength point of this new product providing interesting future perspective for the improvement of the reflectance values.

Chapter references

Akbari H., Matthews H.D. (2012) Global Cooling Updates: Reflective Roofs and Pavements, Energy and Buildings, 55 2-6

Akbari H., Pomerantz M., Taha H. (2010) Cool Surfaces and Shade Trees to Reduce Energy Use and Improve Air Quality in Urban Areas, Solar Energy, 70(3) 295-310.

ASTM (1996). ASTM E 903-96 – Standard test method for solar absorptance, reflectance, and transmittance of materials using integrating spheres. Standard of the American Society for Testing and Materials.

Carty W.M., Senapati U. (1998) Porcelain—Raw Materials, Processing, Phase Evolution, and Mechanical Behavior, Journal of the American Ceramic Society 81 (1998) 3–20

De Brito Filho J.P., Henriquez J.R., Dutra J.C.C. (2011) Effects of Coefficients of Solar Reflectivity and Infrared Emissivity on the Temperature and Heat Flux of Horizontal Flat roofs of Artificially Conditioned Nonresidential Buildings, Energy and Buildings, 43(2-3) 440-445.

Ferrari C., Libbra A., Muscio A., Siligardi C., (2013) Design of ceramic tiles with high solar reflectance through the development of a functional engobe, Ceramics International. 39(8), 9583-9590

I.Cer.S. Colore, Pigmenti e Colorazione in Ceramica. Editore S.A.L.A srl, Modena, Italia, 2003

Levinson R., Berdahl P., Akbari H., Miller W., Joedicke I., Reilly J., Suzuki Y., Vondran M. (2007) Methods of Creating Solar-Reflective Nonwhite Surfaces and their Application to Residential Roofing Materials, Solar Energy Materials & Solar Cells, 91(4),304-314.

SACMI, Raw materials for frits and glazes, in Applied Ceramic Technology, Vol. 1, 2nd edition, 139-174, La Mandragola, Bologna, Italy, 2005.

Santamouris, M. (2012). Cooling the cities – A review of reflective and green roof mitigation technologies to fight heat island and improve comfort in urban environments. Solar Energy, In press (2012).doi:10.1016/j.solener.2012.07.003.

Siligardi C., Lusvarghi L., Giolli C., Scrivani A., Venturelli D. (2014) Recycling in cerami glazes of zirconia overspray from thermal barrier coating manufacturing, Journal of the European Ceramic Society, 34, 147-154

Shi Z., Zhang X. (2011) Analyzing the Effect of the Long wave Emissivity and Solar Reflectance of Building Envelopes on Energy-Saving in Buildings in Various Climates, Solar Energy, 85(1) 28-37.

Synnefa A., Santamouris M., Apostolakis K.,(2007) On the development, optical properties and thermal performance of cool colored coatings for the urban environment, Solar Energy, 81(4), 488-497, 10.1016/j.solener.2006.08.005.

Synnefa A., Santamouris M. (2012) Advances on Technical, Policy and Market Aspects of Cool Roof Technology in Europe: The Cool Roof Project, Energy and Buildings, 55 35-41.

Taha H., Akbari H., Rosenfeld A., Huang J. (1998) Residential Cooling Loads and the Urban Heat Island – The Effects of Albedo, Building and Environment, 23(4) 271-283.

CHAPTER 6
FORMULATION OF A SOLAR REFLECTIVE CERAMIC GLAZE FOR ASPHALT SHINGLES

Brief introduction

Asphalt shingles are one of the most widely used cool roof building material (EPA, 2008; EPA, 2010; CRRC Rated Product Database). As illustrated in Chapter 3 they are mainly made by two different layers: a bitumen layer and mineral grit (basalts or slate). In order to improve mineral grit solar reflectance (ρsol=0.18) paint was usually applied on the shingle, with all the problems, first of all the low durability of the surface and the necessity of refurbishment of the surface every three years (Berdhal, 2012). Recently both white and colored ceramic-based glazes were formulated and applied on the surface of the granules through a rotary kiln. Usually these glazed are based on TiO2 white pigment which is quite expensive . New solutions are necessary in order optimize the cost without affect negatively solar reflectance and possibly without modify the manufacturing process.

Aim of the project

This study is aimed to prepare roofing products based on ceramic coatings and providing solar reflectance as high as market-ready organic materials, but having higher chemical durability after aging and weathering. Common cool roof materials are based on white pigments with high solar reflectivity in the NIR wavelength range such as the titanium dioxide (TiO_2). Talc powder with chemical formulation $Mg_3Si_4O_{10}(OH)_2$ is exploited here to improve the behavior of titanium dioxide in terms of solar reflectivity and, at the same time, to decrease the glaze cost.

Preliminary studies were carried out in collaboration with a company in order to evaluate the effect of temperature and different $Mg_3Si_4O_{10}(OH)_2$ / TiO_2 ratios. Subsequently the

problem was faced using a more complete approach through a 2^k full factorial design. The final aim of this approach is to find the optimal formulation varying of both the pigments and the liquid phase represented by Na_2SiO_3 and water (keeping the temperature constant T= 900 °C)

The obtained glazes have been characterized by solar reflectance analysis, XRD and SEM analysis. Moreover, aesthetical properties have been characterized in term of Hunter parameters (L*a*b). The results of the testing activities show that the glazes containing talc presents similar solar properties of conventional products, but they allow the reduction of the glaze cost (decrease of almost 50% of the TiO_2 pigment cost).

Experimental approach: Preliminary study

Starting from the analysis of an industrial product, industrial formulation (tab 6.1) and heat treatment (T=900 °C) were modified in order to produce five different samples to reduce production costs without affect the solar reflectance.

Table 6.1 – Starting industrial composition

	Wt(%)
Na_2SiO_3	50
$Al_2Si_2O_5(OH)_4$	10
H_2O	10
TiO_2	30

Two different strategies were approached: the replacement of TiO_2 with $Mg_3Si_4O_{10}(OH)_2$ and the variation of firing temperature. In this case the molar ratio between the two pigments was varied from 1:1 up to 1:10 and the temperature was changed from 700 °C up to 1100 °C- (tab 6.2). Kaolin, water and sodium silicate are kept constant. The raw materials were poured in a becker and mixed through a magnetic stirrer for 2 minutes. Subsequently the glaze was dried, milled in agata jar with agata milling balls. The obtained powder was then pressed at 300 Kg/cm^3 and fired in a 60 min heating cycle with a 15 min isotherm. The samples were then quenched in air in order to better approximate the industrial cycle.

Table 6.2 – Formulations of preliminary samples

	$TiO_2/Mg_3Si_4O_{10}(OH)_2$ mol ratio	$Al_2Si_2O_5(OH)_4$	Na_2SiO_3	H_2O	T °C
T1	1:1	5.3	21.1	10.5	700
T2	10:1	5.3	21.1	10.5	700
T3	1:1	5.3	21.1	10.5	1100
T4	10:1	5.3	21.1	10.5	1100
T5	5,5:1	5.3	21.1	10.5	900

Method

Solar properties of the glazes were measured with a Spectrophotometer Uv-Vis-Nir (Jasco V-670) in accomplishment to ASTM E903 (ASTM, 1996). The solar reflectivity spectra were collected from 300nm up to 2500nm with a step size of 5nm. Then solar reflectance value ρ_{sol} of every analyzed surface was calculated by integrating the measured spectral reflectivity ρ_λ (defined as the ratio of reflected part and total amount of incident radiation at the considered wavelength λ), weighted by the standard spectral irradiance of the sun at the earth surface, $I_{sol,\lambda}$ [W/(m²×nm)]:

$$\rho_{sol} = \frac{\int_{300}^{2500} \rho_\lambda I_{sol,\lambda} d\lambda}{\int_{300}^{2500} I_{sol,\lambda} d\lambda} \quad (6.1)$$

In order to better understand the solar properties of the samples, in addition to ρ_{sol}, also Hunter's parameters were measured a X-Rite colorimeter SP-60. In particular L* was checked to allow correlations with $\rho_{vis.}$

Mineralogical analysis were performed through X-ray diffraction (XRD) using using Cu Kα radiation limited to 40 kV and 40 mA and a X'Celerator counter (X'pert PRO, Panalytical). All the samples were collected with a scanning rate of 0.1°/min for 2θ from 10° to 70°.

Finally glaze microstructure analysis were carried out through environmental scanning electron microscope (FEI XL-30). The microstructure of the samples was checked analyzing powdered fired glaze coated with a 10 nm thick gold layer using the sputtering technique.

Table 6.3 – Solar reflectance and L* values of preliminary samples

	Solar Reflectance	L*
T1	0.702	85.36
T2	0.749	84.51
T3	0.662	89.73
T4	0.638	80.93
T5	0.789	90.27

Table 6.3 and fig. 6.1 shows the values measured both for solar reflectance and L* parameter measured for the samples produced. The effect of the temperature is really interesting since the maximum values in solar reflectance and L* is obtained measuring the samples fired at 900 °C while there is a drop in solar reflectance both increasing the temperature and, even if less significant, also decreasing the temperature, while the trend is not so defined analyzing L* parameter.

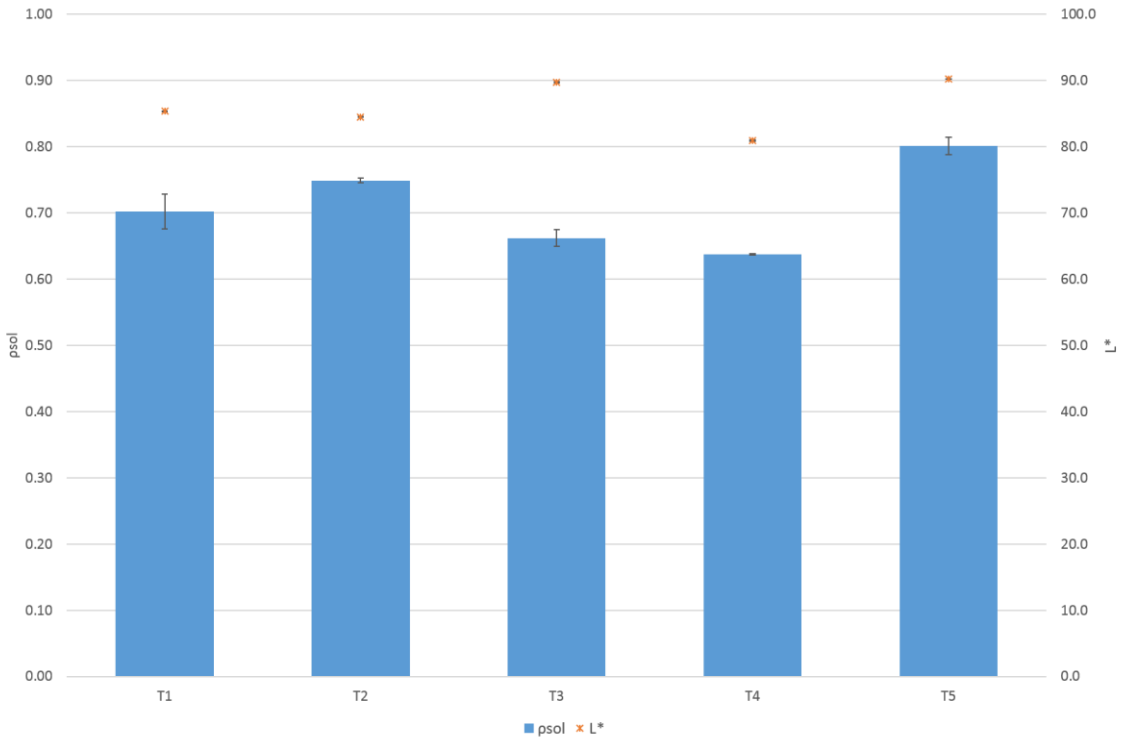

Figure 6.1 – Solar reflectance and L* values measured for the produced samples

From Table 6.3 and fig 6.1 it is also evident how the solar reflectance is affected by the pigment ratio: it is interesting to observe how, at low firing temperature, higher ratio TiO_2/Talc

(10:1) promotes higher solar reflectance, while increasing the firing temperature (T=1100 °C) higher solar reflectance is obtained by the samples with lowest TiO_2/Talc ratio (1:1).

X-ray diffraction and SEM analysis can provide easily explanations supporting solar reflectance trend: in fig. 6.2 diffraction spectra are shown in order to facilitate a comparison between different samples.

The first graph is representative of comparison between different pigment ratio: the orange line represent the sample with higher ratio TiO_2/Talc and the peaks related to Rutile are better developed than the peaks at low 2θ angle related to Talc which are represented by the red spectrum. The influence of the temperature is explained in the second spectra comparison. In this case the samples with higher TiO_2/Talc ratio are compared. The green spectrum represent the sample fired at higher temperature while the orange spectrum is related to the sample fired at lower temperature. From the spectra it is also observed how at 700 °C the amorphous phase is still not well developed, it reaches its maximum in sample T5 (fired at 900 °C) where TiO_2 is embedded in amorphous phase which was enhanced by talc decomposition. From samples heated at 1100 °C Talc melt starts re-crystallization forming magnesium silicate (Enstatite and forsterite). This crystallization contribute to decrease the solar reflectance of the sample. Fig 6.3 support what assumed from XRD comparison: in samples T1 and T2 the presence of the talc is still visible with tabular crystals, T5 sample, as previously assumed, is characterized by a significant amount of amorphous phase which is slightly reduced in samples T3 and T4.

Fig 6.2 shows SEM images obtained through secondary electron detector analysis of powdered glaze. These images confirmed what observed from XRD patterns:

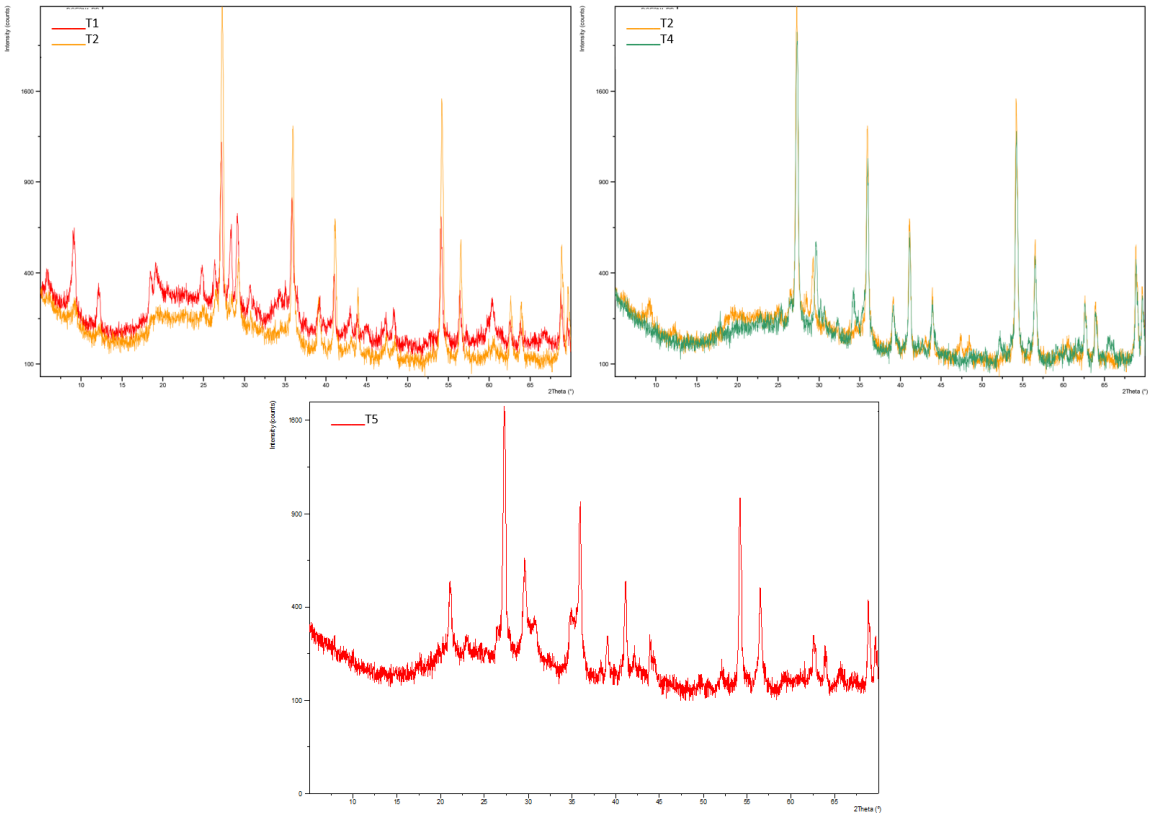

Figure 6.2 - Comparison between diffraction patterns of produced samples

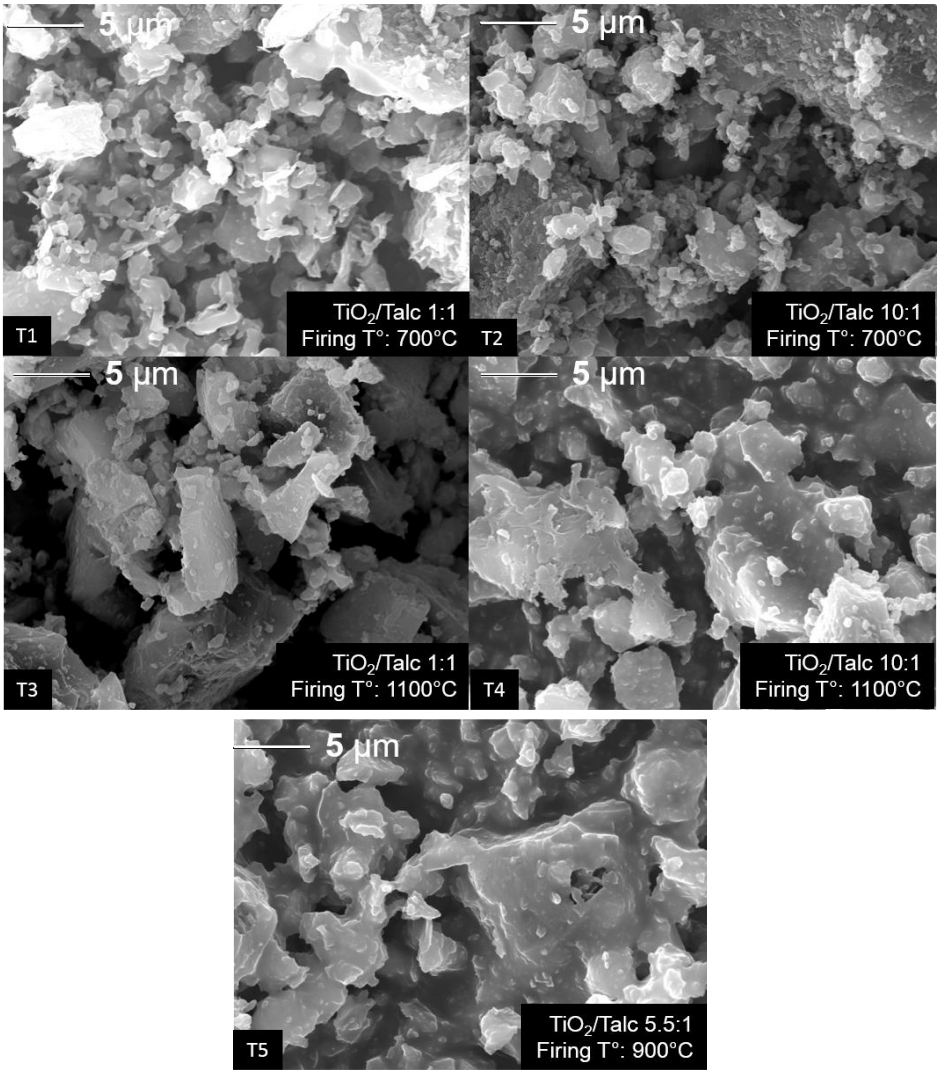

Figure 6.3 - Comparison between SEM micrographs (Secondary electron detector, 4000x)

Optimization of composition to obtain higher solar reflectance

Design of Experiments (DoE) can be used, as a critically important tool, to improve the performances of a process and in particular it can be considered an alternative way to traditional approaches in order to achieve the final goal without performing a large number of experiments. The (statistical) design of experiments (DoE) is an efficient procedure for planning experiments so that obtained data can be analyzed to yield valid and objective conclusions. The final goal of a DoE is to create a predictive model, which can describe the relationships between the input variables and the final properties of the materials.

The guide lines to prepare a DoE are shown in figure 6.4:

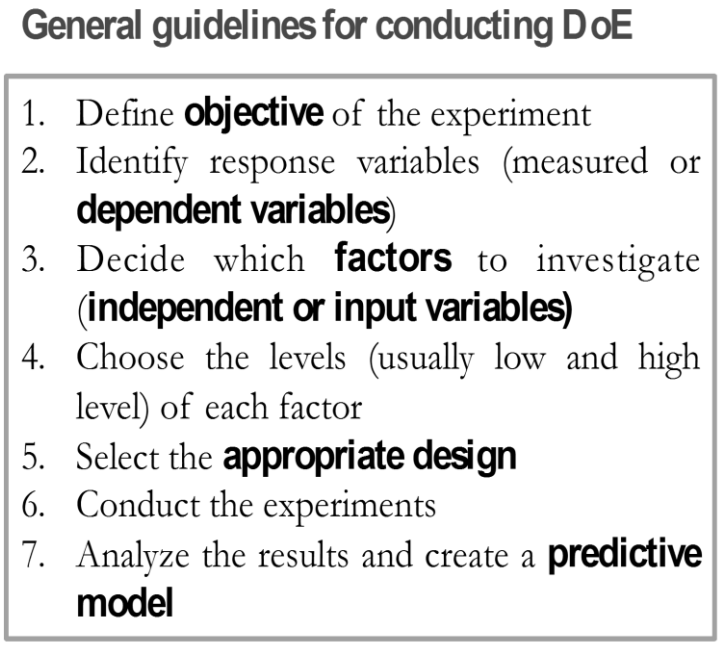

Figure 6.4 – General guidelines for conducting DoE

Factors are the independent variables, which, due to changes in their levels will exert an influence on the system or the process and then on the responses variables. They can be categorized as process factors (temperature, time) or mixture factors (amount of the constituents in a mix) according to the studied system.

They can be quantitative (factors which may change according to a continuous scale) or qualitative (categorical variables, the factor can only assume certain discrete values). At this stage it has been performed a screening study. The primary purpose in screening is to select or screen out the few important main factors from the many less important ones also evaluating the

possible interaction factors. The order in which the experiments run should be randomized to avoid influence by uncontrolled variables (time-related) such as moisture etc. Replications improves the chance of detecting a statistically significant effect (the signal) in the mid of natural process variation (the noise (fig. 6.5)

Dividing experimental runs into homogeneous blocks increase the sensitivity of DoE. Blocking screens out noise caused by known sources of variation, such as raw material batch, machine differences etc. (Eriksson et al.)

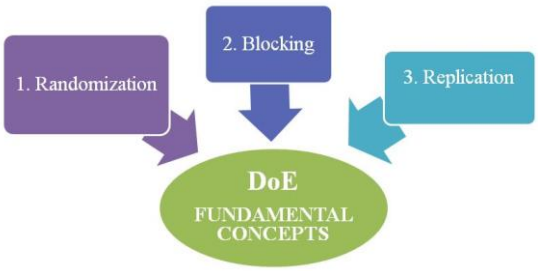

Figure 6.5. - DoE Fundamental concepts

Two-level full factorial design (2^k full factorial design)

Among factorial designs, full factorial design is the most widely used. Here, the experimental work was carried out through a 2k full factorial design, where "2" represents the levels at which the "k" factors are varied. Since this type of design consists of two or more factors with discrete possible values (called levels), the experimental units take on all possible combinations of the levels across all such factors, being 2^k the total number of experiments. In this way, the effect of each factor and their mutual interaction on the response is allowed.

The experimental plan was obtained by using as input factors (independent variables) two quantitative variables (tab. 6.4):

Table 6.4 – Factors considered during experimental plan

Factor	Name	Units	Type	Low Actual	High Actual	Low Coded	High Coded
A	talc	g	Numeric	0	30	-1	1
B	water	g	Numeric	20	50	-1	1

The number of the experiments was calculated through the equation reported below:

The plan is made by 4 experiment and 3 center points, added to facilitate the subsequent data analysis. Moreover, all the experiments were replicate which allows the calculation of the pure error mean square; which is used to check model goodness-of-fit. (Tab. 6.5)

In this plan the firing temperature is considered constant at 900 °C while kaolin is maintained at constant weight (10 wt%)

The response variable considered in this study is represented by ρ_{sol}.

According to the geometry illustrated in fig. 6.6 the plan was developed as reported in tab 6.5. With respect to glaze composition, just two parameters (talc and water amount) are considered since the wt(%) of the pigments sum is 30 while the total amount of liquid phase wt(%) is 60. TiO_2 and Sodium Silicate are calculated in function of Talc and Water content as reported in tab 6.6.

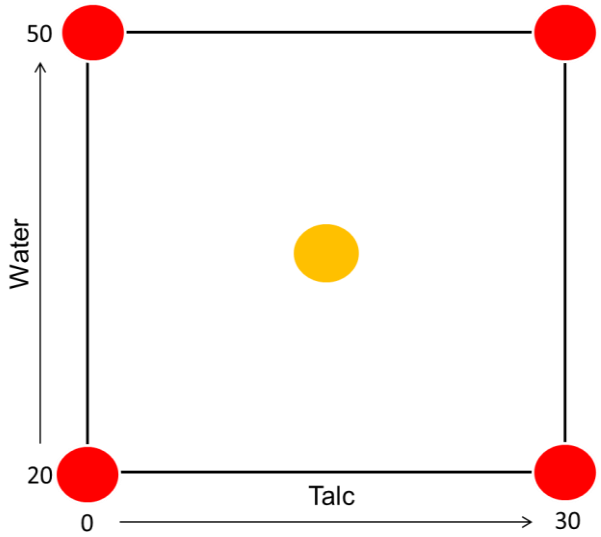

Figure 6.5 - Geometry of 2^2 full factorial design with center point (orange point)

Table 6.5 – Experimental plan for DoE

STD	RUN	TALC	WATER	KAOLIN
9	1	0	20	10
4	2	30	20	10
7	3	0	50	10
11	4	30	50	10
13	5	15	35	10
8	6	15	35	10
5	7	15	35	10
14	8	0	20	10
6	9	30	20	10
12	10	0	50	10
2	11	30	50	10
1	12	15	35	10
3	13	15	35	10
10	14	15	35	10

Likely to what performed in the first part of this study, the raw materials were poured in a becker and mixed through a magnetic stirrer for 2 minutes. Subsequently the glaze was dried, milled in agata jar with agata milling balls. The obtained powder was then pressed at 300 Kg/cm^3 and fired in a 60 min heating cycle with a 15 min isotherm at 900 °C. The samples were then quenched in air in order to better approximate the industrial cycle.

Methods

Even in this case solar reflectance of the samples was measured through a Spectrophotometer Uv-Vis-NiR (Jasco V-670) according to ASTM E903 (ASTM, 1996). All the solar reflectivity spectra were collected from 300nm up to 2500nm with a stepsize of 5nm. Starting from spectral reflectivity, solar reflectance value ρ_{sol} of every analyzed surface was calculated by integrating the measured spectral reflectivity ρ_λ (defined as the ratio of reflected part and total amount of incident radiation at the considered wavelength λ), weighted by the standard spectral irradiance of the sun at the earth surface, $I_{sol,\lambda}$ [W/(m^2×nm)]. The irradiance spectrum used for spectral integrations is AM1GH (Levinson, 2010)

In addition to the development of the DoE, other characterizations were performed.

Mineralogical analysis were carried out through X-ray diffraction (XRD) using Cu Kα radiation limited to 40 kV and 40 mA and a X'Celerator counter (X'pert PRO, Panalytical). All the samples were collected with a scanning rate of 0.1°/min for 2θ from 10° to 70°.

Moreover glaze microstructure analysis were carried out through environmental scanning electron microscope (FEI XL-30). The microstructure of the samples was checked analyzing powdered fired glaze coated with a 10 nm thick gold layer using the sputtering technique.

Results and discussion

In tab. 6.6 are reported the values of measured ρ_{sol} according to AM1GH irradiance spectrum

Table 6.6. Experimental plan for DoE and the obtained solar reflectance data

STD	RUN	TALC	WATER	SOLAR
9	1	0	20	0.791
4	2	30	20	0.700
7	3	0	50	0.825
11	4	30	50	0.725
13	5	15	35	0.753
8	6	15	35	0.744
5	7	15	35	0.757
14	8	0	20	0.791
6	9	30	20	0.678
12	10	0	50	0.817
2	11	30	50	0.721
1	12	15	35	0.753
3	13	15	35	0.746
10	14	15	35	0.759

Evaluation of the data

The data elaboration was made using Design Expert 7

The regression analysis and models interpretation, involves the calculation of the mathematical models in order to correlate the input factors with the measured properties of the material. In this study, a Partial Least Square (PLS) regression method is used to explore the dependence of the responses (spectral properties) on varied factors.

When fitting regression model different parameters: "goodness of fit" (R2), Adjusted R-squared and "goodness of prediction" (Predicted R-Squared) are analyzed: the R2 coefficient of determination is a statistical measure of how well the regression line approximates the real data points. An R2 of 1.0 indicates that the regression line perfectly fits the data. Adjusted R square measures the proportion of the variation in the dependent variable accounted for by the explanatory variables. Unlike R square, adjusted R square allows for the degrees of freedom associated with the sums of the squares. Therefore, even though the residual sum of squares decreases or remains the same as new explanatory variables are added, the residual variance does not. For this reason, adjusted R square is generally considered to be a more accurate goodness-of-fit measure than R square. Predicted R-squared is used in regression analysis to indicate how well the model predicts responses for new observations, whereas R-squared indicates how well the model fits your data. Predicted R-squared can prevent over-fitting the model and it can be more useful than adjusted R-squared for comparing models because it is calculated using observations not included in model estimation. An important tool for the design of experiments analysis is the analysis of variance (ANOVA) which, it can be used in the regression analysis to separate and estimate the different causes of variation such as those associated with systematic errors and those arising from random errors. ANOVA involves two tests that assess the truth of a hypothesis which is known as the null hypothesis. It is the hypothesis to be tested and the term null implies that there is no difference between the considered means. ANOVA is based on partitioning the total variation of a selected response into one part due to the regression model and another part due to the residuals. When replicated experiments are available, as in this study, ANOVA also decomposes the residual variation into one part related to the model error and another part linked to the replicate error. Subsequently, the numerical sizes of these variance

estimates are compared by means of F-tests. The first F-test named regression model significance test compares the variance related to the regression model and the variance of the residuals (MS regression/MS residual); then retrieving the probability, p that this two variances originate from the same distribution. It is common practice to set p=0.05 as the critical limit. A p-value lower than 0.05, indicates a good model; the two variances are unequal and not drawn from the same distribution and the null hypothesis is rejected. The second F-test named lack of fit test compares the size of the two variances MS model error and MS replicate error. In the ideal case, the model error and the replicate error are small and of similar size then the F-test show a low result and the p-value is larger than the critical value (p=0.05), hence, the model has a small model error and good fitting power, that is, shows no lack of fit.

Other important information on the goodness of the model can be revealed by the residuals analysis. It is known that a good model should be characterized by normally distributed errors, so the N-probability plot is taken into account in order to verify the normal behaviour of the residuals and then to detect deviating experiments. In addition to regression analysis, also model interpretation plays an important role in the data analysis: studying the coefficient plot it is possible to decide if the model can be used for model interpretation, and, eventually, model pruning. The regression coefficients of the model and their confidence intervals are obtained and it is possible to know the real effect of the coefficients on the measured properties, identifying which factors improve the mechanical properties of the green body. Finally, through the response contour plot we can analyze the studied region in order to choose the best point at which conduct test experiments or anchor a subsequent design.

In the replicate plot (Fig. 6.7) the measured values of a response are plotted against the number of each experiment. The replicate experiments (and the six centre points) are plotted in the same bar.

The replicate plot reports that the variation among the replicate experiments (Exp C5, C6, C7, C12, C13, C14) is lower than the variation of the entire data, indicating that the replicate error will not complicate the data analysis.

Moreover, the six central points are positioned in the center of the range of the obtained values suggesting that the linear model could be suitable to describe the studied system.

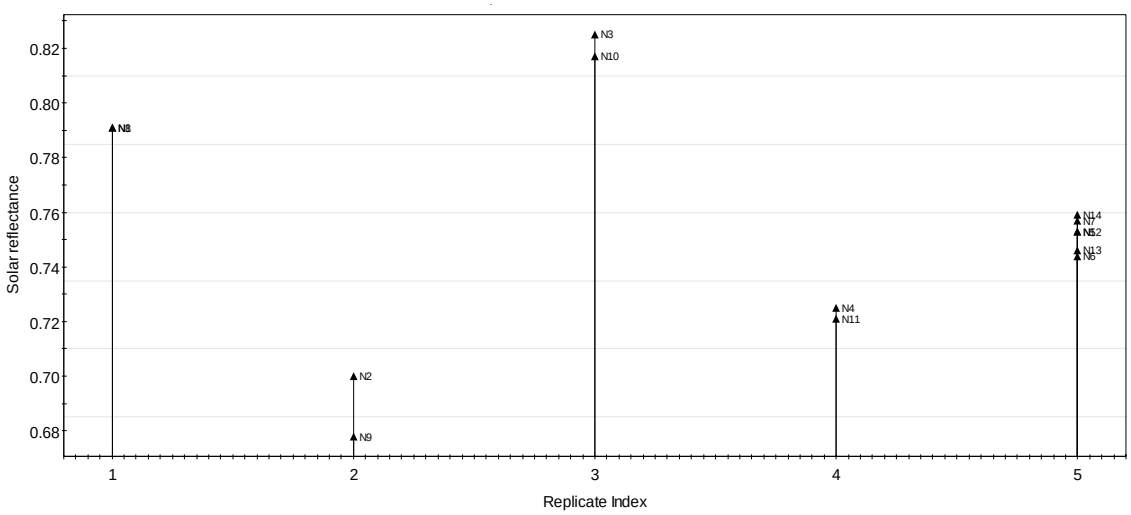

Figure 6.7 - Replicate plot for solar reflectance

Regression Analysis

Table 6.7 - ANOVA results for the interaction model

Source	Sum of Squares	df	Mean Square	F Value	p-value Prob > F	
Model	0.022	3	0.007	144.439	< 0.0001	significant
A-talc	0.020	1	0.020	392.663	< 0.0001	
B-water	0.002	1	0.002	40.580	0.0001	
AB	3.7E-06	1	3.70E-06	0.073	0.793	
Curvature	5.02E-05	1	5.02E-05	0.986	0.347	not significant
Pure Error	0.001	9	5.10E-05			
Cor Total	0.022	13				

Lack of Fit (Model Error)	1	5.49E-05	5.49E-05	1.078	**0.326**	0.007
Pure Error (Replicate Error)	9	0.001	5.09E-05			0.007

The F-Value of the model implies that the linear model is significant. The regression model significance test compares the MS regression and the MS residual; the ratio between these two variances (F-value) is equal to 144 and the p-value is <0.05 thus, the compared variance are not equal and the considered models are statistically significant for the studied properties for a confidence interval of 95% (the null hypothesis is rejected.)

The Lack of fit is not significant. The lack of fit test shows an F-value (MS model error /MS replicate error) of 1.08 and a p value higher than 0.05 suggesting that, the two variances are closed to each other and no lack of fit can be noted. Hence, the test is satisfied (the null hypothesis is retained) and a good fitting of the data is obtained.

As regard the R-Squared a value approaching one is desirable. In our case, the value is close to one thus the model is good. At the same time, R-squared is also high and close to R square. Adequate precision measures the signal to noise ratio. A ratio great than 4 is desirable. In our case, the value equal to 30.9 indicates an adequate signal. This model can be used to describe the design space.

Table 6.8 - Model parameters

R-Squared	0.980
Adj R-Squared	0.973
Pred R-Squared	0.938
Adeq Precision	30.984

R-Squared: A measure of the amount of variation around the mean explained by the model.

Adj R-Squared: A measure of the amount of variation around the mean explained by the model, adjusted for the number of terms in the model. The adjusted R-squared decreases as the number of terms in the model increases if those additional terms don't add value to the model.

The predicted R-squared and the adjusted R-squared should be within 0.20 of each other. Otherwise there may be a problem with either the data or the model. Look for outliers, consider transformations, or consider a different order polynomial.

Adequate Precision: This is a signal to noise ratio. It compares the range of the predicted values at the design points to the average prediction error. Ratios greater than 4 indicate adequate model discrimination.

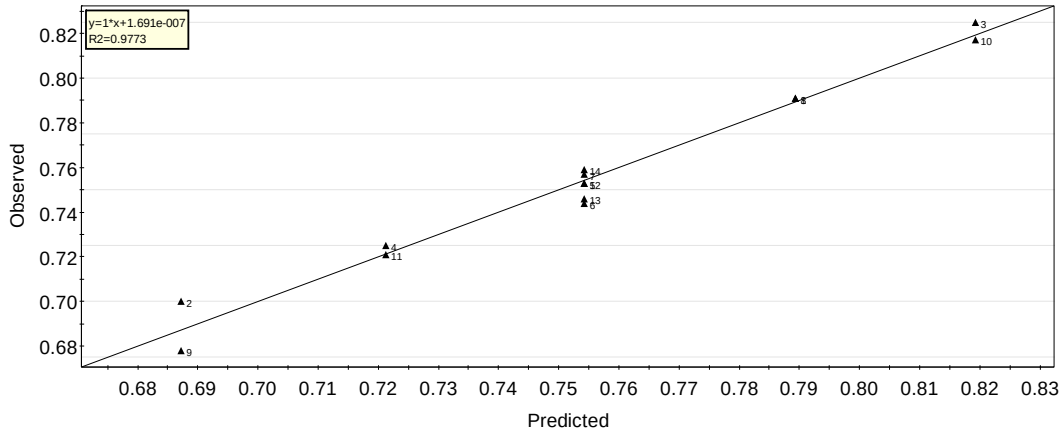

Figure 6.8 - Predicted versus actual

In Figure 6.8 the relationship between calculate and observed response values are is illustrated. As it is possible to observe that the measured values are located near the line of the predictive ones.

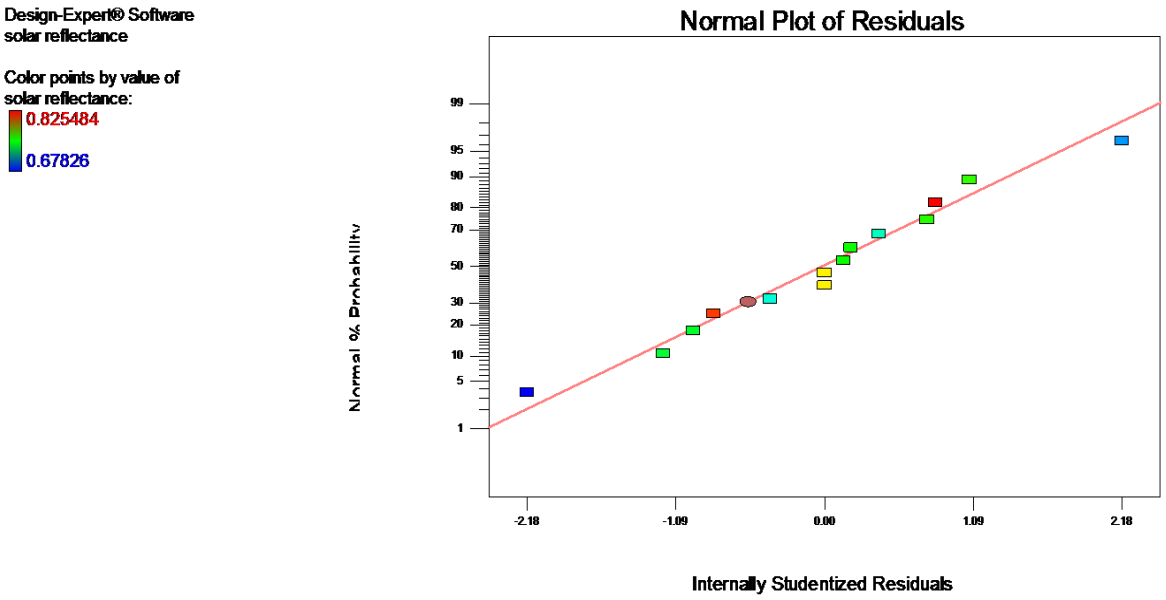

Figure 6.9 - N-Probability plot

Normal distribution of the residuals. As previously mentioned, important information on the goodness of the model can be revealed by the residuals analysis in order to detect deviating experiments. Observing the Normal probability plot (Figure 6.9) of the standardized residuals, it is possible to see that the residuals are normal distributed thus, it is possible to move towards the model interpretation to check the significant factors.

Model interpretation

Table 6.9 - Estimated coefficients

Factor	Coefficient Estimate	df	Standard Error	95% CI Low	95% CI High	VIF
Intercept	0.756	1	0.003	0.750	0.762	
A-talco	-0.050	1	0.003	-0.056	-0.044	1
B-acqua	0.016	1	0.003	0.010	0.022	1
AB	0.001	1	0.003	-0.005	0.006	1
Center Point	-0.004	1	0.004	-0.013	0.005	1

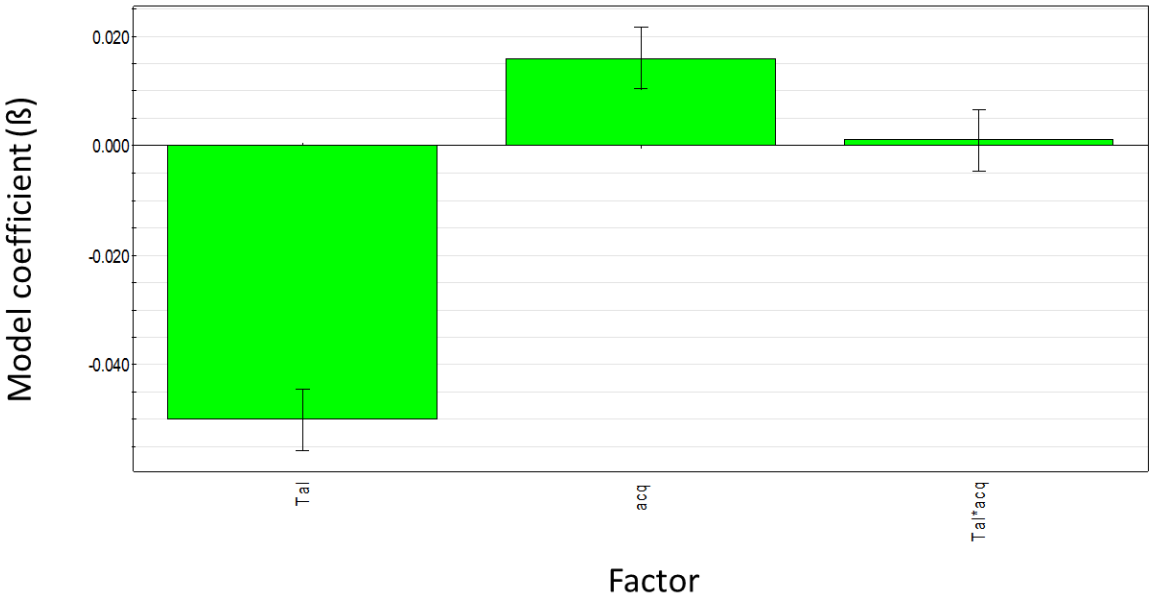

Figure 6.10 - Bar chart with scaled and centered regression coefficients with 95% confidence intervals

Significant components

The effect of a single factor is also called a main effect. Interactions occurs when the effect of one factor on a response depends on the level of another factor. The two selected input factors are significant, since the confidence interval (95% CI) does not include "0".

The interaction term is not significant.

In Table 6.9 and Figure 6.10 the scaled and centered regression coefficient values are reported. Particularly, in the Figure 6.11 and 6.12 each factor is illustrated in the x-coordinate

while their regression coefficient value is shown in the y-coordinate. It is possible to note that there are two coefficients statistically significant.

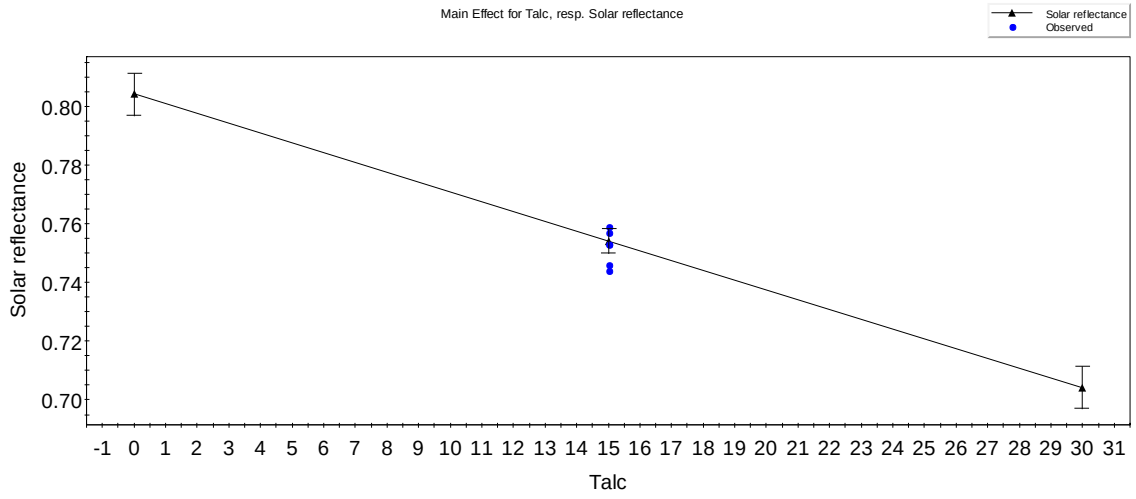

Figure 6.11 - Main effect for talc

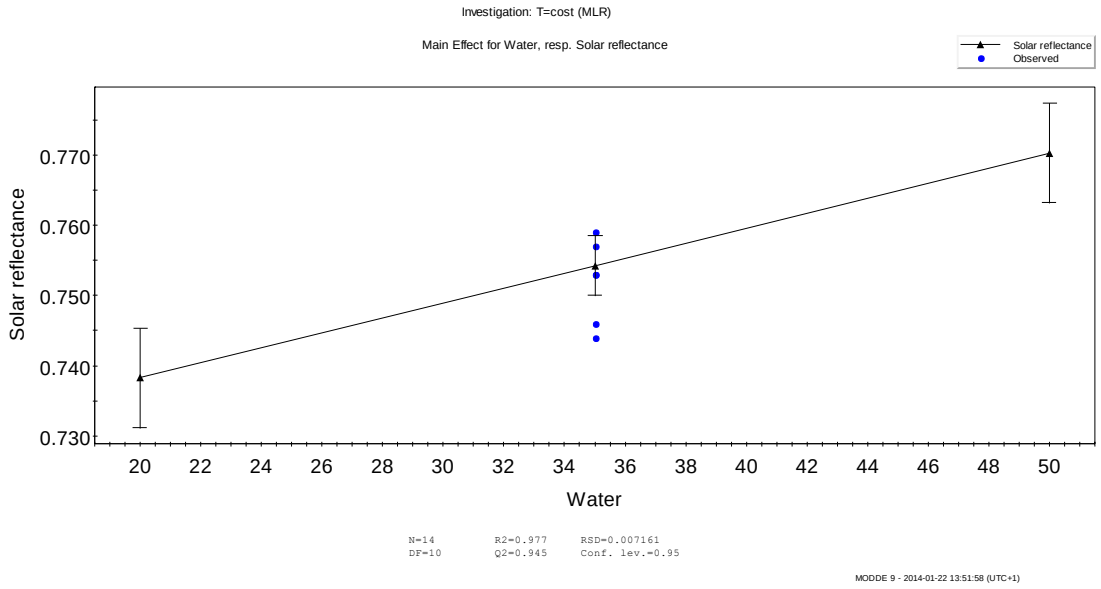

Figure 6.12 - Main effect for water

The response contour (fig. 6.13 and 6.14) plot allows to analyze the studied region in order to choose the best point at which conduct test experiments or anchor a subsequent design.

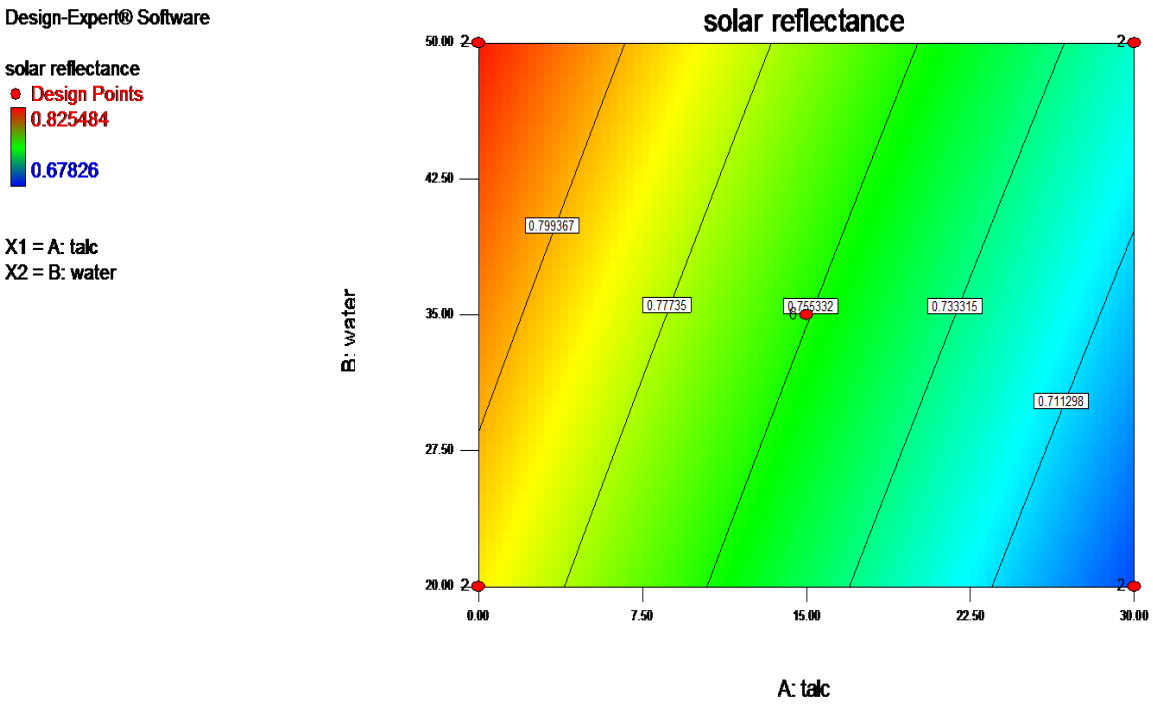

Figure 6.13 - 2D Contour plot for solar reflectance

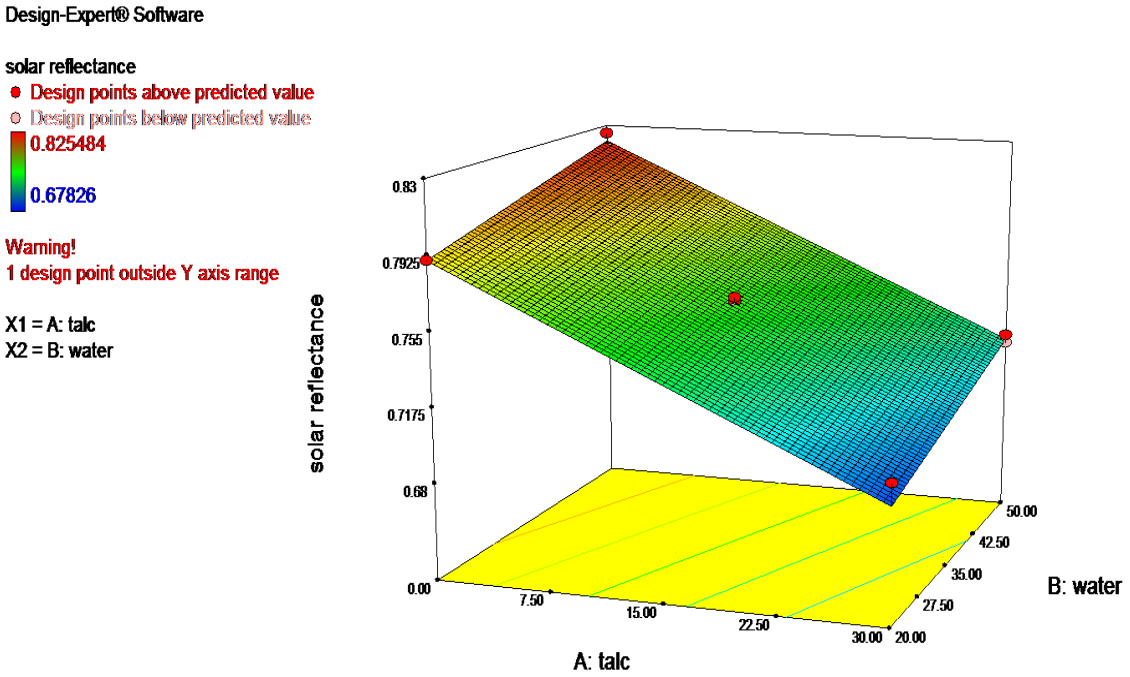

Figure 6.14 - 3D Contour plot for solar reflectance

In order to validate the model, three test point (tab 6.10) were prepared and measured

Table 6.10 – Validation samples formulation

STD	RUN	TALC	TiO_2	WATER	SODIUM SILICATE
15	15	10	20	50	10
16	16	10	20	40	40
17	17	0	30	30	30

Samples were prepared and fired at 900 °C according to the procedures adopted for all the samples produced in this study in order to not introduce new variables in the system. Solar reflectance was measured for each sample. Measured values were reported in tab 6.11 with predicted values. As it is shown by the table it can be assumed that the model predicts in a quite good way the solar reflectance of the samples even if the predicted values are always slightly underestimate.

Table 6.11 – Solar reflectance measured for each validation sample

STD	RUN	SOLAR REFLECTANCE Measured	SOLAR REFLECTANCE Predicted	Lower	Upper
15	15	0.805	0.787	0.779	0.794
16	16	0.791	0.755	0.748	0.763
17	17	0.816	0.799	0.792	0.807

After DoE analysis, microstructural and mineralogical analysis were carried out on most significant samples, in particular samples C1, C2, C3, C4 and C5 were considered

In fig 6.15 XRD patterns are reported: in the first picture two samples with the same amount of liquid phase, the spectrum drawn with red line represent a sample containing the maximum amount of TiO_2 while the spectrum drawn with the orange line represent a sample containing the maximum amount of Talc. In the second picture, samples containing the maximum amount of TiO_2 are compared. The sample C1 contain lower amount of water (and higher amount of sodium silicate) if compared with C3. This is recognizable by the higher background line of the red spectrum typical of higher amount of amorphous phase.

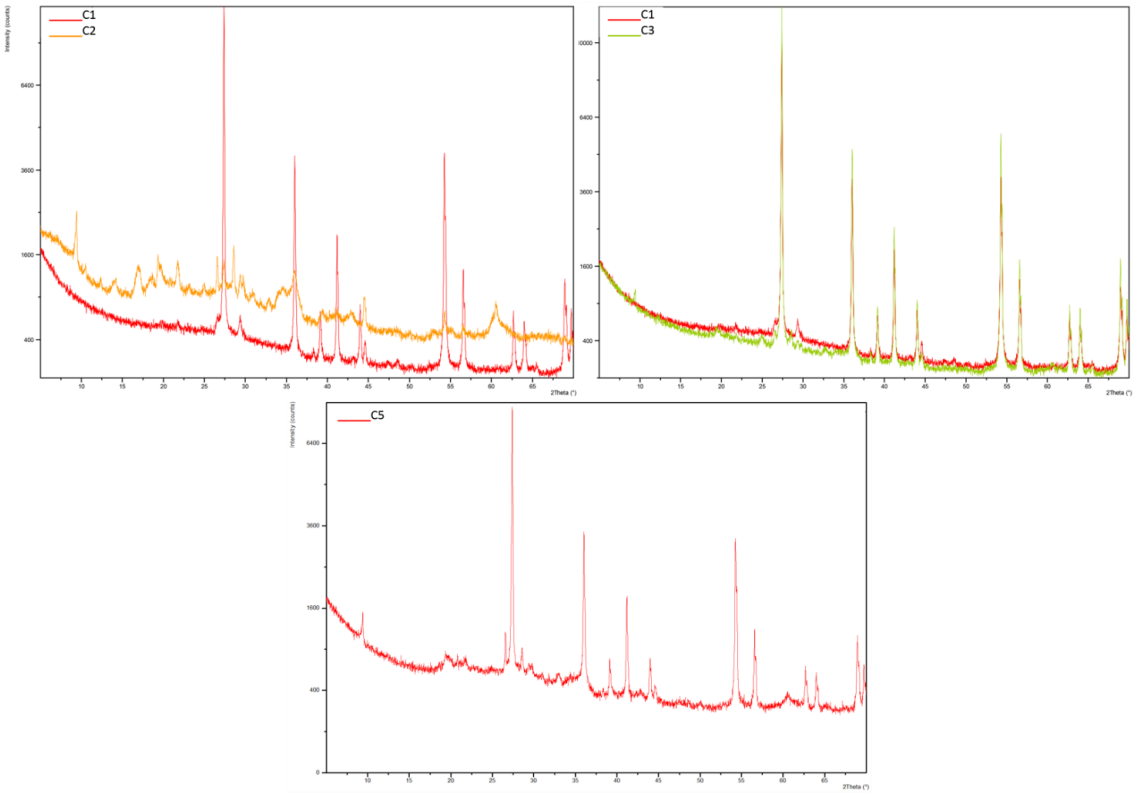

Figure 6.15 – XRD pattern of most significant DoE samples

In Fig. 6.16 microstructural analysis of powdered glazes are reported. All the SEM images are collected through Secondary Electron Detector.

On samples containing a low amount of water, and high amount of sodium silicate (C1, C2), the presence of higher amorphous phase is evident

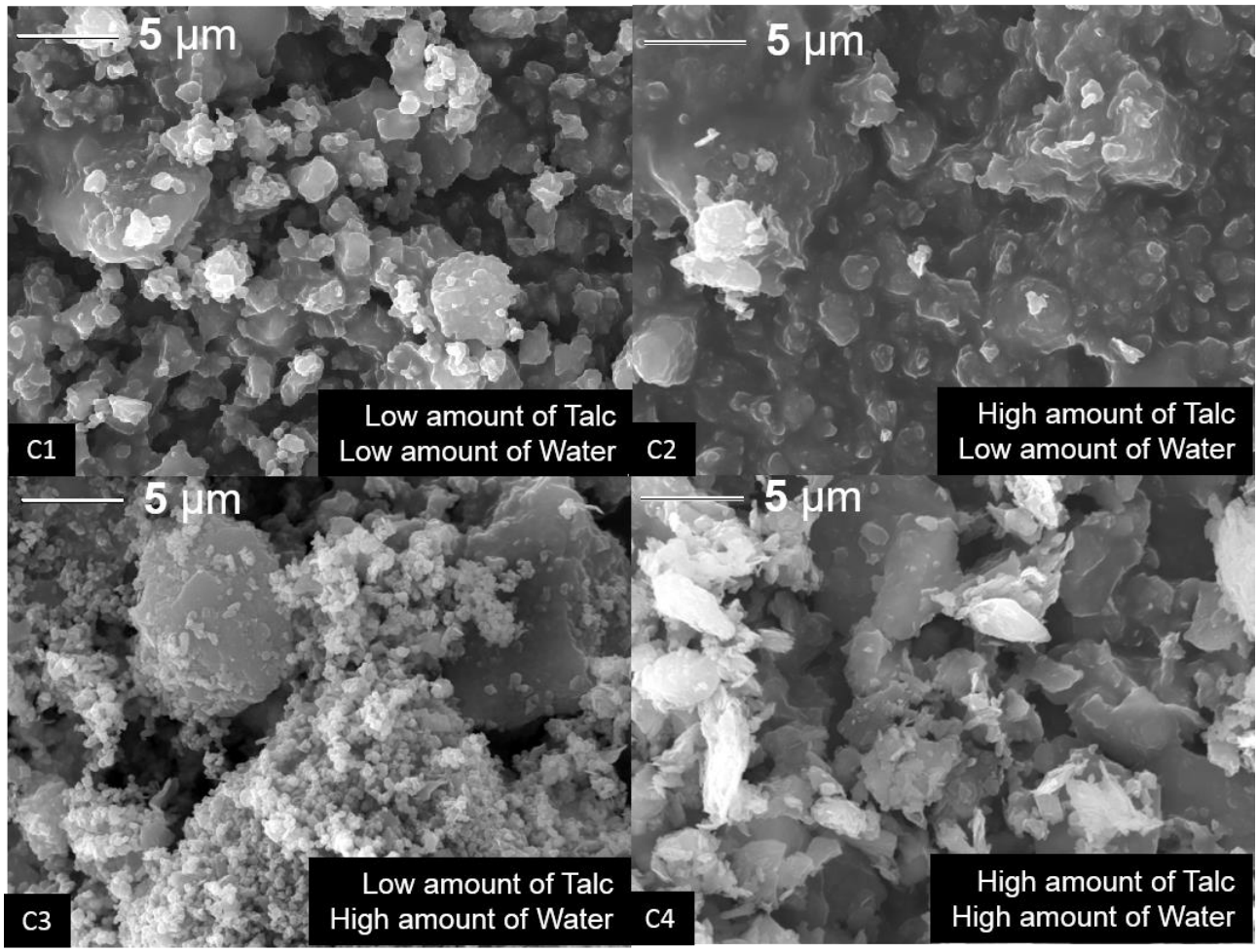

Figure 6.16 - Comparison between SEM micrographs (Secondary electron detector, 4000x)

Conclusion

New ceramic glazes for asphalt shingles were formulated with regards to solar reflectance trying to reduce costs. In order to reduce the cost of the glaze two parameters can be tuned: the firing temperature, the pigments embedded into the glaze and the liquid phase.

Concerning the temperature, industrial firing cycle (T=900 °C) was the temperature developing better solar reflectance.

Concerning the pigments, industrially, titanium dioxide was the pigment industrially used for these glazes; since it high cost TiO_2 was replaced with talc which has a cost 10 times smaller than TiO_2.

In order to evaluate the contribute of pigment and liquid phase a 2k mixture design was studied where the independent values considered are talc and water amount. Since the sum of pigments and the sum of liquid phase is constant, the amount of TiO2 and sodium silicate is obtained as a difference between the weight of pigments or liquid phase and the weight given by the plan. The model present a linear trend where the talc present a negative influence on the solar reflectance while the water has a positive influence on the solar reflectance.

The model applied presents a very low number of experiments, due to this a limitate number of information can be retrieved from the data. This is, in fact, considered as a screening analysis, in order to formulate a wider DoE analyzing a more accurate pigment ratio, the temperature and the duration of firing cycle, the substrate influence… in order to obtain more precise informations about low cost and high performance system.

Chapter references

ASTM (1996). ASTM E 903-96 – Standard test method for solar absorptance, reflectance, and transmittance of materials using integrating spheres. Standard of the American Society for Testing and Materials.

Berdahl, P., Akbari, H., Levinson, R., Jacobs, J., Klink, F., and Everman, R. (2012). Three-year weathering tests on asphalt shingles: Solar reflectance. Solar Energy Materials and Solar Cells, 99, 277-281.

Cool Roof Rating Council Rated Product Database - http://coolroofs.org/products/results

Design Expert 7 - http://legacy.statease.com/dx7descr

EPA, 2008, Reducing Urban Heat Islands: Compendium of Strategies: Basic and Cool Pavements Compendium Environmental Protection Agency.EPA

EPA, 2010, http://www.epa.gov/climatechange/wycd/waste/downloads/asphalt-shingles10-28-10.pdf (Accessed 20th January 2014).

Eriksson L., Johansson E., Kettaneh-Wold N., Wikström C., and Wold S.: Design of Experiments: Principles and Applications - Learn about the fundamentals of design of experiments and how such principles aid in quality-by- design and design space investigations. ISBN 91-973730-4-4

Levinson R., Akbari H., Berdahl P. (2010a), Measuring solar reflectance—Part I: Defining a metric that accurately predicts solar heat gain, Solar Energy, 84(9), 1717-1744

CHAPTER 7
INFLUENCE OF NATURAL AND ARTIFICIAL AGEING ON THE SOLAR REFLECTANCE OF CLAY ROOF TILES

Brief introduction

Clay roof tiles are widely used as roofing materials because of their good mechanical and aesthetical properties. The exposure to atmospheric agents and, most of all, to pollutants and smog affects negatively the solar reflectance of a tile surface. The aim of this study is to analyze the influence of ageing on the solar reflectance of clay roof tiles. We studied samples provided by manufacturer in Greece and USA. Samples were coated with either organic or inorganic coatings. Natural ageing processes were used for samples with inorganic coating, and artificial ageing simulation was performed on all samples. Samples were naturally aged in a test farm in Arizona, with an exposure time of 3 years. In artificial ageing processes, the surface of the tiles was subjected to the application of two different mixtures simulating exposure to i) Arizona weathering agents such as clay, salts and soot and ii) Arizona, Florida and Ohio weathering agents through an average mixture made by clay, salts, particulate organic matter and soot. The amount of soiling mixture deposited on the surface of the samples was aimed at reproducing a 3 years exposure. Soiled samples were subjected to air blowing and rinsing under running water to simulate the wind and rain effects, respectively. The effects of both natural ageing and artificial soiling on the surface reflectivity of the clay roof tiles were assessed in the UV-Vis-NIR range (range from 300 to 2500 nm). The two different soiling conditions were found to affect significantly the solar reflectance of the samples, in particular the samples soiled with the average mixture present a decrease up to 0.20, while Arizona weathering condition affects the solar reflectance up to 0.05, and neither air blowing nor rinsing seem to permit a significant recovery

of the surface properties. All solar reflectance measurements were computed by averaging the spectral reflectivity weighted by the AM1GH solar spectral irradiance

Aim of the project

In this study the solar reflectance according ASTM E903 and ASTM C1549 was measured considering AM1GH irradiance spectrum. The study is divided into two different parts: the first one analyzes the differences between natural and artificial ageing, while the second one regards the application of ageing studies on samples from Italy characterized by an ancient nouveau aesthetical finishing. This particular surface finishing try to reproduce in an artificial way, with the application on the surface of the sample of inorganic glazes, the aspect of an aged tile in order to facilitate the integration of new roof tiles in restoration of roof tiles which presents on their surfaces moss, algae and lichens.

In the first part of this project, two different sets of fresh samples coated with inorganic and organic cool coatings and a set of samples coated with inorganic coating and aged for 3 years in Arizona climate were analyzed. On fresh samples were applied accelerated soiling protocols simulating both Arizona and Average (Arizona, Ohio and Florida) conditions. On each weathered sample (both natural and artificial) wiping and rinsing were applied in order to simulate wind and rain effect and solar reflectance was measured after each step. These analysis allowed us to understand that there is a good match between natural ageing under Arizona conditions and artificial ageing at the same conditions and neither rain simulation nor wind simulation can restore solar reflectance on clay roof tiles

In the second part of this project three different sets of samples, from three different part of the Country, were considered. Different supplier provided both fresh and aged samples. In addition to the solar reflectance analysis, in this case, mineralogical and microstructural analysis were carried out in order to try to correlate the variations on the solar reflectance behavior with the surface structure of the various samples.

Experimental approach: Natural vs ageing

Two different macro-set of samples were used in order to carry out this study: from California we received four sets of samples made by five fresh and five 3-years-aged coupons; from Greece we received four sets of samples made of 4 fresh samples (Tab.7.1).

All the samples, like traditional terracotta red ceramics, present a substrate made by ceramic material obtained by mixing quartz, feldspar, calcium carbonate and different clays. In order to reduce the cost of the finished product, raw material sources located close to the tile plant are used; this often affects the quality of the clay due to the high levels of iron.

All samples, both fresh and aged, were in good mechanical conditions.

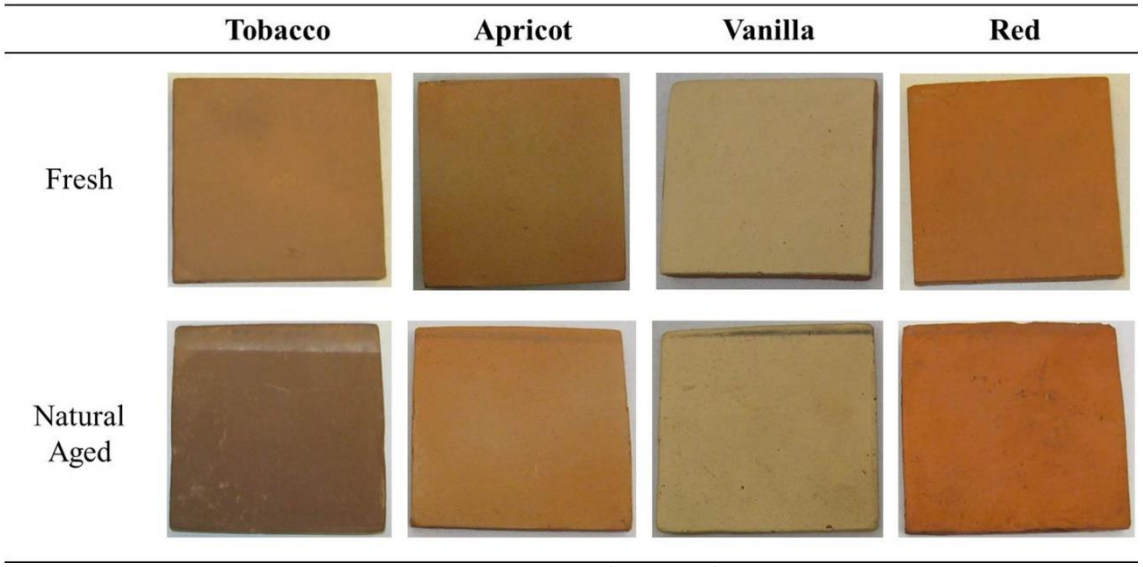

Figure 7.1 – Samples from California

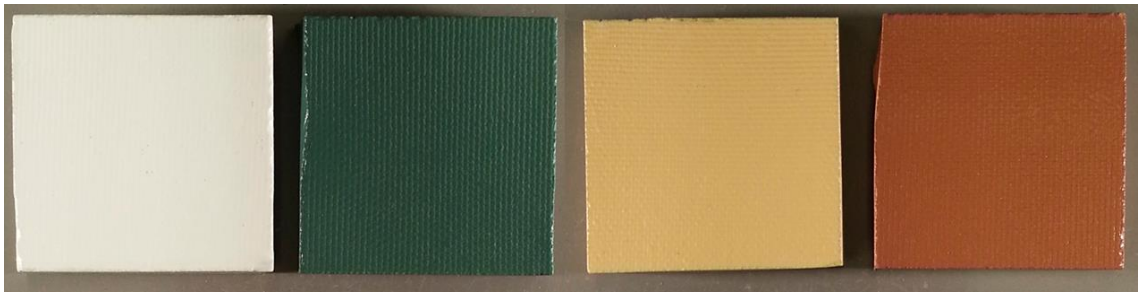

Figure 7.2 - Samples from Greece

Table 7.1 - Samples from Greece and California

Location	Color	Condition	Place of ageing	Time of ageing	Substrate nature	Coating nature
California	Tobacco	Unweathered	N/A	N/A	Clay tile	Inorganic
		Weathered	Arizona	08.2007/ 09.2010	Clay tile	Inorganic
	Vanilla	Unweathered	N/A	N/A	Clay tile	Inorganic
		Weathered	Arizona	08.2007/ 09.2010	Clay tile	Inorganic
	Apricot	Unweathered	N/A	N/A	Clay tile	Inorganic
		Weathered	Arizona	08.2007/ 09.2010	Clay tile	Inorganic
	Red	Unweathered	N/A	N/A	Clay tile	Inorganic
		Weathered	Arizona	08.2007/ 09.2010	Clay tile	Inorganic
Greece	Beige	Unweathered	N/A	N/A	Clay tile	Organic (Paint)
	Brown	Unweathered	N/A	N/A	Clay tile	Organic (Paint)
	Green	Unweathered	N/A	N/A	Clay tile	Organic (Paint)
	White	Unweathered	N/A	N/A	Clay tile	Organic (Paint)

Method

As reported by Levinson (2010a) and Levinson (2010b), the near-normal hemispherical solar spectral reflectance (300–2500 nm @ 5 nm intervals) and the total reflectance corresponding to air-mass 1 global horizontal radiation (AM1GH) of a 10mm2 area at the center of each sample were calculated according to ASTM Standard E903 (ASTM, 1996), using a PerkinElmer Lambda 1050 UV/Visible/NIR Spectrometer with 150 mm integrating sphere.
The global solar reflectance of each tile was estimated as the mean of ASTM Standard C1549 air-mass 1.5 solar reflectance (ASTM, 2002) measured with a Devices & Services Solar Spectrum Reflectometer (model SSR-ER v.6) at several 2.5-cm diameter spots (five per samples from California, four per samples from Greece) over the whole sample area.

Sample preparation

In the first step, the solar reflectance was measured for both weathered and unweathered samples as received by the suppliers. The unweathered samples from California and Greece were, then, artificially weathered in the LBNL laboratories applying three different conditions identified as “After weatherometer”, “Arizona” and “Average”. The first set made by one coupon

from each sample a 24 hours weathering cycle was applied with a QUV/SPRAY from Q-LAB (2013) according to ASTM G154 (ASTM, 2012). The cycle was made by 8 hours of UV light exposure at the conditions of 0.89 W/m2 and T=60°C, and 4 hours of water condensation at T=50°C, repeated twice.

Other two sets made by one coupon from each sample were artificially soiled applying, after a 24 hours weathering cycle as described above, Arizona soiling condition (Fig. 7.3) and an Average (Fig. 7.4) of the soiling conditions presented in the three location selected by the CRRC as a reference for the weathered samples (Ohio, Arizona and Florida) (Tab. 7.2)

Figure 7.3 - Samples from Greece after accelerated ageing simulating (Arizona weathering conditions)

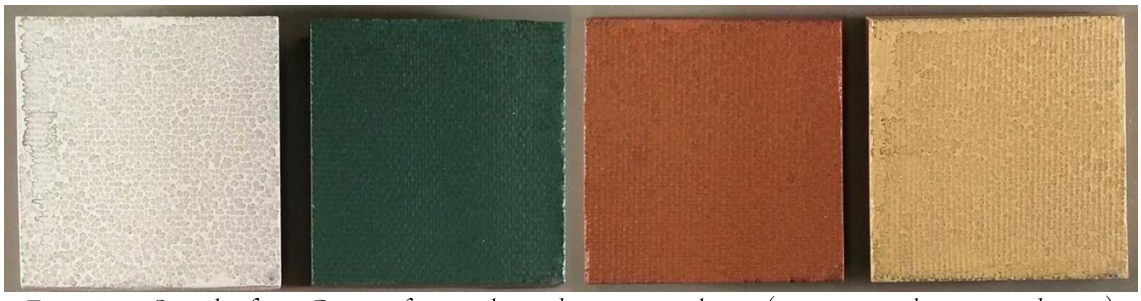

Figure 7.4 - Samples from Greece after accelerated ageing simulating (average weathering conditions)

Table 7.2 - Soiling mixture wt% composition

	Dust	Salts	POM	Soot
Arizona Mixture	79 wt%	20 wt%	0 wt%	1 wt%
Average Mixture	47 wt%	20 wt%	28 wt%	5 wt%

After the weatherometer exposure, all the samples were dried for one hour under a heating lamp. Once the surface was completely dried, the soiling mixture was applied on the samples surface through a device, which allows to deposit, through a spray nozzle, a mixture of soiling agents in aqueous suspension put in a pressurized vessel and. Once ageing was applied, all the artificially soiled samples were dried under heating lamp for 1 hour in order to bind the

soiling mixture to the surface and then they were treated with another 24 hours weathering cycle, and then dried again.

Both naturally and artificially aged coupons were treated with two different surface processes, which tried to simulate the most common natural weathering agents, i.e. wind and rain. The surface of the samples was blown with a hairdryer set on cold air flux to simulate wind and was rinsed under cold running water to simulate rain. Both processes were applied for two minutes on each coupon and after each process the samples were dried under a heating lamp. Solar reflectance was measured with both the spectrophotometer and the reflectometer. These processes yielded eleven different cleaning steps for each sample analyzed considering the two cleaning mechanism shown above and both the unweathered, the samples just weathered, the naturally soiled, the two artificially soiled, and their respective artificially weathered conditions

Results and discussion

The samples images (Fig. 7.3 and Fig. 7.4) show how the soil layer affects visibly the surface. It is interesting to notice the different deposition patterns of Arizona and Average soiling mixture on the samples surface. Only organic coated surfaces pictures are shown here, since because of the very homogeneous surface structure, the soiling layer is more visible than on the samples with inorganic coatings.

Figs. 7.5 and 7.6 shows the spectral reflectivity of the samples coated with an inorganic layer, whereas Figs. 7.7 and 7.8 present the spectra related to the samples coated with an organic paint. Moreover, in each graph the AM1GN solar irradiance spectrum is also reported in order to graphically shows the variation of the solar radiation reaching the earth in the measurement range.

Graphs in figure 7.5 and 7.7 show the spectral reflectivity behavior of the untouched samples. In Figs. 7.6 and 7.8 all the soiling and the related cleaning steps are reported for the most significant sample of each category.

Analyzing inorganic coatings, the lighter colored samples such as vanilla and apricot present higher loss after soiling, moreover the differences between Arizona natural and artificial ageing range from 0.05 to 0.11 except for tobacco samples which present a difference of 0.017

between natural and artificial soiling. Analyzing the cleaning steps the higher gain both in Wiping and Rinsing is reached by apricot sample which in Artificial Arizona soiling recovered 0.007 and in Natural Arizona soiling recovered 0.012 in solar reflectance. In order to better analyze the reflectance gain through the different cleaning steps, in Tab. 7.3 the ratios between the unsoiled solar reflectance and the different reflectance values measured according to ASTM E903 (ASTM, 96) are reported.

Concerning the samples coated with organic layers, the beige samples present a higher loss in solar reflectance when treated with Arizona mixture, while the brown sample presents the lower one. The brown sample presents also the lower loss in solar reflectance considering the surfaces treated with average mixture, while the white one presents the higher loss. Considering the cleaning steps, the higher gain is reached by the white samples rinsed after average soiling mixture exposure, but the gain is as small as 0.001. Since the precision of the instrument is 0.002, it can be assumed that no real gain occurs.

If inorganic coating (fig. 7.5 and fig. 7.6) spectra are compared to organic coatings (fig.7.7 and 7.8) the most important aspect to highlight is the deep difference between the trend in the NiR fraction. In the range between 1750 nm and 2500 nm, and more accentuated in the range between 2250 nm and 2500 nm, a drop in solar reflectivity of organic based coatings occur. This trend is not present in the spectra related to inorganic based samples. Comparing fig. 7.2 and 7.7 it is important to notice how the green sample, which present the lowest reflectance not only among organic based samples but among all the studied samples, presents, is also characterized by an absorption band located in the 1250-1750 nm wavelength range which affect in a significant way the reflectance of this sample.

Only organic coatings pictures are shown in Figs. 7.2-7.4 because, for samples with inorganic coatings, due to the higher roughness of the surface, the soiling mixture deposition did not affect visibly the surface of the coupons. The two soiling mixtures were applied using the same setup and the same protocol; however, it is interesting to notice how they create two completely different patterns on the two surfaces. This can be due to the different chemical composition of the mixtures. The peculiar surface morphology of the two coupons, in addition, affected the distribution of the soiling droplets on the surfaces, according to what is evident in Fig. 7.4.

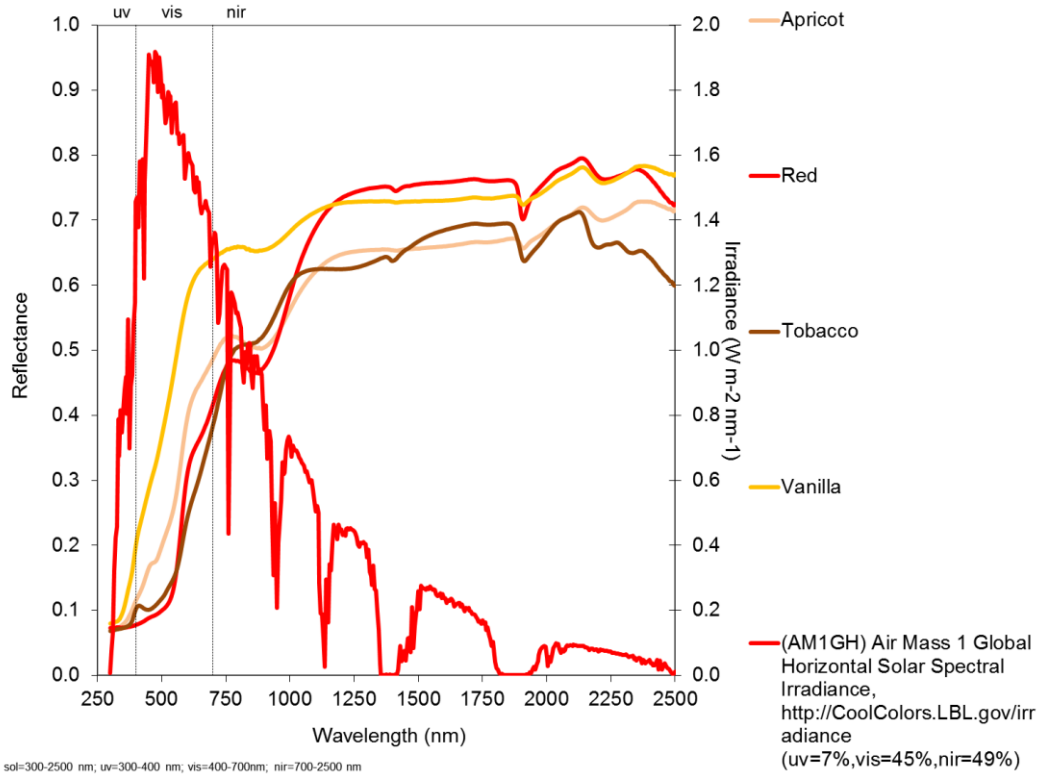

Figure 7.5 - Spectral reflectivity of unweathered samples with Inorganic coating and AM1GH irradiance spectrum

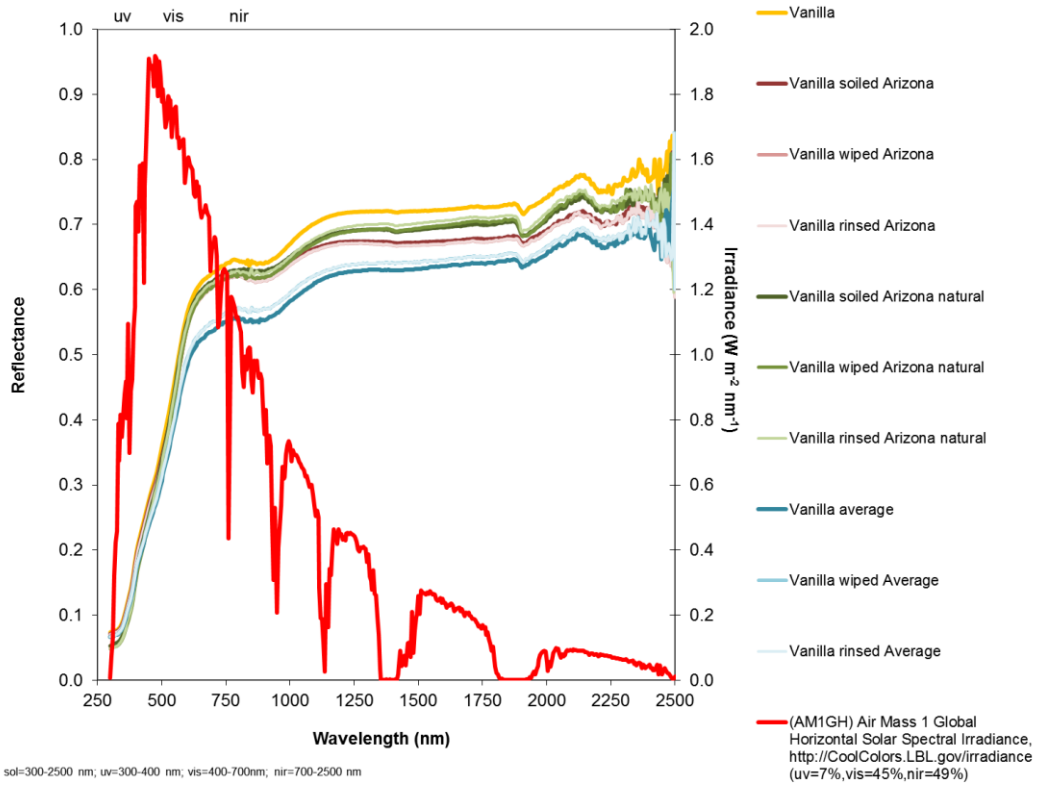

Figure 7.6 - Spectral reflectivity of the soiling and cleaning step on Vanilla sample and AM1GH irradiance spectrum

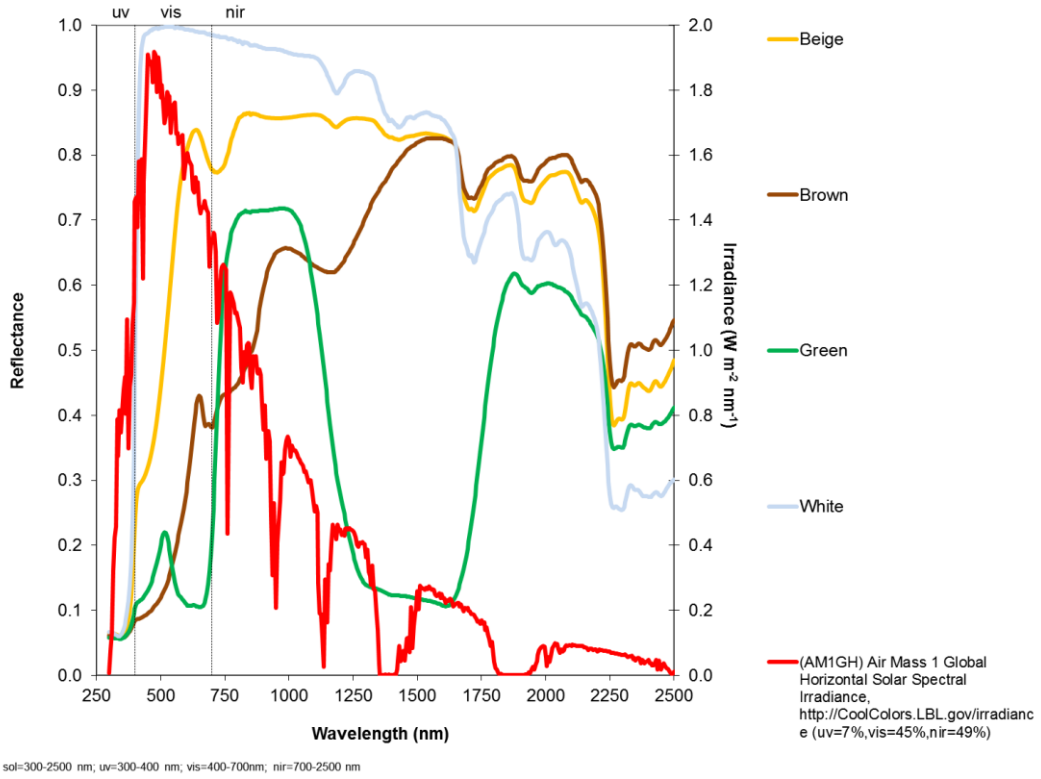

Figure 7.7 - Spectral reflectivity of unweathered samples with Organic coating and AM1GH irradiance spectrum

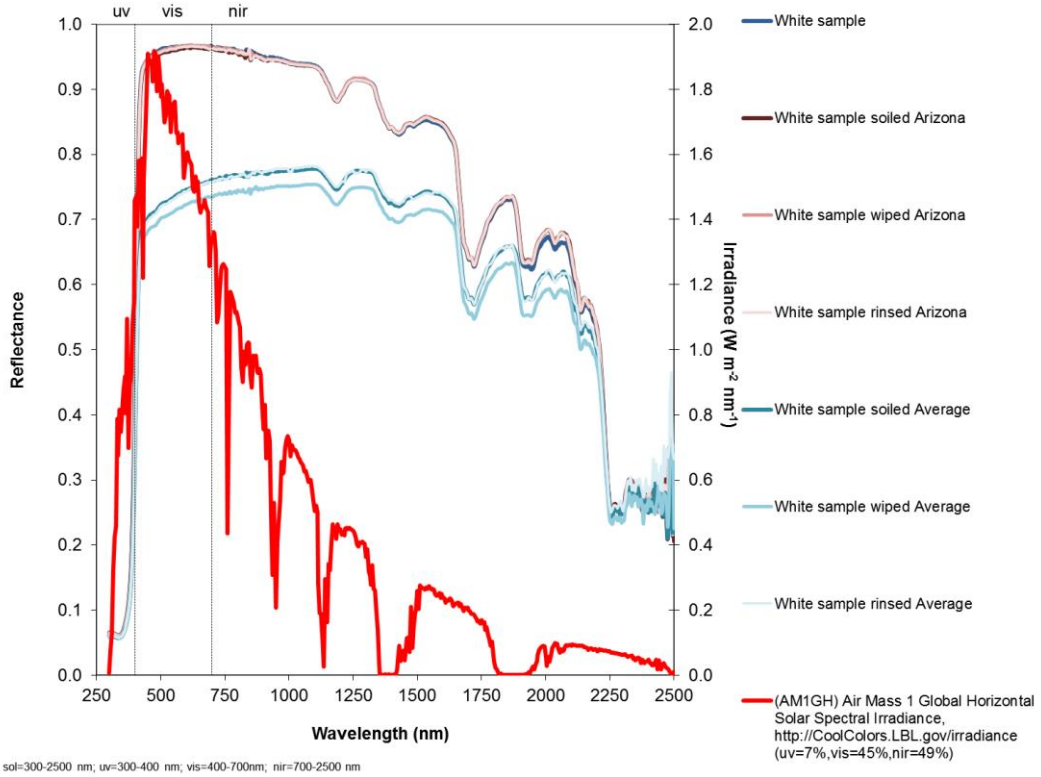

Figure 7.8 - Spectral reflectivity of the soiling and cleaning step on White sample and AM1GH irradiance spectrum

Table 7.3 - Solar reflectance R0 and solar reflectance ratio Rn/R0 of all the samples in each experimental step (all solar reflectance values in this table were measured via ASTM E903)

	Solar reflectance R_0	**Solar reflectance ratio R_n/R_0**									
	Unsoiled	**After weatherometer**	**Soiled Arizona**	**Wiped Arizona**	**Rinsed Arizona**	**Soiled Natural**	**Wiped Natural**	**Rinsed Natural**	**Soiled Average**	**Wiped Average**	**Rinsed Average**
Tobacco	0.345	0.983	0.983	0.989	0.986	0.934	0.921	0.921	0.891	0.892	0.893
Vanilla	0.537	0.969	0.969	0.945	0.945	0.958	0.956	0.964	0.868	0.865	0.865
Apricot	0.413	0.904	0.904	0.921	0.925	0.932	0.939	0.959	0.887	0.882	0.875
Red	0.381	0.960	0.960	0.924	0.922	0.947	0.944	0.991	0.894	0.897	0.889
Beige	0.659	1.000	0.986	0.988	0.983	N/A	N/A	N/A	0.842	0.821	0.847
Brown	0.382	1.004	1.000	1.000	1.000	N/A	N/A	N/A	0.882	0.853	0.890
Green	0.311	1.000	0.994	0.994	0.994	N/A	N/A	N/A	0.868	0.842	0.871
White	0.867	1.005	0.997	0.998	0.995	N/A	N/A	N/A	0.795	0.767	0.805

Only organic coatings pictures are shown in Figs. 7.2-7.4 because, for samples with inorganic coatings, due to the higher roughness of the surface, the soiling mixture deposition did not affect visibly the surface of the coupons. The two soiling mixtures were applied using the same setup and the same protocol, however it is interesting to notice how they create two completely different patterns on the two surfaces. This can be due to the different chemical composition of the mixtures. The peculiar surface morphology of the two coupons, in addition, affected the distribution of the soiling droplets on the surfaces, according to what is evident in Fig. 7.4.

Considering samples with inorganic coating, the difference between natural and artificial Arizona soiling is up to 0.01 for data measured with ASTM C1549 (ASTM, 2002) and up to 0.02 for data measured with ASTM E903 (ASTM, 96). Moreover, the ratio between the reflectance values measured for unweathered and soiled samples after the various cleaning processes, applied both on natural and accelerated aged samples, remains almost constant.

Looking at the different cleaning process, there is not a big recovery of solar reflectance neither after wiping nor after rinsing. On light color samples (vanilla, apricot, beige, and white) observations can be made easier if compared with other coupons and, analyzing the ratio of solar reflectance values measured on unsoiled and soiled samples, for each group of samples (organic and inorganic), the lighter samples are more influenced by the different soiling treatments.

Finally, inorganic coated samples are characterized by higher heterogeneity if compared with organic coated ones. However, this feature does not affect the feasibility of the study.

Experimental approach Natural ageing: Italian Experience

In this study, all the samples were collected from three Italian suppliers with the collaboration of ANDIL (Associazione Nazionale degli Industriali del Laterizio).They provided unweathered and weathered samples. For weathered samples, suppliers gave us information about the place of ageing and the time of ageing.

On all samples solar reflectivity measurements are carried out through both UV-Vis-NiR spectrophotometer with a 150 mm integrating sphere and reflectometer analysis.

The approach in the studies regarding the influence of different cleaning process carried out by Levinson et al (2005) and Akbari et al (2005), should probably be modified considering that in typical buildings it is not a common procedure to clean with phosphate free soap and bleaching agents a roof made by traditional clay roof tile. For this reason all the samples are modified with two different cleaning processes with increasing influence on the surface state, starting from a wiping process to simulate wind action through rinsing to simulate rain action. After each step, solar reflectance of the samples is measured once again with both a UV-Vis-NiR Spectrophotometer with a 150 mm integrating sphere and a reflectometer.

Table 7.4 - Samples ID

Set	Colour	Condition	Place of ageing	Time of ageing
Set 1	Campione 1	Unweathered	N/A	N/A
		Weathered	Siena	4 yrs
	Campione 2	Unweathered	N/A	N/A
		Weathered	Siena	4 yrs
	Campione 3	Unweathered	N/A	N/A
		Weathered	Siena	4 yrs
Set 2	Campione 1	Unweathered	N/A	N/A
		Weathered	Noale	7 yrs
	Campione 2	Unweathered	N/A	N/A
		Weathered	Catanzaro	6 yrs
	Campione 3	Unweathered	N/A	N/A
		Weathered	Valenza	5 trs
Set 3	Campione 1	Unweathered	N/A	N/A
		Weathered	Castiglion Fiorentino	3 yrs

These operations allow us to discover the influence of natural ageing on ceramic roof tiles, evaluate the influence of atmospheric agents on aged surfaces.

On table 7.4 are listed all the samples analyzed while figure 7.9 shows a coupon selected by the samples from the set 1, on figure 7.10 are shown the samples of the set 2 while in figure 7.11 coupons from set 3 are reported

Figure 7.9 - Samples from Set 1

Figure 7.10 - Samples from Set 2

Figure 7.11 - Sample from Set 3

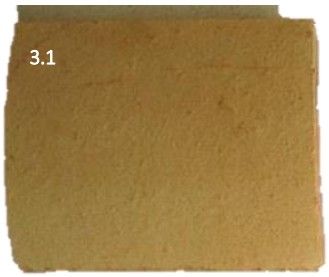

Method

Similarly to the first part of the study, both near-normal hemispherical solar reflectance, from 300 up to 2500 nm, with a step size of 5nm and the total solar reflectance measured with air mass 1 global horizontal (AM1GH). Both a Perkin Elmer Lambda 1050 UV/Visible/NIR Spectrometer with 150 mm integrating sphere and a Devices & Services Solar Spectrum Reflectometer (model SSR ER v.6) were used in order to measure the spectral properties of the surfaces.

A relevant issue we had to face with was the roundness of the surfaces of samples from set 1 and 3 since the measurement methods were designed for flat surfaces it was quite difficult try to measure using both spectrophotometer and reflectometer.

Moreover, in order to obtain a good statistic, five different coupons were selected from each samples provided. This was necessary because of the particular heterogeneous surface typical of ancient nouveau finishing. For each coupon at least 2 different measurements were carried out and in all the histogram reported double standard deviation was reported since the value is representative of almost 95% of the samples, contrary to simply σ which statistically represent just the 65% of the uncertainty of the measure

In addition to solar reflectance measurements the surface of the samples was investigated by means of X-Ray Diffraction, XRD, with a X'pert PRO diffractometer (PANalytical, Almelo, The Netherlands) equipped with X'Celerator detector. Diffraction patterns were collected using Cu Kα radiation, in the 5°-70° 2θ range (step size: 0.017°, step time: 19.68 s). A microstructural analyses was carried out on the sample' surfaces by means of an environmental scanning electron microscope, ESEM (ESEM Quanta 200-FEI Company, Eindhoven, The Netherlands) equipped with a X-EDS microanalysis system (Inca, Oxford Instruments, U.K.). The microscope was operated in high-vacuum mode.

Results and discussion

Likely to what performed in the first part of this study, solar reflectance was measured both according to ASTM E903 and ASTM C1549 methods in order to check the reliability of the measurements since, according to Levinson et al (2010c) the two measurement techniques should matches to within about 0.01. For this reason just solar reflectance measurements performed according to ASTM E903 will be reported in this part since the spectra collected can provide more information about the samples analyzed.

The ageing condition of each set were reported by the histogram in Fig. 7.12, Fig. 7.14 and Fig. 7.16 while in Fig. 7.13, Fig. 7.15 and Fig 7.17 are reported the different spectra related to the different set.

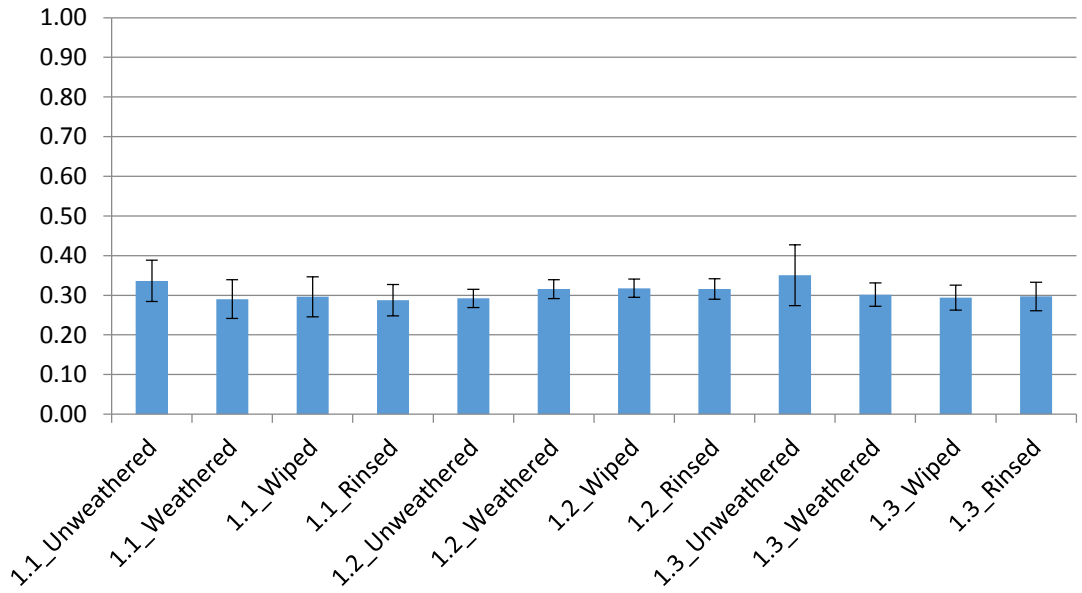

Figure 7.12 - Average reflectance of Set 1 samples measured according to ASTM E903 and calculated considering AM1GH as irradiance spectrum

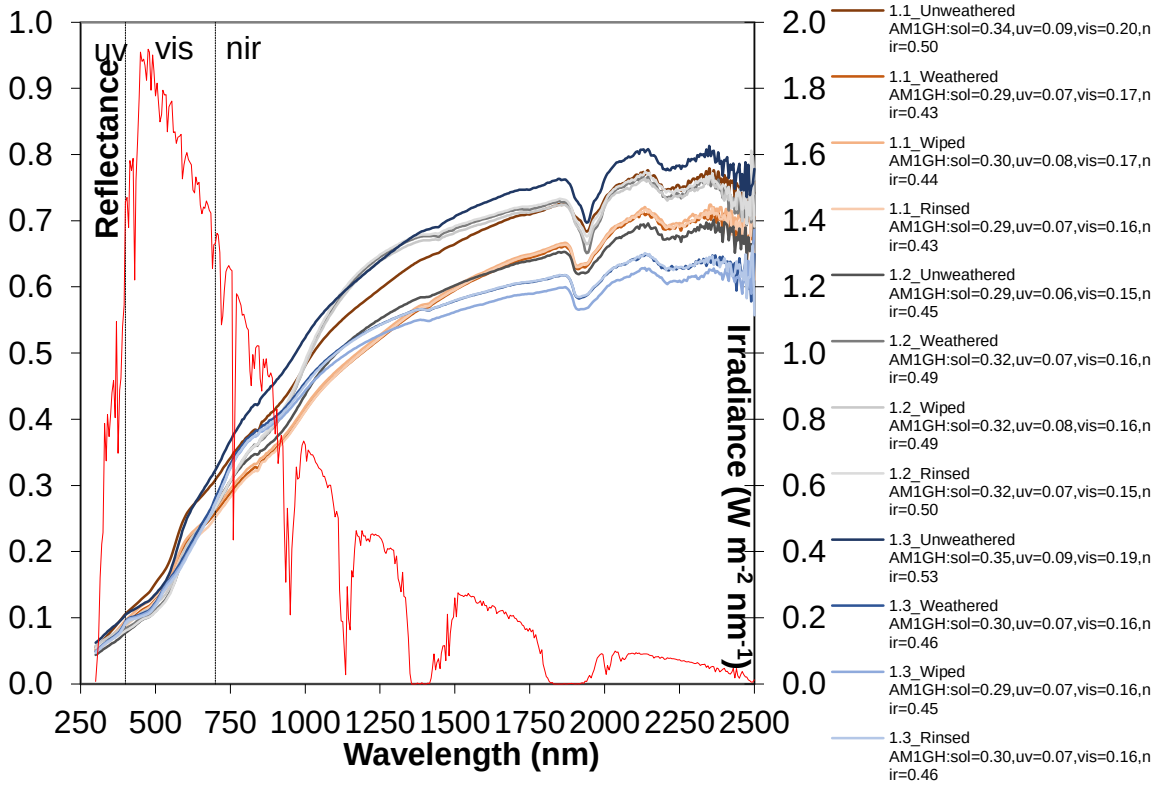

Figure 7.13 – Reflectance spectra of Set 1 samples measured according to ASTM E903 and AM1GH as irradiance spectrum

As reported in the histogram in figure 12, the samples from set 1 present similar reflectance. The sample 1.1 presents a decrease of solar reflectance after ageing, the sample 1.2, instead, shows a slight increase of solar reflectance, while the sample 1.3 presents again a relevant

decrease of reflectance after ageing process. Due to the heterogeneity of the surface and the roundness of the same the standard deviation bar is still higher than the variation of the solar reflectance across the different processes so it is impossible to assert if the variations, in particular regarding samples 1.1 and 1.2, are related to ageing processes or just to the surface morphology.

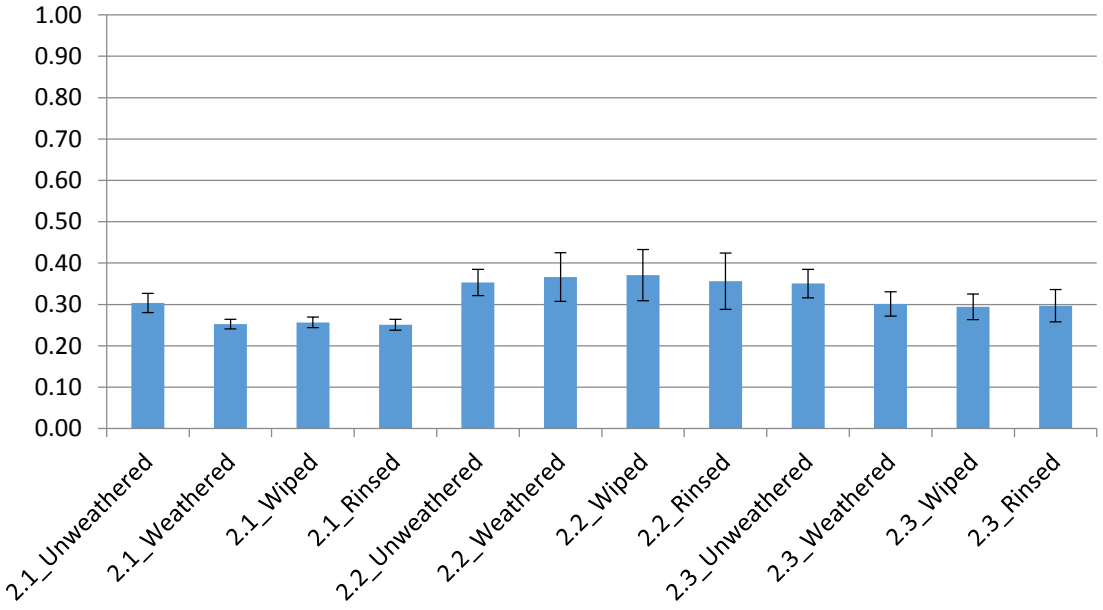

Figure 7.14 - Average reflectance of Set 2 samples measured according to ASTM E903 and calculated considering AM1GH as irradiance spectrum

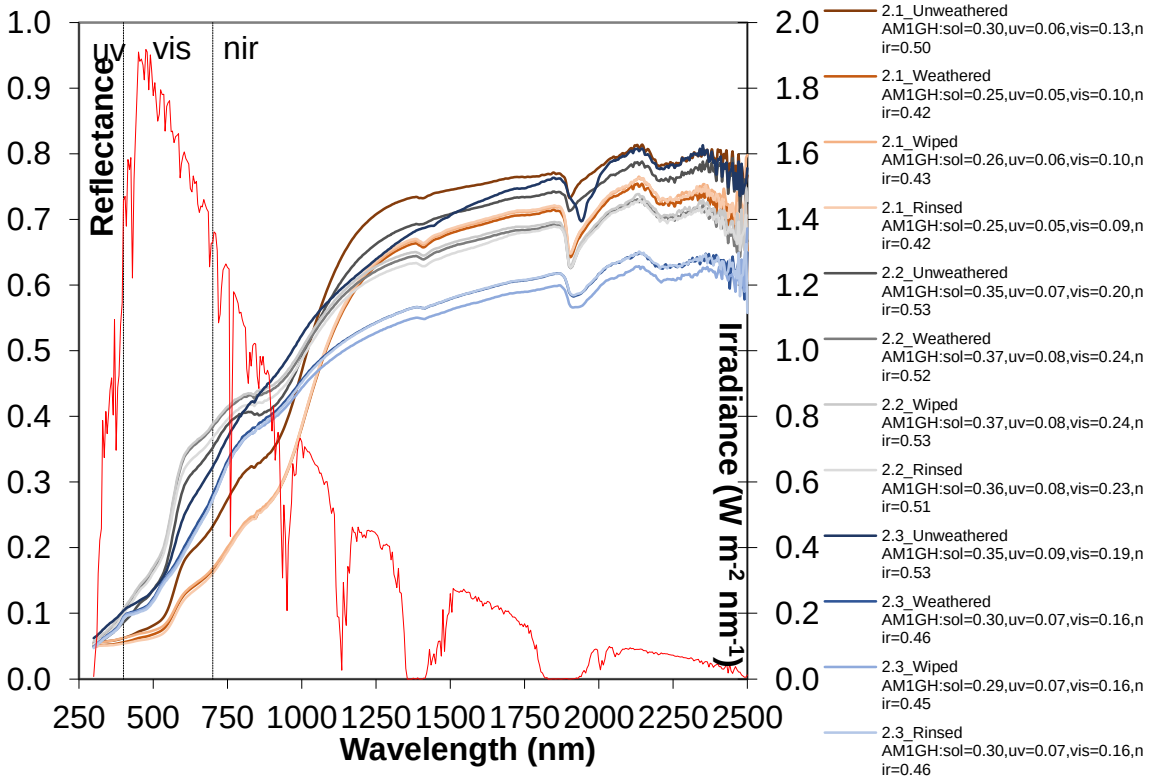

Figure 7.15 – Reflectance spectra of Set 1 samples measured according to ASTM E903 and AM1GH as irradiance spectrum

In this second set the sample 2.1 (Fig. 7.14, 7.15) present a decrease of solar reflectance of almost 0.05. Regarding samples 2.2 and 2.3 they are similar to the samples in previous set. As well as observed in Set 1 the solar reflectance is not really affected by the various cleaning processes, while, for surfaces more homogeneous like 2.1 the variation because of the ageing is more appreciable. Looking at sample 2.2 it seems the reflectance slightly increase after rinsing and wiping processes of about 0.001. Analyzing the error bar it is evident how, in reality, no real difference is appreciable.

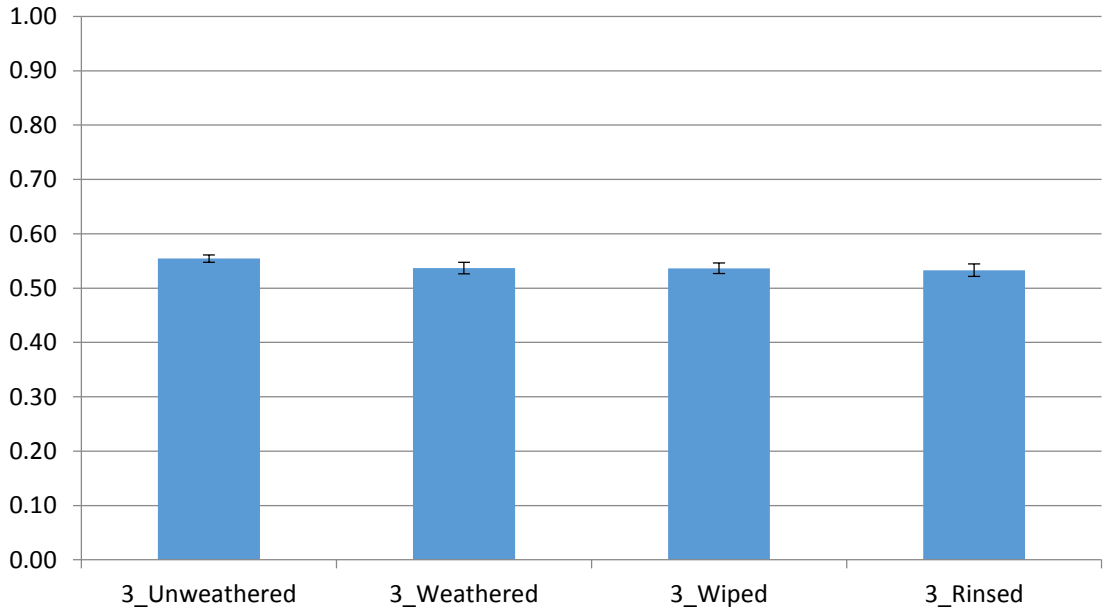

Figure 7.16 - Average reflectance of Set 3 samples measured according to ASTM E903 and calculated considering AM1GH as irradiance spectrum

Higher values of solar reflectance are achieved by the samples from Set 3 (Fig. 7.16, 7.17). In this case, thanks to the higher homogeneity of the surface, the 2σ standard deviation bar is significantly reduced if compared with the ones calculated for the other samples analyzed in this study. In Set 3, moreover, the difference between unweathered and weathered are not relevant. This can be explained in two different ways: the light color of the surface that is just slightly affected by the atmosphere pollution and the samples from Set 3 present the shorter ageing if compared with samples from Set 1 and Set 2.

Solar reflectance measurements, concerning these samples, are not properly relevant for both set 1 and 2 since the small measured area (1 cm^2 each spot) and the high variability of their surface does not allow a good repeatability of the measurements: this is also confirmed by the high value of standard deviation measured on the samples. An approach with a Portable Solar Spectrum Reflectometer and CRRC-1 standard test method is suggested or, as alternative, if a surface wide at least 1m^2 is available the use of a pyranometer or albedometer and the application of E1918a method is suggested. This method is an evolution of ASTM E1918 standard for smaller surface and it is under approval to become a recognized standard for measurement of solar reflectance.

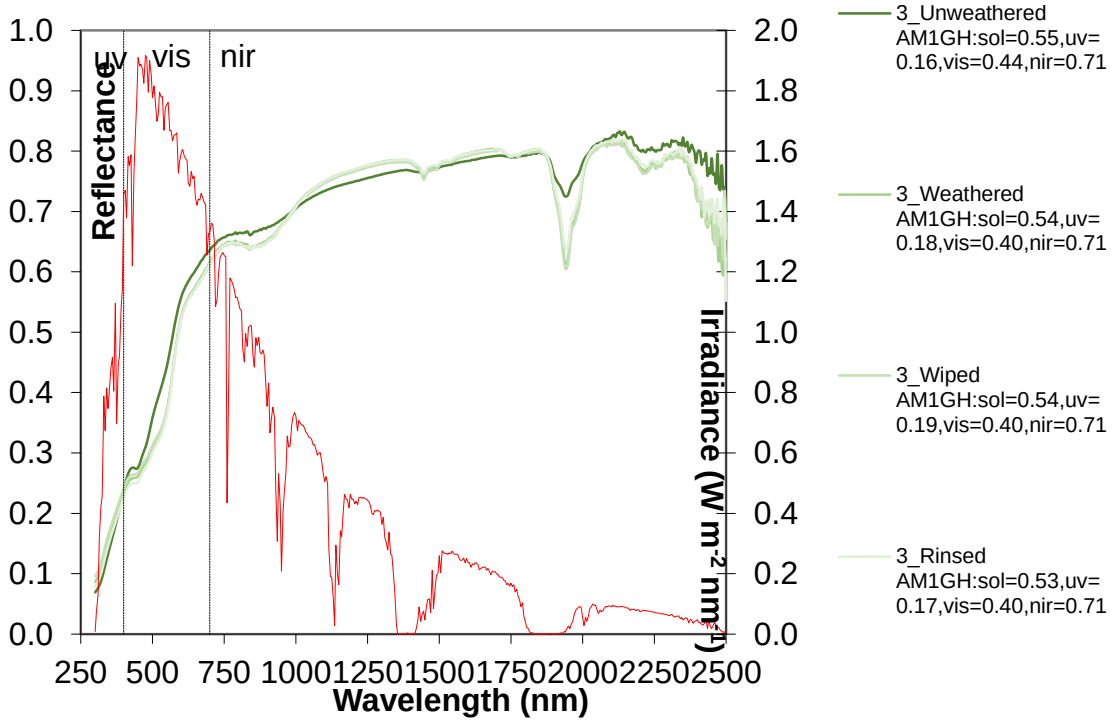

Figure 7.17 – Reflectance spectra of Set 1 samples measured according to ASTM E903 and AM1GH as irradiance spectrum

In this case it is important to compare the XRD spectra of the different samples before and after ageing processes in order to discover if, during ageing process, new crystalline phases were formed during the ageing process. The measurement were quite difficult to perform considering that the surface of the samples were not only heterogeneous and profiled but also with a considerably roughness. Generally all the samples present the same peaks both in the unweathered and weathered surface. The difference is limited in the intensity of the different peaks. Considering that the analysis of mineralogical composition of the sample will be

performed on Set 3 samples. This set was selected because the surface is more regular and smoother than the other surfaces analyzed. In fig. 7.18 the comparison between the weathered and unweathered samples is reported. In both samples were detected as main consitiuent phases Quartz, Calcium Carbonate

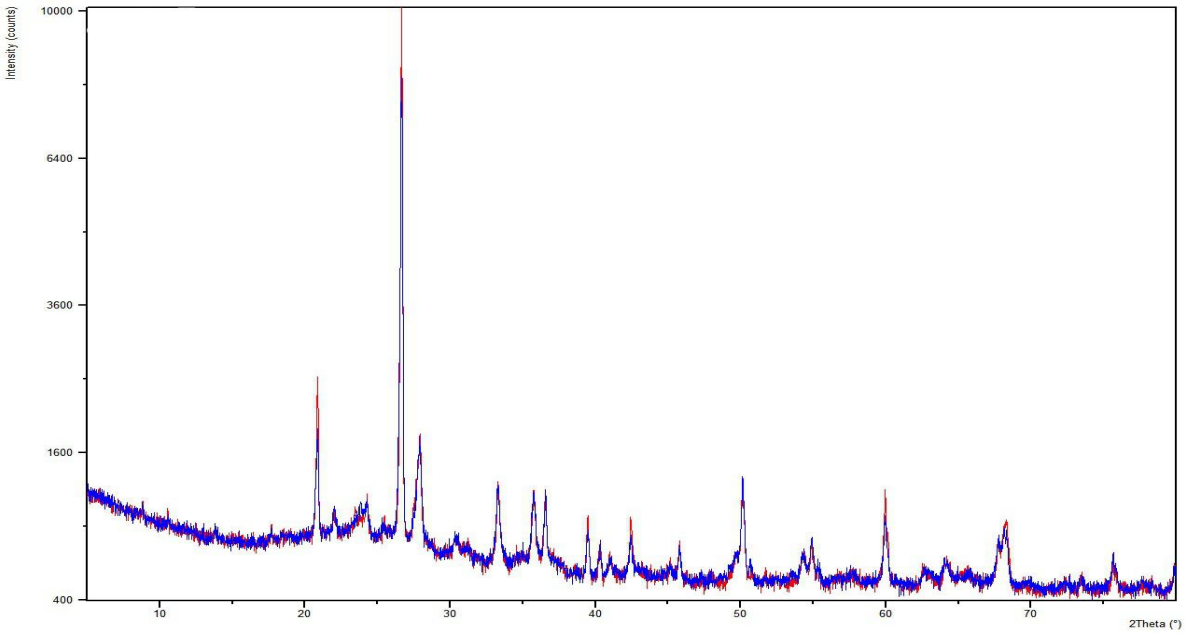

Figure 7.18 – Set 3 X-ray diffraction pattern. (Red: unweathered, Blue: weathered)

The microstructural analysis was carried out just on the untouched surfaces of the unweathered and weathered samples in order to check if the contaminants present in the pollution deposited on the tiles affect the microstructure of the samples. Moreover the micrographs help to better understand the ancient nouveau surfaces structure. First of all in figure 7.19 the comparison between the surfaces unweathered and weathered of sample 1.2 (Fig. 7.9) are reported. There are no appreciable differences in the surface structure.

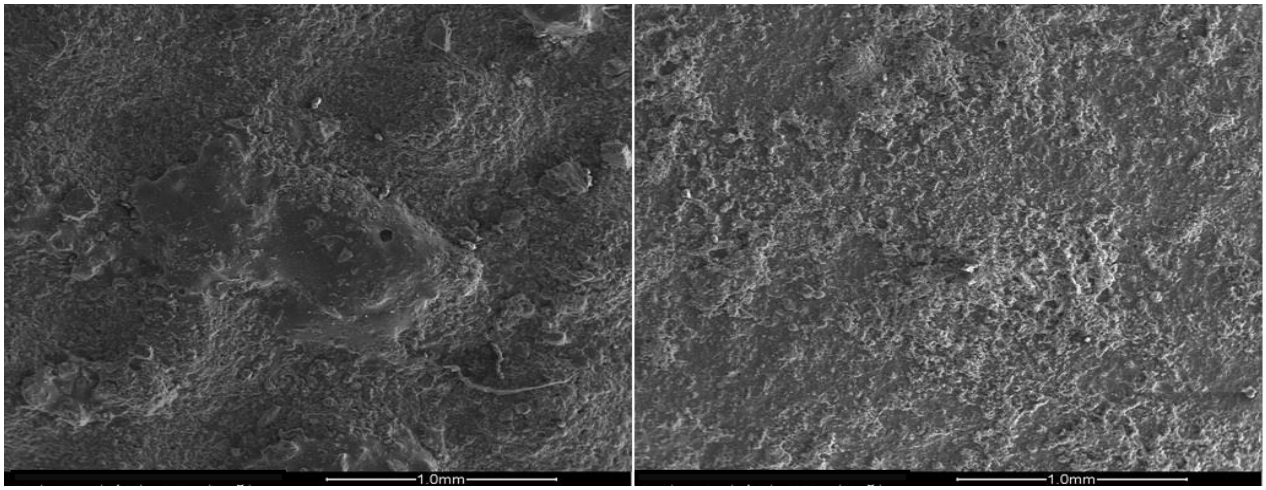

Figure 7.19. Comparison between surface weathered (left) and unweathered (right) of sample 1.2 (Magnification 100x)

The only interesting difference is related to the presence, on the aged samples, of a sort of structured surfaces that is better appreciable if the magnification will be reduced to 50x. (Figure 7.20)

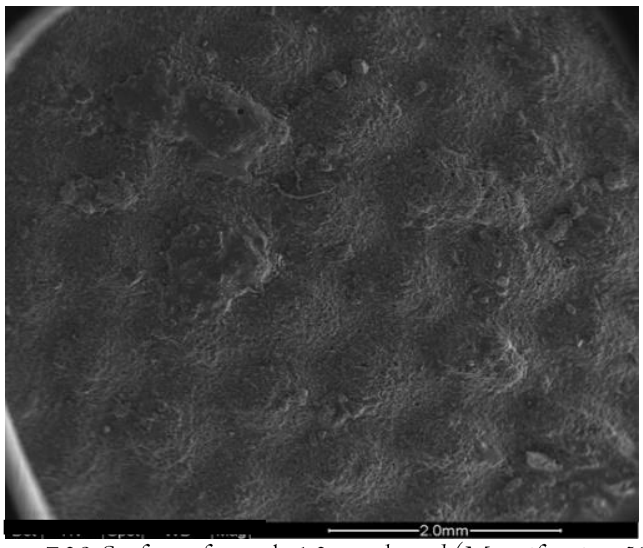

Figure 7.20. Surface of sample 1.2 weathered (Magnification 50x)

In figure 7.21 two micrographs from a sample belonging to the Set 2 are reported. On the first sample the roughness are absent (micrograph on the left) while are appreciable, in the micrograph on the left, irregular areas representative of the presence of glaze which simulate mold on the surface of the sample.

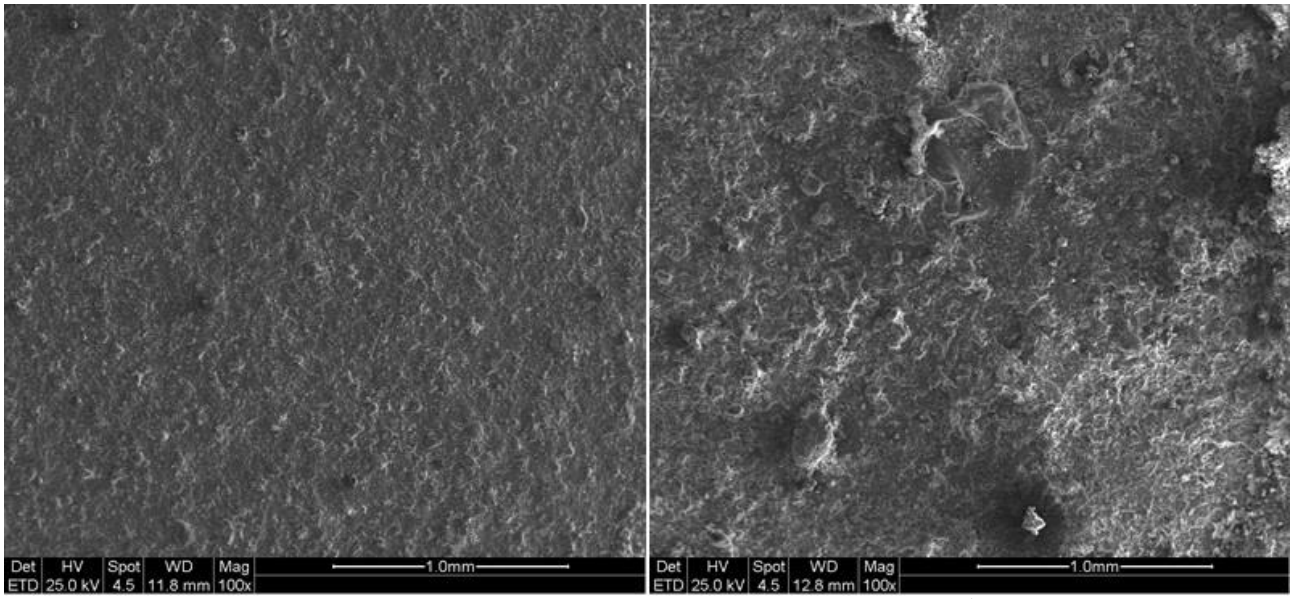

Figure 7.21. Micrograph of a unglazed surface and a glazed surface of a sample in Set 2 (Magnification 100x)

The surface of a sample from Set 3 is shown in Figure 7.22. As observed in figure 11, an engobe light colored covers the surface in a homogeneous way. The presence of this layer is confirmed by the SEM micrograph that present a smoother surface than the previous micrographs. The engobe presence, moreover, attenuate the roughness of the surface helping to increase the soiling resistance of the sample

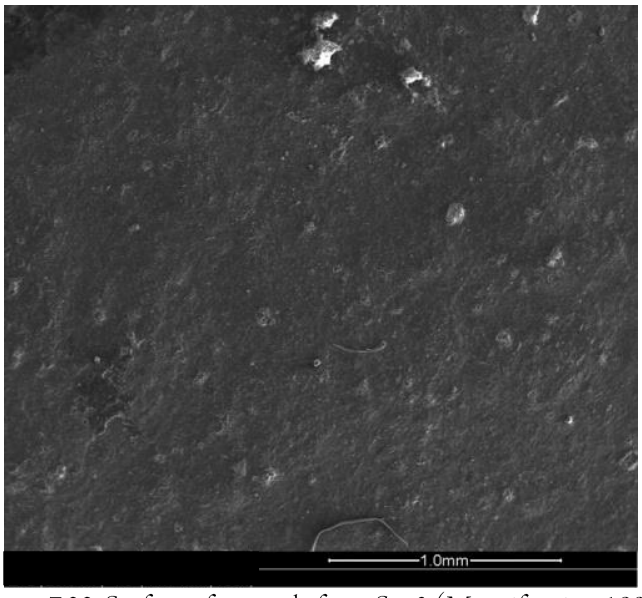

Figure 7.22. Surface of a sample from Set 3 (Magnification 100x)

Conclusions

The aim of the first part of this study was to investigate how accelerated ageing can affect solar reflectance of samples, characterized with both inorganic (4 coupons) and organic (4 coupons) and how natural weathering agents such as rain and wind, simulated in laboratory through wiping and rinsing processes, can eventually restore the solar reflectance.

The different soiling and cleaning processes show a good reproducibility of the process but also that the soiling mixture adheres to the fresh substrate in a way that excellently simulates the real soiling conditions of the naturally aged samples.

In contradiction to what is shown in Levinson et al (2005) concerning single ply membrane, cleaning processes do not seem to restore the solar reflectance of the samples, however washing and bleaching processes were not suitable for these samples since they cannot be applied to roofs covered with clay based tiles. A suitable reason of this lack in recovery of solar reflectance can be attributed to the morphology of the samples. For this reason microstructural, mineralogical and chemical analyses will be carried out on all the samples, both unsoiled and soiled, in order to better understand this particular behavior.

Since roof tiles are deeply integrated into buildings structure it is appropriate to spend a few words concerning how this kind of product affects the energy performance of buildings. In particular, a recent study carried out by Libbra et al (2013) concerns the energy performance of Italian buildings, which are commonly covered by clay roof tiles. They showed that raising the solar reflectance of clay tiles with terracotta color from an average value of 0.25 up to the maximum value technically possible, assumed equal to 0.55, may allow a decrease of the thermal load in summer up to 10 W per square meter of roof. In the USA studies on this line were carried out by Levinson et al (2007) demonstrating the reduction of peak roof surface temperature and peak ceiling heat flux.

In the second part of the study, seven different samples from whole Italy were analyzed through ASTM E903 with irradiance spectra AM1GH and ASTM C1549 with irradiance spectra AM1GH. Both fresh and aged samples were provided by suppliers and, with each aged sample, information about ageing conditions were provided.

Four different step were considered for this study: Fresh samples, Aged samples, Wiped samples and Rinsed samples.

High values of standard deviations can be due both to the variegated surfaces we had to deal with and to the curvature (or, in general the shape) of the samples analyzed

Considering the cleaning steps neither wiping neither rinsing can recover the reflectance of the samples. This can be due to the irregular surface of the samples which, thanks to the ancient nouveau technique is characterized by the application of droplets of inorganic glaze.

X-ray diffraction analysis on the surfaces of the samples were carried out in order to analyze the difference on the samples' mineralogy but no relevant changes were noticed

As attended, solar reflectance, after ageing, decrease from 0.01 up to 0.05. This promising result can be related to the high roughness of the surfaces: the pollutants on the surface, in fact, were deposited first of all into the asperities of the surface and after the filling of this micro cavities the contaminants will be deposited on the surface of the samples.

Clay roof tile, definitely, represents an excellent candidate for an high energy efficiency building. The weakness of the product, mainly related to the dark color of the natural surface of the tile, can be improved if the product will be integrated with an appropriate insulation system.

Chapter references

Akbari,H. (2005). Energy Saving Potentials and Air Quality Benefits of Urban Heat Island Mitigation. Lawrence Berkeley National Laboratory Report LBNL, Berkeley, CA.

Akbari, H., Berhe, A., Levinson, R., Graveline, S., Foley, K., Delgado, A.H., and Paroli, R.M. (2005). Aging and weathering of cool roofing membranes. Proceedings of the First International Conference on Passive and Low Energy Cooling for the Built Environment, May 17, 2005, Athens, Greece, Also published as Lawrence Berkeley National Laboratory Report LBNL-58055, Berkeley, CA.

Akbari, H., and Matthews, H.D. (2012). Global cooling updates: Reflective roofs and pavements, Energy & Buildings, 55, 2-6. Doi: 10.1016/j.enbuild.2012.02.055

ASTM (1996). ASTM E 903-96 – Standard test method for solar absorptance, reflectance, and transmittance of materials using integrating spheres. Standard of the American Society for Testing and Materials.

ASTM (2002). ASTM C 1549-02 – Standard test method for determination of solar reflectance near ambient temperature using a portable solar reflectometer. Standard of the American Society for Testing and Materials.

ASTM (2003). ASTM G 173-03 – Standard tables for reference solar spectral irradiance at air mass 1.5: direct normal and hemispherical on 37° tilted surface. Standard of the American Society for Testing and Materials.

ASTM(2012). ASTM G154-12a – Standard Practice for Operating Fluorescent Ultraviolet (UV) Lamp Apparatus for Exposure of Nonmetallic Materials. Standard of the American Society for Testing and Materials.

Berdahl, P., Akbari, H., Levinson, R., Jacobs, J., Klink, F., and Everman, R. (2012). Three-year weathering tests on asphalt shingles: Solar reflectance. Solar Energy Materials and Solar Cells, 99, 277-281. Doi: 10.1016/j.solmat.2011.12.010

Bretz, S., and Akbari, H. (1997). Long-term performance of high-albedo roof coatings. Energy & Buildings, 25, 159-167. Doi: 10.1016/S0378-7788(96)01005-5

Cheng, M.D., Miller, W., New, J., and Berdahl, P. (2012). Understanding the long-term effects of environmental exposure on roof reflectance in California. Construction and Building Materials 26, 516–526 (2012) Doi: 10.1016/j.conbuildmat.2011.06.052

Ferrari C., Libbra A., Muscio A., Siligardi C., (2013) Design of ceramic tiles with high solar reflectance through the development of a functional engobe, Ceramics International, 39(8), 9583-9590, ISSN 0272-8842, 10.1016/j.ceramint.2013.05.077.

George, G., Vishnu, V.S., Reddy, M.L.P. (2011). The synthesis, characterization and optical properties of silicon and praseodymium doped Y6MoO12 compounds: Environmentally benign inorganic pigments with high NIR reflectance. Dyes and Pigments, 88(1), 109-115.

Konopacki, S.J., Akbari H., Pomerantz M., Gabersek, S., and Gartland, L.M. (1997). Cooling Energy Savings Potential of Light-Colored Roofs for Residential and Commercial Buildings in 11 US Metropolitan Areas. Lawrence Berkeley National Laboratory Report LBNL-39433, Berkeley, CA.

Levinson, R., and Akbari, H. (2010a). Potential benefits of cool roofs on commercial buildings: conserving energy, saving money, and reducing emission of greenhouse gases and air pollutants. Energy Efficiency, 3(1), 53-109.

Levinson, R., Akbari, H., and Berdahl, P. (2010b). Measuring solar reflectance – Part I: defining a metric that accurately predicts solar heat gain. Solar Energy, 84, 1717-1744. Doi: 10.1016/j.solener.2010.04.018

Levinson, R., Akbari, H., and Berdahl, P. (2010c). Measuring solar reflectance – Part II: Review of practical methods. Solar Energy, 84, 1745-1759. Doi: 10.1016/j.solener.2010.04.017

Levinson, R., Berdahl, P., Berhe, A., and Akbari, H. (2005). Effects of soiling and cleaning on the reflectance and solar heat gain of a light-colored roofing membrane. Atmospheric Environment, 39, 7807-7824. Also published as Lawrence Berkeley National Laboratory Report LBNL-57555, Berkeley, CA.

Levinson R., Akbari H., Reilly J.C. (2007). Cooler tile-roofed buildings with near-infrared-reflective non-white coatings, Building and Environment, 42 (7) 2591-2605, DOI:10.1016/j.buildenv.2006.06.005.

Levinson, R., Berdahl, P., Akbari, H., Miller, W., Joedicke, I., Reilly, J., Suzuki, Y., and Vondran, M. (2007). Methods of creating solar-reflective nonwhite surfaces and their application to residential roofing materials. Solar Energy Materials and Solar Cells, 91, 304–314. Doi: 10.1016/j.solmat.2006.06.062

Levinson, R., Akbari, H., Berdahl, P., Wood, K., Skilton, W., and J. Petersheim, J. (2010). A novel technique for the production of cool colored concrete tile and asphalt shingle roofing products. Solar Energy Materials and Solar Cells, 94, 946-954. Doi: 10.1016/j.solmat.2009.12.012

Libbra, A., Tarozzi, L., Muscio, A., and Corticelli, M.A. (2011). Spectral Response Data for Development of Cool Coloured Tile Coverings. Optics and Laser Technology, 43(2), 394-400. Doi: 10.1016/j.optlastec.2009.07.001

Libbra, A., Muscio, A., Siligardi, C., and Tartarini, P. (2011). Assessment and improvement of the performance of antisolar surfaces and coatings. Progress in Organic Coatings, 72, 73-80. Doi: 10.1016/j.porgcoat.2011.02.019

Libbra, A., Muscio, A., Siligardi, C. (2013) Energy performance of opaque building elements in summer: Analysis of a simplified calculation method in force in Italy, Energy and Buildings, 64, 384-394, DOI: 10.1016/j.enbuild.2013.05.022.

Noelia L. Alchapar, Erica N. Correa, M. Alicia Cantón (2014). Classification of building materials used in the urban envelopes according to their capacity for mitigation of the urban heat island in semiarid zones. Energy and Buildings, 69, 22-32, Doi: 10.1016/j.enbuild.2013.10.012

Pisello, A.L., Cotana, F., Nicolini, A., Brinchi, L. (2013). Development of Clay Tile Coatings for Steep-Sloped Cool Roofs. Energies 6, 3637-3653

Q-Lab (2013). QUV ACCELERATED WEATHERING TESTER. Retrievable in 2013 at the web address: http://www.q-lab.com/products/quv-weathering-tester/quv

Santamouris, M. (2012). Cooling the cities – A review of reflective and green roof mitigation technologies to fight heat island and improve comfort in urban environments. Solar Energy, In press (2012).doi:10.1016/j.solener.2012.07.003.

Sleiman, M., Kirchstetter, T., Berdahl, P., Gilbert, H., Francois, D., Spears, M., Levinson, R., Destaillats, H., and Akbari, H.(2010).Development of an accelerated soiling method that mimics natural exposure of roofing materials.Proceedings of the 3rd International Passive and Low Energy Cooling for the Built Environment (Palenc 2010), September 29 to October 1, 2010, Rhodes, Greece, pp. 19-21.

A. Synnefa, M. Santamouris, I. Livada, (2006) A study of the thermal performance of reflective coatings for the urban environment, Solar Energy, 80(8), 968-981, 10.1016/j.solener.2005.08.005.

A. Synnefa, M. Santamouris, K. Apostolakis,(2007) On the development, optical properties and thermal performance of cool colored coatings for the urban environment, Solar Energy, 81(4), 488-497, 10.1016/j.solener.2006.08.005.

Zhao, M., Han, A., Ye, M., Wu, T. (2013). Preparation and characterization of Fe3+ doped Y2Ce2O7 pigments with high near-infrared reflectance. Solar Energy, 97, 350-35

CHAPTER 8
GENERAL CONCLUSIONS AND FURTHER PERSPECTIVES

General conclusions

Urban Heat Island is a phenomenon affecting in a significant way the planet. Different strategies are adopted in order to mitigate dangerous effect due to UHI, first of all the increasing of temperature which causes, among all, an increasing thermal discomfort with an increase of relate air conditioning costs, the increasing of greenhouse gases emission and relevant structural stresses for buildings.

Among the strategies for counteracting the UHI effect cool roofs are one of the most widely used. This technique, introduced in the US thanks to Lawrence Berkeley National Laboratory Heat Island Group, is based on materials characterized by high solar reflectance and high thermal emissivity.

Cool roof market is mainly dominated by organic based building products, but ceramic based and in general clay based building materials, thanks to their naturally excellent thermal emissivity (ε=0.8/0.9) are excellent candidates for cool roof application. It is, however, necessary to work in order to improve their solar reflectance.

This thesis was aimed to increase the solar reflectance of various building products, starting from a traditional ceramic tile where a new solar reflective engobe was formulated and different colored glazes were applied, a glazed clay roof tile and ceramic glaze for asphalt shingles which reduced significantly the production cost of this glaze keeping interesting values of solar reflectance.

With all these products significant improvement of the solar reflectance were made in addition to an increased durability to weathering agents thanks to the glazed applied on all the products.

The resistance to ageing weathering and pollutants exposure is one of the bigger issues concerning cool roof since three year of exposure in selected US climate are necessary for a product in order to obtain the "Cool Roof" label from the Cool Roof Rating Council. These three location are in Florida, Ohio and Arizona.

In the third part of this study, the ageing matter was analyzed applying both natural and artificial weathering protocols to cool roof surfaces. Their response to ageing was analyzed, and in order to check if a 3-day-laboratory simulation, well working on polymeric materials, can be adopted also for clay roof tiles in order to condensate the three years exposure required from CRRC. Moreover, the influence of ageing in Italy was checked on samples characterized by ancient nouveau surface finishing.

Different cleaning processes were then applied to these surfaces to analyze if wind or rain can restore totally or partially the solar reflectance of the samples. The reflectance was not restored maybe due to the high roughness of clay roof tiles, since the cleaning operations were not efficient to remove pollutants formed into the asperities of the surface.

Further Perspectives

Cool roof analysis on inorganic based materials is still in a preliminary phase and really many new perspectives are considered every days. Starting from the results of this thesis, first ageing studies should be carried out on all the glazed tiles and clay roof tiles produced.

Moreover, energy simulation can be made in order to analyze, at city scale, which is the effective reduction of energy consumption and CO2 emission after cool roof applications.

Concerning the analysis of asphalt shingles glaze the Experimental Plan can be integrated in order to add variation of isotherm duration and temperature and eventually pigment amount considering the same pigments used in the first part of this thesis.

An interesting new perspective, opened not just to cool roof but to every materials subjected to weathering, is the installation of a test farm, following the US Cool Roof Rating Council test farms concept, in the Po Valley.

According to recent studies, Po Valley, is one of the most polluted area in the whole Europe and the behavior of spectral properties, and in general the durability of cool roof and all building materials under natural weathering, it is really interesting. Moreover, a soiling mixture simulating Po valley pollutants should be created in order to apply accelerated weathering protocols simulating ageing conditions of this area.

Acknowledgements

Alla fine di un viaggio è naturale fare un bilancio del percorso svolto. In questi anni ci sono tante persone che mi sono state vicine e alle quali va la mia più sincera gratitudine. La prima persona che vorrei ringraziare è la *Prof.ssa Cristina Siligardi*. Grazie per avere scommesso su di me, per avermi dato fiducia e non avermi mai fatto mancare il prezioso supporto sia scientifico sia umano. Unitamente alla Prof.ssa Siligardi il mio grazie incondizionato va al *Dott. Alberto Muscio*. Tutto quello che ho imparato in questi anni è essenzialmente merito vostro e di questo non potrò mai smettere di esservi grata. E' stato veramente inspiring poter lavorare con voi. Un ringraziamento sentitissimo va anche al *Prof. Hashem Akbari* che mi ha accolto per sei mesi nell'Heat Island Group della Concordia University a Montreal, dimostrandosi guida preziosa e modello di lavoro. Grazie all'*Ing. Antonio Libbra* che mi ha insegnato i fondamenti pratici sulle misure delle proprietà radiative dei materiali.

Un buon ricercatore deve saper lavorare in team, ed avere un ottimo team di appoggio è stato essenziale per la mia crescita professionale quindi grazie a tutto il *SiMo Group*, per il supporto costante in questi anni a Modena, a tutti i *colleghi di ufficio* e agli amici dell'*EELab*. Grazie all'*Heat Island Group a Montreal* (in particolare *Ali, Farhad, Ata e Hatef*) per l'accoglienza e il reciproco arricchimento. Grazie anche allo staff dell'*Heat Island Group del Lawrence Berkeley National Laboratory* (*Ronnen, Hugo, Mohamad, Paul e Haley*) per avermi accolto e insegnato tanto nelle due settimane trascorse insieme.

Un viaggio importante, come quello che è stato il mio percorso di dottorato, è ancora più bello se condiviso con persone eccezionali quindi, *Ale e Paolo*, vorrei ringraziarvi per esservi dimostrati così meravigliosi che a volte ho avuto quasi paura di non meritarvi! Senza di voi questi anni non sarebbero stati uguali!

Grazie di cuore anche a chi non mi ha mai fatto mancare il suo supporto sostenendomi e facendomi sentire sempre la sua presenza mentre ero a Montreal, incoraggiandomi e spronandomi nei momenti di difficoltà e debolezza sia di qua sia al di là dell'oceano e condividendo i momenti di gioia e di conquista che hanno costellato questo mio cammino.

Non posso non ringraziare *Giovanni*, in tutti questi anni, da quando eravamo decisamente meno "saggi" mi ha accompagnato in un'amicizia che non esiterei a definire unica nel suo genere. Grazie per avermi appoggiato, spronato, sgridato, gioito e per esserci stato sempre. Grazie a *Massimiliano*, che mi ha accompagnato nel cammino dalla laurea specialistica ad oggi prima nella veste di correlatore e ora nella veste di amico prezioso. Grazie a *Pamela*, *Margherita*, Elisa, Elisa e *Francesca* per essere state amiche grandiose e sempre presenti, grazie a *Lidia* per essere stata la mia famiglia durante i sei mesi e mezzo a Montreal

Grazie di cuore anche a chi, con enormi sacrifici, mi ha permesso di arrivare fin qua oggi. Siete la *famiglia* migliore che si possa desiderare e spero di avervi resa fiera di voi oggi. Anche grazie a chi oggi non può esserci, non fisicamente, almeno, sperando che ovunque siano, anche loro possano essere fieri di me.

Come già detto, tre anni sono tanti e il rischio di aver tralasciato persone importanti per il mio cammino professionale e personale diventa terribilmente alto, quindi voglio ringraziarvi tutti quanti in queste righe, dal primo all'ultimo, e contemporaneamente vi chiedo scusa per non essere riuscita a nominarvi personalmente in questo spazio ristretto.